

entropy

Entropy and Non-Equilibrium Statistical Mechanics

Edited by

Róbert Kovács, Antonio M. Scarfone and Sumiyoshi Abe

Printed Edition of the Special Issue Published in *Entropy*

Entropy and Non-Equilibrium Statistical Mechanics

Entropy and Non-Equilibrium Statistical Mechanics

Special Issue Editors

Róbert Kovács

Antonio M. Scarfone

Sumiyoshi Abe

MDPI • Basel • Beijing • Wuhan • Barcelona • Belgrade • Manchester • Tokyo • Cluj • Tianjin



Special Issue Editors

Róbert Kovács
Budapest University of
Technology and Economics
Hungary

Antonio M. Scarfone
Consiglio Nazionale delle
Ricerche (ISC-CNR)
Italy

Sumiyoshi Abe
Huaqiao University
China

Editorial Office

MDPI
St. Alban-Anlage 66
4052 Basel, Switzerland

This is a reprint of articles from the Special Issue published online in the open access journal *Entropy* (ISSN 1099-4300) (available at: https://www.mdpi.com/journal/entropy/special_issues/noequilibrium).

For citation purposes, cite each article independently as indicated on the article page online and as indicated below:

LastName, A.A.; LastName, B.B.; LastName, C.C. Article Title. <i>Journal Name</i> Year , Article Number, Page Range.

ISBN 978-3-03936-232-5 (Hbk)

ISBN 978-3-03936-233-2 (PDF)

Cover image courtesy of Péter Verhás.

© 2020 by the authors. Articles in this book are Open Access and distributed under the Creative Commons Attribution (CC BY) license, which allows users to download, copy and build upon published articles, as long as the author and publisher are properly credited, which ensures maximum dissemination and a wider impact of our publications.

The book as a whole is distributed by MDPI under the terms and conditions of the Creative Commons license CC BY-NC-ND.

Prof. József Verhás, D.Sc. (1939–2020)

The present Special Issue is dedicated to the memory of our beloved, respected friend, colleague and teacher, the late Professor József Verhas.

Prof. Verhás played a pioneering role in establishing and strengthening the Hungarian tradition of thermodynamics.

He was active both scientifically and socially, having membership in the Roland Eötvös Physical Society, the János Bolyai Mathematical Society, the International Society for the Interaction of Mechanics and Mathematics, and in the Editorial Advisory Board of *Journal of Non-Equilibrium Thermodynamics*. He was also a member of the Accademia Peloritana dei Pericolanti.

Prof. Verhás was a master of irreversible thermodynamics with extremely broad interests and knowledge. He contributed to the progress of the variational principles of irreversible thermodynamics and wave theory of thermodynamics, and introduced the concept of dynamic degrees of freedom and developed the nonequilibrium thermodynamic theory of liquid crystals.

He also worked on the theory of cellular division, turbulence, plasticity, and in many other applications and areas of irreversible thermodynamics.

The Kluitenberg-Verhás body and the rheological Verhás element bear his name, in honor of his work in elaborating the thermodynamic basis of rheology.



Contents

About the Special Issue Editors	ix
Róbert Kovács, Antonio M. Scarfone, Sumiyoshi Abe Entropy and Non-Equilibrium Statistical Mechanics Reprinted from: <i>Entropy</i> 2020 , <i>22</i> , 507, doi:10.3390/e22050507	1
Giorgio Kaniadakis and Antonio M. Scarfone Classical Model of Quons Reprinted from: <i>Entropy</i> 2019 , <i>21</i> , 841, doi:10.3390/e21090841	3
Karl-Erik Eriksson and Kristian Lindgren Statistics of the Bifurcation in Quantum Measurement Reprinted from: <i>Entropy</i> 2019 , <i>21</i> , 834, doi:10.3390/e21090834	15
Róbert Kovács On the Rarefied Gas Experiments Reprinted from: <i>Entropy</i> 2019 , <i>21</i> , 718, doi:10.3390/e21070718	29
Rudolf A. Treumann and Wolfgang Baumjohann A Note on the Entropy Force in Kinetic Theory and Black Holes Reprinted from: <i>Entropy</i> 2019 , <i>21</i> , 716, doi:10.3390/e21070716	43
Václav Klika, Michal Pavelka and Miroslav Grmela Dynamic Maximum Entropy Reduction Reprinted from: <i>Entropy</i> 2019 , <i>21</i> , 715, doi:10.3390/e21070715	61
Xiaohan Cheng A Fourth Order Entropy Stable Scheme for Hyperbolic Conservation Laws Reprinted from: <i>Entropy</i> 2019 , <i>21</i> , 508, doi:10.3390/e21050508	89
Congjie Ou, Yuho Yokoi and Sumiyoshi Abe Spin Isoenergetic Process and the Lindblad Equation Reprinted from: <i>Entropy</i> 2019 , <i>21</i> , 503, doi:10.3390/e21050503	97

About the Special Issue Editors

Róbert Kovács graduated with a degree in Mechanical Engineering in 2015 before attaining his Ph.D. in 2017 from Budapest University of Technology and Economics (BME) in collaboration with the Hungarian Academy of Sciences. He is currently working on continuum thermodynamics, both experimental and theoretical problems, including the development of numerical schemes, analytical solutions of evolution equations, and other mathematical aspects. He has been a Visiting Researcher at Northeastern University, MA, USA; Messina University, Sicily, Italy; and Université du Québec à Chicoutimi, Québec, Canada.

Antonio M. Scarfone is a theoretical physics researcher working mainly in the field of statistical mechanics. He graduated from University of Torino in 1996 and completed his Ph.D. in Physics at Politecnico of Torino in 2000. He has been a Postdoctoral Researcher at INFN (2000–2002) and received a Research Fellowship at the University of Cagliari in 2003. Since 2004, he has carried out research activities at CNR-ISC based in Politecnico of Torino. To date, he has authored approximately 100 scientific papers published in international journals on the topics of statistical mechanics, kinetic theory, geometry information, nonlinear classical and quantum dynamics, and noncommutative algebras. He is Editor-in-Chief of the Section Statistical Physics of *Entropy*, a member of the Editorial Board of *Advances in Mathematical Physics*, and belongs to the advisory panel of *Journal of Physics A*. Finally, he is one of the organizers of the SigmaPhi international conference series that has been held every three years starting from 2005.

Sumiyoshi Abe has recently been serving as Full Professor at Mie University in Japan until March 2020. Currently, he is a Visiting Professor at Huaqiao University in China, Kazan Federal University in Russia, Turin Polytechnic University in Tashkent in Uzbekistan, and ESIEA in France.

Entropy and Non-Equilibrium Statistical Mechanics

Róbert Kovács ^{1,2,3,*} , Antonio M. Scarfone ⁴  and Sumiyoshi Abe ^{5,6,7,8}

¹ Department of Energy Engineering, Faculty of Mechanical Engineering, Budapest University of Technology and Economics, 1111 Budapest, Hungary

² Department of Theoretical Physics, Wigner Research Centre for Physics, Konkoly-Thege M. 29-33, 1121 Budapest, Hungary

³ Montavid Thermodynamic Research Group, 1112 Budapest, Hungary

⁴ Istituto dei Sistemi Complessi, Consiglio Nazionale delle Ricerche (ISC-CNR), c/o, Politecnico di Torino, Corso Duca degli Abruzzi 24, I-10129 Torino, Italy; antonio.scarfone@polito.it

⁵ Physics Division, College of Information Science and Engineering, Huaqiao University, Xiamen 361021, China; suabe@sf6.so-net.ne.jp

⁶ Institute of Physics, Kazan Federal University, 420008 Kazan, Russia

⁷ Department of Natural and Mathematical Sciences, Turin Polytechnic University in Tashkent, Tashkent 100095, Uzbekistan

⁸ ESIEA, 9 Rue Vesale, 75005 Paris, France

* Correspondence: kovacs.robert@wigner.mta.hu

Received: 24 April 2020; Accepted: 27 April 2020; Published: 29 April 2020

Keywords: non-equilibrium phenomena; kinetic theory; second law of thermodynamics; statistical distributions; stochastic processes

The present Special Issue, ‘Entropy and Non-Equilibrium Statistical Mechanics’, consists of seven original research papers. Although the issue has a long history, still it remains as one of the most fundamental subjects in physics. These seven papers actually cover various latest relevant topics, ranging from gravity as an entropic force to exotic statistics, including conservation laws, dynamics generated by entropy production, quantum measurements and the limits on the constitutive laws in classical gaseous systems.

We hope that the Special Issue will be able to play a role in further progress to come in the future.

In this paper, ‘Classical Model of Quons’, by G. Kaniadakis and A. M. Scarfone [1] by using a kinetic interaction principle an evolution equation describing quons statistics is proposed by properly generalizing the inclusion/exclusion principle of standard boson and fermion statistics. In this way, a nonlinear Fokker-Planck equation for quons particles of type I and type II is introduced and the corresponding steady distribution is derived.

The paper ‘Statistics of the Bifurcation in Quantum Measurement’, by K.-E. Eriksson and K. Lindgren [2], deals with a quantum measurement of a two-level system improving the already known methods, basing the analysis of the interaction with the measurement device on the quantum field theory. In this way, a microscopic details of the measurement apparatus affect the process so that it takes the eigenstates of the measured observable by recording the corresponding measurement result.

The paper written by R. Kovács [3] deals with the experiments on rarefied gases. The generalized system of Navier-Stokes-Fourier equations is presented, which is required to model the ballistic effects appearing in gases at low pressures. The experimental evaluation consists of the investigation of scaling properties of models originating from the kinetic theory and continuum thermodynamics, especially emphasizing the importance of mass density dependence of material properties.

In the paper ‘A Note on the Entropy Force in Kinetic Theory and Black Holes’ by R. A. Treumann and W. Baumjohann [4] is derived a kinetic equations of a large system of particles including a collective integral term to the Klimontovich equation for the evolution of the single-particle distribution function. The integral character of this equation transforms the basic single particle kinetics into an

integro-differential equation showing that not only the microscopic forces but the hole system gets its probability distribution in a holistic way.

In their paper [5], motivated by the contact geometric structure in thermodynamics, V. Klika, M. Pavelka, P. Vágner, and M. Grmela present an approach to multilevel modeling based on the recognition that the state variables and their conjugate variables are independent. That procedure is called Dynamic MaxEnt, and demonstrated on various examples from continuum physics such as hyperbolic heat conduction and magnetohydrodynamics.

In the paper 'A Fourth Order Entropy Stable Scheme for Hyperbolic Conservation Laws' [6], Xiaohan Cheng presents the development of a numerical procedure with fourth order accuracy in order to solve hyperbolic system of partial differential equations of conservative form, for one-dimensional situations. Here, the novelty is to endow great importance for the entropy balance equation in updating the state variables, thus the numerical compatibility with the second law of thermodynamics is ensured. Its efficiency is demonstrated on several examples, e.g., on shock tubes and on the nonlinear Burgers equation.

In the paper [7], Ou, Yokoi and Abe note a possible diversity of baths in quantum thermodynamics. They discuss the isoenergetic processes in terms of the concept of weak invariants, where the time-dependent Hamiltonian is a weak invariant associated with a relevant master equation. In particular, they analyze as an explicit example the finite-time isoenergetic process of the nonequilibrium dissipative system of the Pauli spin in a varying external magnetic field based on the Lindblad master equation.

Acknowledgments: We would like to express our gratitude to the Editorial Board of Entropy for they helpful attitude and also to the Authors who made this Special Issue successful.

Conflicts of Interest: The authors declare no conflict of interest.



References

1. Kaniadakis, G.; Scarfone, A.M. Classical Model of Quons. *Entropy* **2019**, *21*, 841. [[CrossRef](#)]
2. Eriksson, K.-E.; Lindgren, K. Statistics of the Bifurcation in Quantum Measurement. *Entropy* **2019**, *21*, 834. [[CrossRef](#)]
3. Kovács, R. On the Rarefied Gas Experiments. *Entropy* **2019**, *21*, 718. [[CrossRef](#)]
4. Treumann, R.A.; Baumjohann, W. A Note on the Entropy Force in Kinetic Theory and Black Holes. *Entropy* **2019**, *21*, 716. [[CrossRef](#)]
5. Klika, V.; Pavelka, M.; Vágner, P.; Grmela, M. Dynamic Maximum Entropy Reduction. *Entropy* **2019**, *21*, 715. [[CrossRef](#)]
6. Cheng, X. A Fourth Order Entropy Stable Scheme for Hyperbolic Conservation Laws. *Entropy* **2019**, *21*, 508. [[CrossRef](#)]
7. Ou, C.; Yokoi, Y.; Abe, S. Spin Isoenergetic Process and the Lindblad Equation. *Entropy* **2019**, *21*, 503. [[CrossRef](#)]



© 2020 by the authors. Licensee MDPI, Basel, Switzerland. This article is an open access article distributed under the terms and conditions of the Creative Commons Attribution (CC BY) license (<http://creativecommons.org/licenses/by/4.0/>).

Classical Model of Quons

Giorgio Kaniadakis ^{1,*}  and Antonio M. Scarfone ² 

¹ Dipartimento di Scienza Applicata e Tecnologia, Politecnico di Torino, Corso Duca degli Abruzzi 24, 10129 Torino, Italy

² Istituto dei Sistemi Complessi, Consiglio Nazionale delle Ricerche (ISC-CNR), c/o Politecnico di Torino, Corso Duca degli Abruzzi 24, 10129 Torino, Italy

* Correspondence: giorgio.kaniadakis@polito.it; Tel.: +39-011-090-7331

Received: 29 July 2019; Accepted: 24 August 2019; Published: 27 August 2019

Abstract: By using the kinetic interaction principle, the quons statistics in the framework of kinetic theory is introduced. This is done by properly generalizing the inclusion/exclusion principle of standard boson and fermion statistics within a nonlinear classical model. The related nonlinear Fokker-Planck equation is introduced and the corresponding steady distribution describing quons statistics of type I and type II is derived.

Keywords: classical model of boson and fermion statistics; inclusion/exclusion principle; nonlinear Fokker-Planck equation; type I quon statistics; type II quon statistics

1. Introduction

As is well known, one of the most fundamental theorems in quantum field theory and in quantum statistical mechanics, at the basis of many physical and chemical phenomena, is the spin-statistics theorem stated by Pauli [1,2].

This theorem fixes the statistical behavior of a many-body quantum system according to its spin. Bosons are integer spin particles whose creation and annihilation operators obey bilinear commutation relations. Their many-body wave function is symmetrical and the occupation number of particle in a given state is unlimited. On the opposite side, fermions are half-integer spin particles whose creation and annihilation operators obey bilinear anti-commutation relations. Their many-body wave function is anti-symmetric and the occupation number of the particle in a given state can never exceed the unity.

Experimental tests [3–5] have placed a straight limit to the possible violations of this theorem so that, today, it is widely accepted that elementary particles can be only bosons or fermions.

However, statistical deviations from bosons or fermions can be observed in quasi-particle excitations that occur in various condensed matter systems. Therefore, the study of physical systems that obey non-conventional statistics is one of the pillars of contemporary statistical physics [6–12]. Their interest spans from the theoretical foundation of generalized statistical mechanics [13,14], Fermi gas superfluid [15], high-temperature gas [16] and high- T_c superconductivity [17], Laughlin particle with fractional charge related to fractional quantum Hall effect [18,19], Josephson junctions [20] and applications to quantum computation [21,22].

Basically, there are two different approaches to introduce non-conventional statistics. The first one is by modifying the bilinear algebraic relation between creation and annihilation operators and therefore the exchange factor between permuted particles. The second is by modifying the number of possible ways to put particles in a collection of single-particles state.

Within the first method we find: parastatistics [23], obtained by generalizing, respectively, the bilinear commutative and anti-commutative relation of creation annihilation operators in trilinear relation for para-Boson and para-Fermion; quons statistics of type I [24,25], with asymmetric q -numbers and type II [26,27], with symmetric q -numbers, obtained in the framework of q -deformed

harmonic oscillator based on q -calculus [28]; fractional statistics of anyons [29–31] that are topological bi-dimensional quasi-particles derived in the framework of quantum groups arising from the study of quantum integrable systems and Yang-Baxter equation; Majorana fermions quasiparticles [32]; and Gentilionic statistics [33], obtained by using the permutation group theory with the indistinguishability principle of identical particles in the framework of non relativistic quantum mechanics.

Differently, within the second approaches we find: Haldane-Wu statistics [34,35], including semion [36], obtained by generalizing Pauli exclusion principle; intermediate statistics by Gentile [37], derived in a thermodynamical context by assuming that the maximum occupation particle number of an energy level is between one (standard fermions) and infinity (standard bosons); and more recently the interpolating boson-fermion statistics [38–42], used to study non relativistic quantum systems that obey to a generalized inclusion/exclusion principle, obtained by modifying the dependency of the transition probability from the occupation particle number of the starting and the arriving site [43,44].

In this paper, we propose an algebraic approach to introduce non-conventional statistics within a semiclassical kinetic framework. Following the kinetic interaction principle proposed in [43], which fixes the form of the transition probability $\pi(t, v_i \rightarrow v_{i+1})$ in such a way to take into account its dependence on the particle population of the starting site $a(f_i)$ and of the arrive site $b(f_{i+1})$, we obtain a nonlinear Fokker-Planck equation describing the particle evolution.

In standard boson and fermion statistics, the inclusion/exclusion principle is taken into account by the relation

$$b(f) \mp a(f) = 1. \tag{1}$$

In fact, when, $a(f) = f$ is fixed, it follows $b(f) = 1 \pm f$, and the Bose (+) and Fermi (-) factors are obtained.

The relation (1) can be generalized in

$$b(f) \oplus a(f) = 1, \tag{2}$$

where $x \oplus y$ is a deformed composition law, depending on a deformation parameter ξ , and is reduced to the standard sum and subtraction in a suitable limit $\xi \rightarrow \xi_0$. Equation (2) defines the functional dependence between $a(f)$ and $b(f)$, and fixes the steady particle distribution. The relationship between the generalized composition law $x \oplus y$ and the induced statistics is the main goal of this work.

The plane of the paper is as follows. In the next Section 2, we briefly recall the kinetic interaction principle used to introduce the nonlinear Fokker-Planck equation governing the time evolution of the particles system toward the equilibrium. Section 3 contains our main result. Non-conventional statistics are introduced by means of a generalized composition law between the functions $a(f)$ and $b(f)$, which introduces nonlinear terms in the Fokker-Planck equation and then modifies substantially its steady state solution. Several well known statistics can be easily derived within this algebraic approach and new statistics can be obtained through the introduction of suitable composition laws. This is discussed in the subsequent Sections 4 and 5, which introduce, within the present formalism, type II quons statistics and type I quons statistics, respectively. In the last Section 6 we report our conclusions.

2. The Exclusion-Inclusion Principle

Let us consider a classical stochastic Markovian process in the n -dimensional velocity space. It is described by the distribution function $f \equiv f(t, v)$ which obeys the Pauli master equation

$$\frac{\partial f}{\partial t} = \int \left[\pi(t, v' \rightarrow v) - \pi(t, v \rightarrow v') \right] d^n v'. \tag{3}$$

According to the kinetic interaction principle the transition probability $\pi(t, v \rightarrow v')$, from the site v to the site v' , can be written in

$$\pi(t, v \rightarrow v') = W(t; v, v') a(f(v)) b(f(v')). \tag{4}$$

This quantity defines a special interaction between the particles of the system that involve, separately and/or together, the two-particle bunches entertained at the start and arrival sites. It is factorized into the product of three terms. The first term $W(t; v, v')$ is the transition rate that depends on the nature of the interaction between the particles and the bath, and is a velocity function of the starting v and arrival v' sites. The second factor $a(f) \equiv a(f(v))$ is an arbitrary function of the particle population of the starting site and satisfies the condition $a(0) = 0$ because, if the initial site is empty, the transition probability is equal to zero. Without loss of generality, we can always impose on $a(f)$ the further condition $a(1) = 1$ by re-scaling the function $a(f)$ and opportunely redefining the quantity $W(t; v, v')$. The last factor $b(f) \equiv b(f(v))$ is an arbitrary function of the arrival site population and satisfies the condition $b(0) = 1$ since the transition probability does not depend on the arrival site if, in it, particles are absent. The expression of the function $b(f)$ plays a very important role as it allows us to introduce a sort of inclusion/exclusion effect in the system stimulating or inhibiting the transition to the arrival site, as a consequence of the interactions originated from collective effects.

Accounting for Equation (4), by using the Kramer-Moyal expansion, the Pauli master equation can be transformed in the following Fokker-Planck equation

$$\frac{\partial f}{\partial t} = \nabla \cdot \left[D a(f) b(f) \nabla \left(\beta U + \ln \frac{a(f)}{b(f)} \right) \right], \tag{5}$$

where $\nabla \equiv (\partial/\partial v_1, \dots, \partial/\partial v_n)$ is the gradient operator in the velocity space, D is the diffusion coefficient, $\beta = 1/k_B T$ the inverse temperature and $U = \frac{1}{2} m v^2$ is the single particle kinetic energy.

Equation (5) can be rewritten in

$$\frac{\partial f}{\partial t} = \nabla \cdot \left(D m \beta \gamma(f) v + D \Omega(f) \nabla f \right), \tag{6}$$

where

$$\gamma(f) = a(f) b(f), \tag{7}$$

affects the drift current $j_{\text{drift}} = D m \beta \gamma(f) v$, while

$$\Omega(f) = b(f) \frac{\partial a(f)}{\partial f} - a(f) \frac{\partial b(f)}{\partial f}, \tag{8}$$

models the diffusion current $j_{\text{diff}} = D \Omega(f) \nabla f$. The functions $\gamma(f)$ and $\Omega(f)$ are scalar quantities depending only on $f(t, v)$. In this way, both drift and diffusion current depend, in a nonlinear manner, on the distribution function through the population of the starting and arrival site.

The stationary distribution of the system described by Equation (5) follows from the condition

$$\frac{\partial f}{\partial t} = 0, \tag{9}$$

that, without loss of generality, implies the relation

$$\beta U + \ln \frac{a(f)}{b(f)} = \beta \mu, \tag{10}$$

where μ is a constant. This last, can be rewritten in

$$\frac{a(f)}{b(f)} = e^{-\epsilon} . \tag{11}$$

which defines implicitly the statistical distribution of the steady state of the system, where $\epsilon = \beta(U - \mu)$, with μ the chemical potential fixed by the normalization of the distribution function.

As well known, Fokker-Planck equation (5) is strictly related to a generalized entropic form, as discussed in [43], so that the steady state obtained from Equation (11) can also be obtained starting from an optimizing program performed to the corresponding entropic form.

3. Generalized Exclusion-Inclusion Principle

The kinetics of already known statistics can be derived from ansatz (4) by choosing opportunely the functions $a(f)$ and $b(f)$. For instance, the bosons and fermions statistics follow, in the quasi-classical picture, by posing

$$a(f) = f , \tag{12}$$

$$b(f) = 1 \pm f . \tag{13}$$

The corresponding Fokker-Planck equation for quasi-classical Bose and Fermi particles reads

$$\frac{\partial f}{\partial t} = \nabla \cdot (D m \beta f (1 \pm f) v + D \nabla f) , \tag{14}$$

that describes a drift-diffusion process with a constant diffusive current, being $\Omega(f) = 1$, and a nonlinear drift term. The corresponding steady state

$$f(\epsilon) = \frac{1}{e^\epsilon \mp 1} , \tag{15}$$

follows by solving Equation (11) with the position (12) and (13).

To go one step further and introduce more general statistics, let us observe that Equation (13) actually may be rewritten in the two equivalent forms

$$b(f) = 1 \pm a(f) , \tag{16}$$

or, alternatively

$$b(f) = a(1 \pm f) . \tag{17}$$

However, it is easy to see that, although both of these formulations are equivalent for $a(f) = f$, for another choice of $a(f)$ different from the identity, Equations (16) and (17) in general do not coincide.

To overcome this problem and have a consistent relationship between the functions $a(f)$ and $b(f)$, we introduce a generalized operation $x \oplus y$ to denote a new composition law between real numbers, hereinafter named deformed sum. It depends on a deformation parameter ζ such that the generalized sum \oplus reduces to the ordinary sum $+$ in a suitable limit $\zeta \rightarrow \zeta_0$, that is $x \oplus y \rightarrow x + y$.

Reasonably, a deformed sum $x \oplus y$ should preserve the main proprieties of standard sum like commutativity, $x \oplus y = y \oplus x$; associativity $x \oplus (y \oplus z) = (x \oplus y) \oplus z$; the existence of neutral element $x \oplus 0^* = 0^* \oplus x = x$; the opposite $x \oplus \bar{x} = \bar{x} \oplus x = 0^*$, where, in general, $0^* \neq 0$ and $\bar{x} \neq -x$. Equipped with these properties, the algebraic structure $\mathcal{A} \equiv (\oplus : \mathfrak{R} \times \mathfrak{R} \rightarrow \mathfrak{R})$ forms an Abelian group.

In this way, a deformed subtraction can be introduced as the inverse operation of the deformed sum, that is $x \ominus y \equiv x \oplus \bar{y}$.

Within the algebra \mathcal{A} , we can generalize Equations (16) and (17) in

$$b(f) = 1 \oplus a(f), \tag{18}$$

$$b(f) = a(c \pm f), \tag{19}$$

where c is a constant depending on the deformation parameter that must reduce to the identity in the $\xi \rightarrow \xi_0$ limit.

Consistently, by requiring that both Equations (18) and (19) define the same function $b(f)$ for any choice of $a(f)$, we obtain the following functional equation

$$1 \oplus a(f) = a(c \pm f). \tag{20}$$

Thus, the generalized composition \oplus fixes univocally the function $a(f)$. In fact, by posing

$$x \oplus y = a \left(a^{-1}(x) \pm a^{-1}(y) \right), \tag{21}$$

we easily realize that Equations (18) and (19) coincide each to the other whenever we choose $c = a^{-1}(1)$.

According to definition (21), the neutral element is given by $0^* \equiv a(0)$ while the opposite is $\bar{x} \equiv a(-a^{-1}(x))$.

Clearly, Equation (20) imposes $a(f)$, and then $b(f)$, to depend on the deformation parameter too so that, as expected in the $\xi \rightarrow \xi_0$ limit, these functions behave like $a(f) \rightarrow f$ and $b(f) \rightarrow 1 \pm f$, respectively.

Notice also that ansatz (21) requires that $a(x)$ be a monotonic, and then invertible, function at least in the range $[0, 1]$ of a distribution function.

Based on the algebra \mathcal{A} , we can introduce several relevant generalized functions. Among them, the generalized exponential $E(x) \in \mathfrak{R}^+$, defined in

$$E(x) = \exp \left(a^{-1}(x) \right), \tag{22}$$

that satisfies the relation

$$E(x \oplus y) = E(x) E(y), \tag{23}$$

as well as its inverse function, the generalized logarithm $L(x)$ for $x \in \mathfrak{R}^+$, with $L(E(x)) = E(L(x)) = x$, defined in

$$L(x) = a \left(\ln(x) \right), \tag{24}$$

that satisfies the dual relation

$$L(x y) = L(x) \oplus L(y). \tag{25}$$

In the $\xi \rightarrow \xi_0$ limit, in which \oplus reduces to the standard sum, both the functions $E(x)$ and $L(x)$ reduce to the standard exponential and logarithm, respectively and Equations (23) and (25) reproduce the well know algebraic relation of standard exponential and logarithm functions.

4. Type II Quons

Within the formalism introduced above, let us now derive some statistics starting from deformed algebras already proposed in literature.

To start with, let us consider the κ -sum [43] defined in

$$x \oplus y = x \sqrt{1 + \kappa^2 y^2} + y \sqrt{1 + \kappa^2 x^2}, \tag{26}$$

whose deformation parameter $\zeta \equiv \kappa$ is limited to $|\kappa| \leq 1$ and the κ -sum recovers the standard sum in the $\kappa \rightarrow 0$ limit.

The above κ -sum is the momenta relativistic additivity law of special relativity and plays a central role in the construction of κ -statistical mechanics [45].

According to Equation (21), the function $a(x)$ should be determined from the relation

$$a^{-1}(x \oplus y) = a^{-1}(x) + a^{-1}(y). \tag{27}$$

In order to solve this functional equation we use the following identity

$$x = \frac{1}{\kappa} \sinh(\operatorname{arcsinh}(\kappa x)), \tag{28}$$

in the r.h.s. of Equation (26) that becomes

$$\begin{aligned} x \oplus y &= \frac{1}{\kappa} \sinh(\operatorname{arcsinh}(\kappa x)) \sqrt{1 + (\sinh(\operatorname{arcsinh}(\kappa y)))^2} \\ &\quad + \frac{1}{\kappa} \sinh(\operatorname{arcsinh}(\kappa y)) \sqrt{1 + (\sinh(\operatorname{arcsinh}(\kappa x)))^2} \\ &= \frac{1}{\kappa} \sinh(\operatorname{arcsinh}(\kappa x)) \cosh(\operatorname{arcsinh}(\kappa y)) + \frac{1}{\kappa} \sinh(\operatorname{arcsinh}(\kappa y)) \cosh(\operatorname{arcsinh}(\kappa x)) \\ &= \frac{1}{\kappa} \sinh(\operatorname{arcsinh}(\kappa x) + \operatorname{arcsinh}(\kappa y)). \end{aligned} \tag{29}$$

This means that

$$\operatorname{arcsinh}(\kappa(x \oplus y)) = \operatorname{arcsinh}(\kappa x) + \operatorname{arcsinh}(\kappa y). \tag{30}$$

which forces us to define

$$a^{-1}(x) = \frac{1}{\kappa} \operatorname{arcsinh}(\kappa x) \Rightarrow a(x) = \frac{\sinh(\kappa x)}{\kappa}. \tag{31}$$

It is worth observing that function $a(x)$, derived in our approach within the κ -algebra, has already been studied in literature starting from [26,27] where quon statistics of type II has been introduced from a Hermitian version of the q -oscillator algebra of creation and annihilation operators.

In fact, recalling that algebra of type II quons is based on the symmetric q -numbers

$$[x] = \frac{q^x - q^{-x}}{q - q^{-1}}, \tag{32}$$

which are invariant under the exchange $q \rightarrow 1/q$; it is easy to verify as definition (32) is related to function (31) according to

$$[x] = \frac{a(x)}{a(1)}. \tag{33}$$

with $\kappa = \ln q$.

Within the κ -algebra the generalized exponential reads $E(x) \equiv \exp_{\kappa}(x)$ and analogously the generalized logarithm reads $L(x) \equiv \ln_{\kappa}(x)$, where

$$\exp_{\kappa}(x) = \left(\sqrt{1 + \kappa^2 x^2} + \kappa x \right)^{1/\kappa}, \tag{34}$$

$$\ln_{\kappa}(x) = \frac{x^{\kappa} - x^{-\kappa}}{2\kappa}, \tag{35}$$

and fulfill relations (23) and (25), respectively, with the κ -sum given in (26).

The deformed-subtraction is given in

$$x \ominus y \equiv x \sqrt{1 + \kappa^2 y^2} - y \sqrt{1 + \kappa^2 x^2}, \tag{36}$$

being, in this case, $0^* \equiv 0$ and $\bar{x} \equiv -x$.

The function $a(f)$ given in Equation (31) defines univocally the function $b(f)$ throughout Equations (18) or (19) with $c = \operatorname{arcsinh}(\kappa) / \kappa$.

Therefore, the nonlinear kinetic underling type II quons statistics is depicted by a linear Fick diffusive current

$$j_{\text{diff}} = D \nabla f, \tag{37}$$

with a constant diffusive coefficient. In fact, it is straightforward to verify from Equation (8) that in this case $\Omega = 1$ [46]. Thus, like standard bosons and fermions, type II quons also undergo classical diffusion process governed by a linear diffusion current.

The corresponding nonlinear Fokker-Planck equation becomes

$$\frac{\partial f}{\partial t} = \nabla \left(D m \beta \gamma(f) v + D \nabla f \right), \tag{38}$$

where

$$\gamma(f) = \gamma_+ e^{2\kappa f} + \gamma_- e^{-2\kappa f} + \gamma_0, \tag{39}$$

with

$$\gamma_+ = \frac{\pm \sqrt{1 + \kappa^2} + \kappa}{4\kappa^2}, \quad \gamma_- = \frac{\pm \sqrt{1 + \kappa^2} - \kappa}{4\kappa^2}, \quad \gamma_0 = -\gamma_+ - \gamma_-. \tag{40}$$

The steady state follows from Equation (11), that in this case reads

$$\frac{\sinh(\kappa f)}{\sinh(\operatorname{arcsinh}(\kappa) \pm \kappa f)} = e^{-\epsilon}, \tag{41}$$

that solved for $f(\epsilon)$ gives

$$f(\epsilon) = \frac{1}{\kappa} \operatorname{arctanh} \left(\frac{\kappa}{e^\epsilon \mp \sqrt{1 + \kappa^2}} \right). \tag{42}$$

As easy check, in the $\kappa \rightarrow 0$ limit, functions $a(f)$ and $b(f)$ reduce to the one of standard bosons and fermions (12) and (13), as well as the nonlinear Fokker-Planck equation (38) reduces to Equation (14) and, in the same limit, the steady state (42) reproduces distribution (15).

5. Type I Quons

As known, type I quons firstly studied in [23], are based on the asymmetric version of q -numbers

$$[x]_q = \frac{q^x - 1}{q - 1}, \tag{43}$$

that is strictly related to the q -calculus introduced by Jackson [28]. In the present context, type I quons can be derived starting from the following deformed sum

$$x \oplus y = x + y + (q - 1) x y, \tag{44}$$

emerging also in the context of generalized statistical mechanics [47]. The deformation parameter $\xi \equiv q$, is restricted to $q \geq 0$ and the q -sum recovers the standard sum in the $q \rightarrow 1$ limit.

Equation (44) can be rewritten in

$$x \oplus y = \frac{[1 + (q - 1)x][1 + (q - 1)y] - 1}{q - 1}, \tag{45}$$

so that

$$1 + (q - 1)(x \oplus y) = [1 + (q - 1)x][1 + (q - 1)y], \tag{46}$$

which forces us to define the quantity

$$a^{-1}(x) = \frac{1}{\ln q} \ln(1 + (q - 1)x), \tag{47}$$

and its inverse $a(x)$ coincides with function defined in Equation (43), that is

$$a(x) \equiv [x]_q. \tag{48}$$

Asymmetric q -numbers have been employed in [23–25] to introduce quon statistics of type I starting from the q -generalization of the quantum oscillator algebras of creation and annihilation operators, like for the type II.

However, the algebra of asymmetric q numbers differs from those of the symmetric one since

$$[\bar{x}]_q = -q^{-x} [x]_q, \tag{49}$$

being, in general $0^* = 0$ and

$$\bar{x} = -\frac{x}{1 + (q - 1)x}, \tag{50}$$

that is, the opposite in $\mathcal{A} \equiv (\oplus_q, \mathfrak{R})$ does not coincides with the opposite of the ordinary algebras in \mathfrak{R} like in the symmetric case.

Within the q -algebra the generalized exponential reads $E(x) \equiv \exp_q(x)$ and analogously the generalized logarithm reads $L(x) \equiv \ln_q(x)$ where

$$\exp_q(x) = (1 + (q - 1)x)^{1/\ln q}, \tag{51}$$

$$\ln_q(x) = \frac{q^{\ln x} - 1}{q - 1}, \tag{52}$$

that are strictly related to the q -exponential and q -logarithm introduced in the generalized statistical mechanics [47] and fulfill relations (23) and (25), respectively, with the q -sum given in (44).

The function $a(f)$ given in Equation (48) defines univocally the function $b(f)$ throughout Equations (18) or (19) with $c = 1$. However, in this case due to relation (49), we must separate the case of boson-like quons, with

$$b(f) = 1 + q [f]_q, \tag{53}$$

from the case of fermion-like quons, with

$$b(f) = 1 - q^{1-f} [f]_q. \tag{54}$$

5.1. Bosons-Like Quons

The kinetic of boson-like quons is depicted by the nonlinear Fokker-Planck equation

$$\frac{\partial f}{\partial t} = \nabla \left(D m \beta \gamma_{\text{Bose}}(f) v + D \Omega_{\text{Bose}}(f) \nabla f \right), \tag{55}$$

with a nonlinear drift term

$$\gamma_{\text{Bose}}(f) = \gamma_2 q^{2f} + \gamma_1 q^f + \gamma_0, \tag{56}$$

where

$$\gamma_2 = \frac{q}{(q-1)^2}, \quad \gamma_1 = -\frac{1+q}{(q-1)^2}, \quad \gamma_0 = -\gamma_2 - \gamma_1, \tag{57}$$

and a nonlinear diffusive term

$$\Omega_{\text{Bose}}(f) = \frac{\ln q}{q-1} q^f, \tag{58}$$

that reduces to a constant $\Omega_{\text{Bose}}(f) \rightarrow 1$ in the $q \rightarrow 1$ limit. Therefore, differently from the symmetric case, Boson-like type I quons undergo classical diffusive process governed by a nonlinear diffusion current.

The steady state classical Boson-like quons follows from Equation (11) that in this case reads

$$\frac{q^f - 1}{q^{1+f} - 1} = e^{-\epsilon}, \tag{59}$$

that solved for $f(\epsilon)$ gives

$$f_{\text{Bose}}(\epsilon) = \frac{1}{\ln q} \ln \frac{e^\epsilon - 1}{e^\epsilon - q}. \tag{60}$$

As expected, in the $q \rightarrow 1$ limit, the steady state of the Boson-like quons (60) reduces to the stationary distribution of bosons.

5.2. Fermions-Like Quons

The kinetic of fermion-like quons is depicted by the nonlinear Fokker-Planck equation

$$\frac{\partial f}{\partial t} = \nabla \left(D m \beta \gamma_{\text{Fermi}}(f) v + D \Omega_{\text{Fermi}}(f) \nabla f \right), \tag{61}$$

with a nonlinear drift term

$$\gamma_{\text{Fermi}}(f) = \gamma_+ q^f + \gamma_- q^{-f} + \gamma_0, \tag{62}$$

where

$$\gamma_+ = -\frac{1}{(q-1)^2}, \quad \gamma_- = -\frac{q}{(q-1)^2}, \quad \gamma_0 = -\gamma_+ - \gamma_-, \tag{63}$$

and a nonlinear diffusive term

$$\Omega_{\text{Fermi}}(f) = \omega_0 + \omega_+ q^f + \omega_- q^{-f}, \tag{64}$$

where

$$\omega_0 = \frac{2q \ln q}{(q-1)^2}, \quad \omega_+ = -\frac{\ln q}{(q-1)^2}, \quad \omega_- = -\frac{q \ln q}{(q-1)^2}. \quad (65)$$

and reduces to a constant $\Omega_{\text{fermi}}(f) \rightarrow 1$ in the $q \rightarrow 1$ limit. Again, type I quons undergo classical diffusive process governed by a nonlinear diffusion current.

The steady state now follows from relation

$$\frac{q^f - 1}{q^{1-f} - 1} = e^{-\epsilon}, \quad (66)$$

that solved for $f(\epsilon)$ gives

$$f_{\text{fermi}}(\epsilon) = \frac{1}{\ln q} \ln \left(\frac{1 - e^{-\epsilon}}{2} + \sqrt{\left(\frac{1 - e^{-\epsilon}}{2} \right)^2 + q e^{-\epsilon}} \right). \quad (67)$$

and reduces to the stationary distribution of fermion particles in the $q \rightarrow 1$ limit.

6. Conclusions

In this paper we have proposed an algebraic approach to study many body particle systems obeying a non-conventional statistics, in the semiclassical picture. A nonlinear Fokker-Planck equation, describing the kinetic of collectively interacting particles, has been obtained according to a kinetic interaction principle. The particle current is fixed by the two functions $a(f)$ and $b(f)$ that regulate the transition probability from the departing site to the arrival site in a way that depends only on the population of the initial and final sites, respectively. In this formalism, bosons-like and fermions-like particles follow from a very easy assumption on the function $a(f)$ and $b(f)$ by means of a generalized version of the inclusion/exclusion principle given by $b(f) \oplus a(f) = 1$, with $b(f) = a(c \pm f)$ for a generalized composition law that fixes the form of the functions $a(f)$, and then $b(f)$, and consequently fixes the steady particle distribution.

Following this approach, we have studied boson-like and fermion like quons of type II [26], whose underlying algebra is related with the generalized sum (26), as well as boson-like and fermion like quons of type I [13], whose underlying algebra is defined by the generalized sum (44). It has been shown that the kinetic of type II quons is described by a nonlinear Fokker-Planck equation with a nonlinear drift current and a linear diffusive current like in the case of standard Bose and Fermi particles; otherwise, the kinetic of type I quons is described by a nonlinear Fokker-Planck equation with a nonlinear drift current and a nonlinear diffusive current.

Finally, let us remark that, following the same approach described in this work, several non conventional statistics in the classical picture can be obtained employing different composition laws. For instance, in addition to the κ -sum and the q -sum studied in this paper, other examples can be found in the framework of the generalized statistical mechanics [48,49].

Author Contributions: The authors have equally contributed to the manuscript. They all have read and approved its final version.

Funding: This research received no external funding.

Conflicts of Interest: The authors declare no conflict of interest.

References

1. Pauli, W. The connection between spin and statistics. *Phys. Rev.* **1940**, *58*, 716–722. [CrossRef]
2. Luders, G.; Zumino, B. Connection between spin and statistics. *Phys. Rev.* **1958**, *110*, 1450–1453. [CrossRef]

3. Reines, F.; Sobel, H.W. Test of the Pauli exclusion principle for atomic electrons. *Phys. Rev. Lett.* **1974**, *32*, 954. [[CrossRef](#)]
4. Modugno, G.; Inguscio, M.; Tino, G.M. Search for small violations of the symmetrization postulate for spin-0 particles. *Phys. Rev. Lett.* **1998**, *81*, 4790–4793. [[CrossRef](#)]
5. VIP Collaboration. New experimental limit on the Pauli exclusion principle violation by electrons. *Phys. Lett. B* **2006**, *641*, 18–22. [[CrossRef](#)]
6. Campagnano, G.; Zilberberg, O.; Gornyi, I.V.; Feldman, D.E.; Potter, A.C.; Gefen, Y. Hanbury Brown–Twiss interference of anyons. *Phys. Rev. Lett.* **2012**, *109*, 106802. [[CrossRef](#)]
7. Shen, Y.; Ai, Q.; Long, G.L. The relation between properties of Gentile statistics and fractional statistics of anyon. *Physica A* **2010**, *389*, 1565–1570. [[CrossRef](#)]
8. Lavagno, A.; Swamy, P.N. Thermostatistics of deformed bosons and fermions. *Found. Phys.* **2009**, *40*, 814–828. [[CrossRef](#)]
9. Bagarello, F. Quons, coherent states and intertwining operators. *Phys. Lett. A* **2009**, *373*, 2637–2642. [[CrossRef](#)]
10. Kibler, M.R. Miscellaneous applications of quons. *SIGMA* **2007**, *3*, 092. [[CrossRef](#)]
11. El Baz, M.; Hassouni, Y. Deformed exterior algebra, quons and their coherent states. *Int. J. Mod. Phys. A* **2003**, *18*, 3015–3040. [[CrossRef](#)]
12. Greenberg, O.W.; Delgado, J.D. Construction of bosons and fermions out of quons. *Phys. Lett. A* **2001**, *288*, 139–144. [[CrossRef](#)]
13. Greenberg, O.W. Particles with small violations of Fermi or Bose statistics. *Phys. Rev. D* **1991**, *43*, 4111–4120. [[CrossRef](#)]
14. Acharya, R.; Swamy, P.N. Statistical mechanics of anyons. *J. Phys. A*, **1994**, *27*, 7247–7263. [[CrossRef](#)]
15. Truscott, A.G.; Strecker, K.E.; McAlexander, W.L.; Partridge, G.B.; Hulet R.G. Observation of Fermi pressure in a gas of trapped atoms. *Science* **2001**, *291*, 2570–2572. [[CrossRef](#)]
16. Algin, A.; Senay, M. High-temperature behavior of a deformed Fermi gas obeying interpolating statistics. *Phys. Rev. E* **2012**, *85*, 041123. [[CrossRef](#)]
17. Wilczek, F. (Ed.) *Fractional Statistics and Anyon Superconductivity*; World Scientific: Singapore, 1990.
18. Camino, F.E.; Zhou, W.; Goldman, V.J. Realization of a Laughlin quasiparticle interferometer: Observation of fractional statistics. *Phys. Rev. B* **2005**, *72*, 075342. [[CrossRef](#)]
19. Stern, A. Anyons and the quantum Hall effect—A pedagogical review. *Ann. Phys.* **2008**, *323*, 204–249. [[CrossRef](#)]
20. Ezawa, Z.F.; Iwazaki, A. Quantum Hall liquid, Josephson effect, and hierarchy in a double-layer electron system. *Phys. Rev. B* **1993**, *47*, 7295–7311. [[CrossRef](#)]
21. Kitaev, A.Y. Fault-tolerant quantum computation by anyons. *Ann. Phys.* **2003**, *303*, 2–30. [[CrossRef](#)]
22. Das Sarma, S.; Freedman S.M.; Nayak, C. Topologically protected qubits from a possible non-abelian fractional quantum Hall state. *Phys. Rev. Lett.* **2005**, *94*, 166802. [[CrossRef](#)]
23. Green, H.S. A Generalized Method of Field Quantization. *Phys. Rev.* **1953**, *90*, 270–273. [[CrossRef](#)]
24. Greenberg, O.W. Example of infinite statistics. *Phys. Rev. Lett.* **1990**, *64*, 705–708. [[CrossRef](#)]
25. Chaturvedi, S.; Kapoor, A.K.; Sandhya, R.; Srinivasan, V.; Simon, R. Generalized commutation relations for a single-mode oscillator. *Phys. Rev. A* **1991**, *43*, 4555–4557. [[CrossRef](#)]
26. Biedenharn, L.C. The quantum group $SU_q(2)$ and a q -analogue of the boson operators. *J. Phys. A* **1989**, *22*, L873–L878. [[CrossRef](#)]
27. Macfarlane, A.J. On q -analogues of the quantum harmonic oscillator and the quantum group $SU_q(2)$. *J. Phys. A* **1989**, *22*, 4581–4588. [[CrossRef](#)]
28. Jackson, F. q -Form of Taylor’s theorem. *Mess. Math.* **1909**, *38*, 57–61.
29. Leinaas, J.M.; Myrheim, J. On the theory of identical particles. *Il Nuovo Cim. B* **1977**, *37*, 1–23. [[CrossRef](#)]
30. Wilczek, F. Magnetic flux, angular momentum, and statistics. *Phys. Rev. Lett.* **1982**, *48*, 1144–1146. [[CrossRef](#)]
31. Lerda, A. *Anyons: Quantum Mechanics of Particles with Fractional Statistics*; Springer: Berlin/Heidelberg, Germany, 1992.
32. Carollo, A.; Spagnolo, B.; Valenti, D. Uhlmann curvature in dissipative phase transitions, *Sc. Rep. Nat.* **2018**, *8*, 9852.
33. Cattani M.; Fernandes, N.C. Baryon states as colorspinors in gentilionic statistics. *Phys. Lett. A* **1987**, *124*, 229–232. [[CrossRef](#)]

34. Haldane, F.D.M. "Spinon gas" description of the $S = 1/2$ Heisenberg chain with inverse-square exchange: Exact spectrum and thermodynamics. *Phys. Rev. Lett.* **1991**, *66*, 1529–1532. [[CrossRef](#)]
35. Wu, Y.S. Statistical distribution for generalized ideal gas of fractional-statistics particles. *Phys. Rev. Lett.* **1994**, *73*, 922–925. [[CrossRef](#)] [[PubMed](#)]
36. Chaturvedi, S.; Srinivasan, V. Microscopic interpretation of Haldane's semion statistics. *Phys. Rev. Lett.* **1997**, *78*, 4316–4319. [[CrossRef](#)]
37. Gentile, G., Jr. Osservazioni sopra le statistiche intermedie. *Nuovo Cim.* **1940**, *17*, 493–497 [[CrossRef](#)]
38. Kaniadakis, G.; Quarati, P. Classical model of bosons and fermions. *Phys. Rev. E* **1994**, *49*, 5103–5110. [[CrossRef](#)] [[PubMed](#)]
39. Toscani, G. Finite time blow up in Kaniadakis-Quarati model of Bose Einstein particles. *Commun. Part. Differ. Equ.* **2011**, *37*, 77–87. [[CrossRef](#)]
40. Carrillo, J.A.; Hopf, K.; Wolfran, M-T. Numerical study of Bose-Einstein condensation in the Kaniadakis-Quarati model for bosons. *arXiv* **2019**, arXiv:1902.06266.
41. Carrillo, J.A.; Hopf, K.; Rodrigo, J.L. On the singularity formation and relaxation to equilibrium in 1D Fokker-Planck model with superlinear drift. *arXiv* **2019**, arXiv:1901.11098.
42. Kaniadakis, G.; Hristopoulos, D.T. Nonlinear kinetics on lattices based on the kinetic interaction principle. *Entropy* **2018**, *20*, 426. [[CrossRef](#)]
43. Kaniadakis, G. Non-linear kinetics underlying generalized statistics. *Physica A* **2001**, *296*, 405–425. [[CrossRef](#)]
44. Kaniadakis, G.; Quarati, P.; Scarfone, A.M. Kinetical foundations of non-conventional statistics. *Physica A* **2001**, *305*, 76–83. [[CrossRef](#)]
45. Kaniadakis, G. Relativistic entropy and related Boltzmann kinetics. *Eur. Phys. J. A* **2009**, *40*, 275–287. [[CrossRef](#)]
46. Kaniadakis, G.; Lavagno, A.; Quarati, P. Kinetic model for q -deformed bosons and fermions. *Phys. Lett. A* **1997**, *227*, 227–231. [[CrossRef](#)]
47. Tsallis, C. *Introduction to Nonextensive Statistical Mechanics*; Springer: New York, NY, USA, 2009.
48. El Kaabouchi, A.; Nivanen, L.; Wang, Q.A.; Badiali, J.P.; Le Méhauté, A. A mathematical structure for the generalization of conventional algebra. *Cent. Eur. J. Phys.* **2009**, *7*, 549–554. [[CrossRef](#)]
49. Scarfone, A.M. Entropic forms and related algebras. *Entropy* **2013**, *15*, 624–649. [[CrossRef](#)]



© 2019 by the authors. Licensee MDPI, Basel, Switzerland. This article is an open access article distributed under the terms and conditions of the Creative Commons Attribution (CC BY) license (<http://creativecommons.org/licenses/by/4.0/>).

Statistics of the Bifurcation in Quantum Measurement

Karl-Erik Eriksson and Kristian Lindgren * 

Complex Systems Group, Department of Space, Earth and Environment, Chalmers University of Technology, SE-412 96 Gothenburg, Sweden

* Correspondence: kristian.lindgren@chalmers.se

Received: 29 June 2019; Accepted: 24 August 2019; Published: 26 August 2019

Abstract: We model quantum measurement of a two-level system μ . Previous obstacles for understanding the measurement process are removed by basing the analysis of the interaction between μ and the measurement device on quantum field theory. This formulation shows how inverse processes take part in the interaction and introduce a non-linearity, necessary for the bifurcation of quantum measurement. A statistical analysis of the ensemble of initial states of the measurement device shows how microscopic details can influence the transition to a final state. We find that initial states that are efficient in leading to a transition to a final state result in either of the expected eigenstates for μ , with ensemble averages that are identical to the probabilities of the Born rule. Thus, the proposed scheme serves as a candidate mechanism for the quantum measurement process.

Keywords: quantum measurement; scattering theory; statistics; Born's rule

1. Introduction

Quantum mechanics is at the basis of all modern physics and fundamental for the understanding of the world that we live in. As a general theory, quantum mechanics should apply also to the measurement process. From the general experience of non-destructive measurements, we draw conclusions about the interaction between the observed system and the measurement apparatus and how this can be described within quantum mechanics.

We thus consider a quantum system μ , interacting with a measurement device. For simplicity we assume that μ is a two-level system that is not destroyed in the process. Then after the measurement, μ ends up in one of the eigenstates of the measured observable. If μ is prepared in one of these eigenstates, it remains in that state after the measurement. If μ is initially in a superposition of the two eigenstates, it still ends up in one of the eigenstates and the measurement result is the corresponding eigenvalue. The probability for a certain outcome is the squared modulus of the corresponding state component in the superposition (Born's rule).

An essential question is whether the probabilistic nature of quantum measurement with Born's rule is an inherent feature of quantum mechanics or whether it can be shown to hold as a result of a quantum-mechanical treatment of the measurement process combined with a statistical analysis. In the latter case, a single measurement would be a quantum-mechanical process in which the state of the measurement apparatus (possibly including its surroundings) determines the result. Born's rule would then emerge from the statistics of the ensemble that describes the measurement apparatus in interaction with the system subject to measurement.

The requirement that μ , if initially in an eigenstate of the observable, remains in that eigenstate after interacting with the apparatus, is usually considered to lead to a well-known dilemma: If applying the (linear) quantum mechanics of the 1930s to μ in an initial superposition of those eigenstates, the result of the process appears to be a superposition of the two possible resulting states for μ and the apparatus without any change in the proportions between the channels. This has been referred to as von Neumann's dilemma [1], and it has led to paradoxical conclusions such as Schrödinger's cat.

Attempts to get around this problem include Everett's relative-state formulation [2] and its continuation in DeWitt's many-worlds interpretation [3] as well as non-linear modifications of quantum mechanics [4–8]. In the non-linear modifications, one gets the bifurcation of the measurement process but the non-linear character of the basic theory introduces new conceptual difficulties. Mathematically our treatment can be seen to be very close to quantum diffusion [5]; we have chosen to follow the same conventions in handling the statistics of stochastic variables as in Ref. [5]. The ambition to understand quantum measurement as a deterministic process we share with the De Broglie-Bohm theory [9], with the difference that we look for how details in the measurement device influence the process.

Bell pointed out that the Everett-DeWitt theory does not properly reflect the fact that the presence of inverse processes and interference are inherent features of quantum mechanics [10]:

Thus, DeWitt seems to share our idea that the fundamental concepts of the theory should be meaningful on a microscopic level and not only on some ill-defined macroscopic level. However, at the microscopic level there is no such asymmetry in time as would be indicated by the existence of branching and the non-existence of debranching. [...] [I]t even seems reasonable to regard the coalescence of previously different branches, and the resulting interference phenomena, as the characteristic feature of quantum mechanics. In this respect an accurate picture, which does not have any tree-like character, is the 'sum over all possible paths' of Feynman.

Therefore, as suggested by Bell, we investigate work of Feynman for a correct theory. We choose the scattering theory of quantum field theory, including Feynman diagrams, as a basis for our description of the measurement process. This theory contains inverse processes that result in a non-linear dependence on the initial state which removes the von Neumann dilemma.

In the field of investigation of the measurement process, a strong belief has been established that microscopic details of the measurement interaction cannot lead to the bifurcation determining the result of measurement (see, e.g., [11,12]). This belief is based on von Neumann's way of handling linear quantum mechanics. In this situation, many have abandoned the ambition to understand the mechanism of a single measurement and concentrated on the full ensemble of measurements. There one has studied the irreversible decoherence process that takes the initial ensemble, with μ in a pure state, into a mixed state for the final ensemble after measurement. Since 1970, the year of DeWitt's many-worlds theory [3] and Zeh's paper on decoherence [11], a new tradition has developed that includes different views on how to interpret quantum mechanics, see for instance Refs. [13,14]. Epistemological aspects play an important role in these interpretations.

Our idea is that the microscopic details of the measurement apparatus affect the process so that it takes μ into either of the eigenstates of the measured observable and initiates a recording of the corresponding measurement result. This is possible to see in a more developed form of linear deterministic quantum mechanics, namely the scattering theory of quantum field theory.

The development of relativistic quantum mechanics led to quantum field theory. For a situation where a quantum system μ meets a part A of a measurement device, interacts with it and then leaves it, scattering theory can be an adequate description. As we have pointed out already, the scattering theory of quantum field theory has the reversibility that was requested by Bell. These are our reasons for the choice of studying measurement in the scattering theory of quantum field theory.

In our approach, measurement is part of the physics studied, rather than a subject for epistemological analysis. We show how non-linearities can be generated within quantum theory. Our statistical study of measurement processes then shows that those states of the apparatus which are competitive in leading to a final state, also take μ into *one* of the eigenstates of the measured observable. Moreover, this bifurcation, leading to one of the two possible final states for μ , occurs with the frequencies given by Born's rule.

In the following sections, we shall first give our scattering theory description and then make all possible processes subject to a statistical analysis.

2. The Initial Phase of Measurement as A Scattering Process

Here we study the interaction between the small system μ and a larger system A with a large number of degrees of freedom. The larger system is assumed to be characterized by an ensemble of possible *initial* microstates of A . We consider this interaction to be the first part of a measurement process.

Since we are dealing with a two-level system μ , the Pauli matrices provide a suitable formalism with $\sigma_3 = \begin{pmatrix} 1 & 0 \\ 0 & -1 \end{pmatrix}$ representing the observable to be measured, with eigenstates $|+\rangle_\mu = \begin{pmatrix} 1 \\ 0 \end{pmatrix}$ and $|-\rangle_\mu = \begin{pmatrix} 0 \\ 1 \end{pmatrix}$.

Let us investigate the characteristics of the interaction between μ and A in scattering theory for the case with A in a state with (unknown) microscopic details that are summarized in a variable α . We then denote the normalized initial state of A by $|0, \alpha\rangle_A$ (with 0 indicating a state of preparedness). This means that we assume α to represent one microstate in an ensemble of possible initial states.

A basic requirement is that if μ is initially in the state $|j\rangle_\mu$ ($j = +$ or $-$), after the interaction with A , its state remains the same. In this process A changes from the initial state $|0, \alpha\rangle_A$ to a final state $|j, \beta_j(\alpha)\rangle_A$, also normalized. The first j here indicates that A has been marked by the state $|j\rangle_\mu$ of μ . All other characteristics of the final state of A are collected in $\beta_j(\alpha)$. The interaction thus transforms the system A from an initial state of readiness, characterized by α , to a final state, marked by $|j\rangle_\mu$ and characterized by $\beta_j(\alpha)$.

For a general normalized state of μ , $|\psi\rangle_\mu = \psi_+ |+\rangle_\mu + \psi_- |-\rangle_\mu$ (with $|\psi_+|^2 + |\psi_-|^2 = 1$), the combined initial state of $\mu \cup A$ is

$$|\psi\rangle_\mu \otimes |0, \alpha\rangle_A = (\psi_+ |+\rangle_\mu + \psi_- |-\rangle_\mu) \otimes |0, \alpha\rangle_A . \tag{1}$$

A measurement of σ_3 on μ leads to a certain result. Since two different results are possible, the μA -interaction should in general result in a transition to one of the following states,

$$|+\rangle_\mu \otimes |+, \beta_+(\alpha)\rangle_A \quad \text{or} \quad |-\rangle_\mu \otimes |-, \beta_-(\alpha)\rangle_A . \tag{2}$$

The conclusion is then that the outcome must depend on the initial state of A , i.e., on α .

In scattering theory, the interaction between μ and A is characterized by a transition operator M , and this leads to the (non-normalized) final state (see Figure 1),

$$M |\psi\rangle_\mu \otimes |0, \alpha\rangle_A = b_+(\alpha) \psi_+ |+\rangle_\mu \otimes |+, \beta_+(\alpha)\rangle_A + b_-(\alpha) \psi_- |-\rangle_\mu \otimes |-, \beta_-(\alpha)\rangle_A . \tag{3}$$

In general, the amplitudes, $b_+(\alpha)$ and $b_-(\alpha)$, are not equal and therefore the proportions between $+$ and $-$ can change in a way that depends on the initial state $|0, \alpha\rangle_A$ of A . (Please note that M must not be confused with the unitary scattering operator S , see Appendix A).

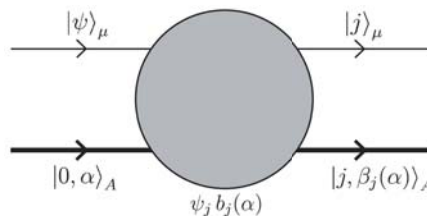


Figure 1. Schematic Feynman diagram for a transition from the initial state $|\psi\rangle_\mu \otimes |0, \alpha\rangle_A$ to the final state $|j\rangle_\mu \otimes |j, \beta_j(\alpha)\rangle_A$, $j = \pm$. The transition amplitude $\psi_j b_j(\alpha)$ depends on the microscopic details of the initial state $|0, \alpha\rangle_A$ of the larger system A and on the initial state $|\psi\rangle_\mu$ of μ .

The requirement of a statistically unbiased measurement means that $\langle\langle |b_+|^2 \rangle\rangle = \langle\langle |b_-|^2 \rangle\rangle$, where $\langle\langle \rangle\rangle$ denotes mean value over the ensemble of initial states $|0, \alpha\rangle_A$ of A .

Equation (3) describes a mechanism of the measurement process in which von Neumann’s dilemma is not present. Relativistic quantum mechanics, in the form of scattering theory of quantum field theory, is a more correct theory than the non-relativistic Schrödinger equation, as used in the 1930s, and we choose to use Equation (3) as our starting point.

In the Feynman-diagram language of quantum field theory, transitions between the two channels, + and −, are possible via returns to the initial state. This is a way to understand how the proportions of the channels can change as described by Equation (3). A formulation based on perturbation theory to all orders, leads to an explicitly unitary description of the whole process. (This is shown in Appendix B)

In scattering theory, transition rate (transition probability per unit time) is a central concept as we have reviewed in Appendix A. The transition rate from the initial state (1) to the final state (3) is $(2\pi)^{-1}w(\alpha)$, where $w(\alpha)$ is the squared modulus of (3),

$$w(\alpha) = |\psi_+|^2|b_+(\alpha)|^2 + |\psi_-|^2|b_-(\alpha)|^2. \tag{4}$$

Each term in (4) represents the partial transition rate for the corresponding channel. Because of our assumption of common mean values for $|b_{\pm}(\alpha)|^2$, the mean value of (4) is the same, $\langle\langle w \rangle\rangle = \langle\langle |b_{\pm}|^2 \rangle\rangle$.

For equation (3) to properly represent a measurement process, i.e., a bifurcation that leads to a final state with μ in either of the eigenstates of σ_3 , it is necessary that the squared moduli of the amplitudes satisfy either $|b_+(\alpha)|^2 \gg |b_-(\alpha)|^2$ or $|b_-(\alpha)|^2 \gg |b_+(\alpha)|^2$. If this holds for (almost) all microstates α in the resulting ensemble of final states, then it can function as a mechanism for the bifurcation of the measurement process.

Part of the basis for the von Neumann dilemma was the assumption that A is in a given initial state $|0, \alpha\rangle_A$. Before the μA -interaction, A can be in any of the states of the available initial ensemble. These states are ready to influence the recording process in different ways. To reach a final state, given by Equation (3), they compete with their transition rates, $(2\pi)^{-1}w(\alpha)$, which can differ widely between different values of α . The competition can lead to a selection and to a statistical distribution over α of the final states that is very different from the distribution in the initial ensemble.

In the following section, we will construct a mathematical model of how A influences the μA -interaction, including a description of the ensemble of possible initial states α . We then make a statistical analysis to show how both the bifurcation and the proper weights for the different measurement results can be understood in this simple setting.

3. Mathematical Model of the μA -interaction

We shall now model the amplitudes describing the μA -interaction, leading to the final state (3), and how it depends on the initial state $|0, \alpha\rangle_A$.

To have a generic model, we think of our system A as consisting of N independent subsystems, each interacting with μ , resulting in amplitudes that are products of N factors [15,16]. Since only factors resulting in differences between the two amplitudes are important, we assume

$$|b_j(\alpha)|^2 = \prod_{n=1}^N (1 + j\kappa_n(\alpha)), \quad \text{with } j = + \text{ or } -, \tag{5}$$

where $\kappa_n(\alpha)^* = \kappa_n(\alpha)$. Small deviations from unity in the factors are characterized by a zero mean, $\langle\langle \kappa_n \rangle\rangle = 0$, while the independence between the subsystems is expressed by $\langle\langle \kappa_n \kappa_{n'} \rangle\rangle = \delta_{nn'}\chi^2$, and $0 < \chi < 1$. We have followed the convention, used in stochastic dynamics (as for instance in Ref. [5]), to calculate to second order in κ_n and then replace $\kappa_n \kappa_{n'}$ by its mean $\delta_{nn'}\chi^2$. This model reflects the unbiased character of the measurement device, and it guarantees that on average the squared moduli of the amplitudes are identical and equal to unity, $\langle\langle |b_j(\alpha)|^2 \rangle\rangle = 1$.

As an illustration, in Appendix C, we describe a situation where μ is a fast charged particle emerging from some process and then interacting electrically with the system A . Here A consists of

a chain of small cylinders of ionizable material along the track where μ is passing in one of its state components. We show how the amplitude factorizes in this case.

We have chosen to keep each factor in the model close to unity in order to illustrate that even very small variations in how the subsystems interact with the system μ may result in one of the channels (one of the amplitudes), dominating over the other one, depending on the microstate α of the device. This makes it necessary to have a very large number N of subsystems. The critical assumptions are (i) the unbiased character of the device, i.e., not favoring any of the channels; and (ii) the independence of the subsystems of the device. The statistics of the interaction is treated in the following section.

4. Statistical Theory of the Transition to the Final State

We are now ready to investigate the statistical consequences of the μA -interaction modelled in the previous section. We introduce the total variance of the parameters in Equation (5), $\Xi = N\chi^2$, and define an aggregate variable $Y = Y(\alpha)$ of A , suitably normalized,

$$Y(\alpha) = \frac{1}{\Xi} \sum_{n=1}^N \kappa_n(\alpha) \tag{6}$$

to represent the overall degree of enhancement/suppression (so that $Y > 0$ for net enhancement of $+$ and $Y < 0$ for net enhancement of $-$). It follows that Y is characterized by mean and variance $\langle\langle Y \rangle\rangle = 0$ and $\langle\langle Y^2 \rangle\rangle = \Xi^{-1}$. Then, for sufficiently small κ_n , we can rewrite (5) as

$$|b_j(\alpha)|^2 = e^{\sum_n \log(1+j\kappa_n)} = e^{\Xi j Y(\alpha) - \frac{1}{2} \sum_n \kappa_n^2} = e^{\Xi(j Y(\alpha) - \frac{1}{2})}, \tag{7}$$

with $j = +$ or $-$. Here, in the exponent, we have done the calculation to second order in κ_n and we have replaced $\sum_n \kappa_n^2$ by $N\chi^2$.

Since all factors in the product (5) are independent, the distribution $q(Y)$ over the aggregate variable $Y = Y(\alpha)$, defined by Equation (6), in the ensemble of initial states of A , is well described by the Gaussian distribution,

$$q(Y) = \sqrt{\frac{\Xi}{2\pi}} e^{-\frac{1}{2}\Xi Y^2}. \tag{8}$$

centered around $Y = 0$ with variance Ξ^{-1} .

Initial states differ in their efficiency in leading to a transition to a final state, since the total transition rate may depend strongly on α . The transition to the final state (3) with $|b_j|^2$ given by (7) has the rate $(2\pi)^{-1}w(Y)$ where

$$w(Y) = |\psi_+|^2 e^{\Xi(Y-\frac{1}{2})} + |\psi_-|^2 e^{\Xi(-Y-\frac{1}{2})}, \tag{9}$$

with $\langle\langle w(Y) \rangle\rangle = 1$. The terms in (9) are the partial transition rates for the $+$ and $-$ channels.

The total transition rate (9) depends strongly on Y . We shall now go into the statistics of the final states which is strongly influenced by $w(Y)$. To get the distribution $Q(Y)$ over Y for the final states, corresponding to $q(Y)$ for the initial states, we must multiply $q(Y)$ by the transition rate (9) which is normalized in the sense that its mean value is 1. This is the standard approach in scattering theory, see, e.g., Ref. [17]. Here, it can be interpreted as a selection process, as previously discussed, that favors initial states which are efficient in leading to a transition, with a selective fitness being proportional to the transition rate (9). Thus, the distribution over final states can be written (see Figure 2)

$$Q(Y) = q(Y)w(Y) = |\psi_+|^2 Q_+(Y) + |\psi_-|^2 Q_-(Y), \tag{10}$$

$$Q_{\pm}(Y) = \sqrt{\frac{\Xi}{2\pi}} e^{-\frac{1}{2}\Xi(Y\mp 1)^2}.$$

The normalized partial distributions, $Q_+(Y)$ and $Q_-(Y)$, also with variance Ξ^{-1} , are centered around $Y = 1$ and $Y = -1$ and refer to μ ending up in the state $|+\rangle_\mu$ and $|-\rangle_\mu$, respectively. The coefficients of $Q_+(Y)$ and $Q_-(Y)$ in $Q(Y)$ are $|\psi_+|^2$ and $|\psi_-|^2$, expressing Born's rule explicitly.

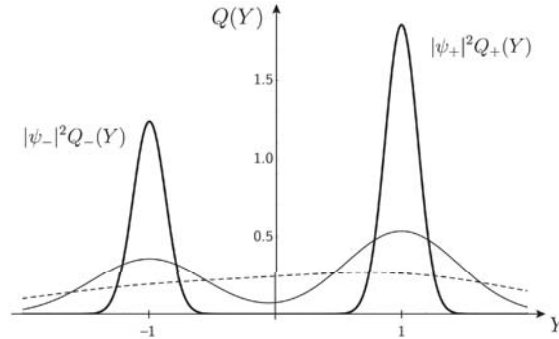


Figure 2. The distribution $Q(Y)$ over Y of transitions taking place in μA -interaction for increasing size of A corresponding to $\Xi = 1$ (broken line), $\Xi = 5$ (thin line), and $\Xi = 60$ (thick line). $Q(Y)$ is composed of two distributions $Q_+(Y)$ and $Q_-(Y)$ with weights $|\psi_+|^2$ and $|\psi_-|^2$, respectively. These distributions become separated as Ξ increases. Each initial state of A , $|0, \alpha\rangle_A$, is represented by a certain $Y = Y(\alpha)$. As the size of A increases and Ξ becomes larger, states that are efficient in leading to a transition are found around $Y = -1$ and $Y = +1$, respectively. These initial states then lead to μ ending up in either $|-\rangle_\mu$ or $|+\rangle_\mu$, respectively, with probabilities confirming the Born rule.

It is instructive to follow the distribution $Q(Y)$ with growing Ξ . For small $\Xi (= N\chi^2)$ it is broad and unimodal; it then turns broad and bimodal with narrowing peaks. For large Ξ , it is split into two well separated distributions with sharp peaks, weighted by the squared moduli of the state components of μ , $|\psi_+|^2 Q_+(Y)$ and $|\psi_-|^2 Q_-(Y)$, at $Y = 1$ and $Y = -1$, respectively. They represent two different sub-ensembles of final states (see Equation (2)). Other values of Y correspond to non-competitive processes. The aggregate variable Y is "hidden" in the fine unknown details of A that can influence the μA -interaction.

From Equation (7) we see that the dominance of either channel is characterized by $|b_+(\alpha)|^2 / |b_-(\alpha)|^2 = e^{2\Xi Y}$ being either very large or very small. For a small system, i.e., small N and hence small Ξ , this ratio does not deviate much from unity which means that we have an entangled superposition of the two final states. As Ξ increases, the ratio deviates more strongly from unity and one of the channels starts to dominate. When Ξ is of the order of 10, the sub-distributions, $Q_+(Y)$ and $Q_-(Y)$, are essentially non-overlapping, $Q(Y)$ is concentrated around ± 1 , and the ratio of dominance between the channels is of the order of $e^{20} \approx 10^{10}$.

The initial state for μ in (1) is a superposition, a 'both-and state', and it ends up in (2) which is again a product state, with μ in either $|+\rangle_\mu$ or $|-\rangle_\mu$. The initial states of A vary widely in their efficiency to lead to a final state. When one transition-rate term in (9) is large, the other one is small. The selection of a large transition rate therefore also leads to a bifurcation with one of the terms in (3) totally dominating the final state.

5. Concluding Remarks

The main contribution in our work is that we have demonstrated that the initial stage of quantum measurement can be described within reversible quantum mechanics. The key components are (i) a scattering theory formulation with inverse processes that both guarantee unitarity and allow for a non-linear mechanism leading to the bifurcation; and (ii) a statistical analysis that reveals how initial states that are efficient in leading to a transition to a final state have a selective advantage and how this results in the correct probabilities of the measurement results as stated by Born's rule.

In our description, we want the system A to be big enough for a bifurcation to take place, i.e., for $\Xi = N\chi^2$ to be sufficiently large. Our idea has been to follow the qualitative recipe given by Bell who formulated a principle concerning the position of the Heisenberg cut [10], i.e., the boundary of the system A , interacting with μ according to quantum dynamics (Ref. [10], p.124):

put sufficiently much into the quantum system that the inclusion of more would not significantly alter practical predictions

On the other hand, the system A should not be so large that $\mu \cup A$ cannot be described by deterministic quantum mechanics. In the model that we have described, the bifurcation of measurement takes place in the reversible stage of the interaction between μ and A before irreversibility sets in and fixes the result. In this respect, our analysis is very different from decoherence analysis [11,18].

Beyond A , the measurement apparatus must be considered to be an open system with its dynamics described by a Lindblad equation [19]. The starting point for the development here is one of the final states before the Heisenberg cut, i.e., $|+\rangle_{\beta_+(\alpha)}_A$ or $|-\rangle_{\beta_-(\alpha)}_A$, in one of the sub-ensembles described by $Q_+(Y)$ or $Q_-(Y)$. Thus, the open dynamics continues only in the channel that happens to have been chosen, $+$ or $-$.

For future work, a more detailed description is needed of a typical μA -interaction, including the statistics of the initial states and the selection of one state $|0, \alpha\rangle_A$ with a large transition amplitude, leading to a final state (2) with μ in one eigenstate, $|+\rangle_{\mu}$ or $|-\rangle_{\mu}$. An important task is to construct a detailed physical model of a non-biased measurement apparatus. The model of Appendix C is a beginning in this respect, but the mathematical assumptions in Equation (3) should be directly tied to physical properties of A . In particular, the non-bias property of A should be analyzed.

The system A should be neither too small nor too large. Then it is reasonable to describe it as mesoscopic, but Bell's principle that we have quoted above gives no indication of its actual size. In the development of realistic models, questions of limits and the accuracy of approximations will have to be handled in more detail.

In practical scientific research, there is a common working understanding of quantum mechanics. Physicists have a common reality concept for a quantum-mechanical system when it is not observed, a kind of pragmatic quantum ontology with the *quantum-mechanical state* of the studied system as the basic concept. Development of this state in time then constitutes the quantum dynamics. If quantum mechanics now can also be used to describe the measurement process, this pragmatic quantum ontology can have a wider validity than has been commonly expected.

Author Contributions: Conceptualization, K.-E.E. and K.L.; methodology, K.-E.E.; software, K.L.; formal analysis, K.-E.E. and K.L.; investigation, K.-E.E. and K.L.; writing—original draft preparation, K.-E.E. and K.L.; writing—review and editing, K.-E.E. and K.L.; visualization, K.-E.E. and K.L.; project administration, K.L.

Funding: This research received no external funding.

Acknowledgments: We thank Erik Sjöqvist and Martin Cederwall for fruitful collaboration in an earlier phase of this project [16]. Financial support from The Royal Society of Arts and Sciences in Gothenburg was important for this collaboration. We are also grateful to Andrew Whitaker for several constructive discussions. We thank two referees, whose critical comments have led us to make several improvements of the paper.

Conflicts of Interest: The authors declare no conflict of interest.

Appendix A. Scattering Matrix S and Transition Matrix M

The unitary (i.e., probability preserving) scattering operator S , takes an initial state $|i\rangle$ into a final state $S|i\rangle$. If a certain final state $|f\rangle$ is of interest to us then we calculate the scattering-matrix element $\langle f|S|i\rangle$. When dealing with particle scattering, it is convenient to do this in momentum space. Eigenstates of momentum are plane waves, i.e., states that occupy all space and cannot be normalized.

We shall be interested in final states $|f\rangle$ that are different from the initial state $|i\rangle$, so that $|f\rangle$ and $|i\rangle$ are orthogonal, i.e., $\langle f|i\rangle = 0$, and we can replace S by $S - 1$.

We use here the Quantum Electrodynamics book by Jauch and Rohrlich as our reference [17], to emphasize the development that had taken place between the physics of the 1930s and the quantum field theory of the 1950s.

To consider energy and momentum conservation, it is usual to write (Ref. [17], Equation (8)–(29))

$$\langle f | (S - 1) | i \rangle = \delta(P_f - P_i) \langle f | M | i \rangle, \tag{A1}$$

where $\delta(P_f - P_i)$ is the 4-dimensional delta function over energy-momentum and M is the transition matrix.

Usually the probability for a transition into the final state $|f\rangle$, given the initial state $|i\rangle$, would be the squared modulus of (A1) but the square of a delta function does not make sense. Then one imposes a very large but finite length L in space and requires normalization for the wave-functions in the volume L^3 , and, similarly, one imposes a time T for the whole process. Energy-momentum conservation is nearly exact for large L and T . One delta function in the squared modified (A1) becomes replaced by $(2\pi)^{-4}L^3T$. When normalization conventions are taken into account, the result becomes independent of L and proportional to T . After this we divide by T to get the transition probability per unit time (see Ref. [17], Equation (8)–(40)),

$$(2\pi)^{-1} \delta(P_f - P_i) |\langle f | M | i \rangle|^2. \tag{A2}$$

Then requesting the states $|i\rangle$ and $|f\rangle$ to have the same energy and momentum, we can interpret

$$(2\pi)^{-1} |\langle f | M | i \rangle|^2 = (2\pi)^{-1} \text{Tr}[|f\rangle \langle f| M \rho^{(0)} M^\dagger]. \tag{A3}$$

as the transition probability per unit time, induced by M , from an initial state described by the density operator

$$\rho^{(0)} = |i\rangle \langle i| \tag{A4}$$

to a final state described by the projection operator $|f\rangle \langle f|$. We thus find that the transition probability-rate matrix obtained from the initial state (A4) is $(2\pi)^{-1}$ times

$$R = M \rho^{(0)} M^\dagger. \tag{A5}$$

Thus, $(2\pi)^{-1}R$ is the total transition rate times the density operator for the final state. Since the trace of a density operator is unity,

$$(2\pi)^{-1}w = (2\pi)^{-1} \text{Tr} R \tag{A6}$$

is the total transition rate. The normalized final-state density matrix is then

$$\rho^{(f)} = \frac{1}{w} R = \frac{M \rho^{(0)} M^\dagger}{\text{Tr}[M \rho^{(0)} M^\dagger]}. \tag{A7}$$

Let us consider the systems μ and A . M makes A entangled with μ without changing the state of μ . Still the transition amplitudes can differ between $+$ and $-$. This can distort the entanglement and induce changes in the relative proportions of $+$ and $-$ in the final state (Equation (2)). Thus, the proportions are no longer fixed by the von Neumann dilemma; the dilemma does not arise in the scattering theory that we are considering.

Appendix B. Calculation of Feynman Diagrams with Explicit Unitarity and Reversibility

The unitarity of the scattering matrix has not been explicitly visible in the main text. Reversibility that we have pointed out as crucial, is also not explicit. To remedy this we shall present a slightly more elaborate description of the whole process where the observed system μ is produced in its initial state

$|\psi\rangle_\mu$ by an external source B before interaction with A and absorbed by a sink D_+ or D_- in one of the possible final states after the interaction. In this version both unitarity and reversibility will be made explicit.

In this picture, the transition rate will instead be hidden and hence also the race to the final state. We therefore use the results that we have already obtained in the article, the transition rate (9) and the distribution (10) of the final states over the aggregated variable Y . The Born rule is also contained in (10).

As in the previous description, A starts in the initial state $|0, \alpha\rangle_A$ but μ is produced by B at an early time $-T$ in the state $|\psi\rangle_\mu$. After μA -interaction around the time zero, μ is absorbed in an eigenstate $|+\rangle_\mu$ or $|-\rangle_\mu$ at the time $+T$ by D_+ or D_- , leaving A in the state $|+, \beta_+(\alpha)\rangle_A$ or $|-, \beta_-(\alpha)\rangle_A$, respectively. We thus have one initial state $|0, \alpha\rangle_A$, a member of the ensemble of initial states, and three available final states, $|0, \alpha\rangle_A$ (no change), $|+, \beta_+(\alpha)\rangle_A$, and $|-, \beta_-(\alpha)\rangle_A$; The system μ takes part only in intermediate states.

Schematic Feynman-diagram elements for the action of the source B , the transition matrix M in Equation (3) and the sinks D_+ and D_- are shown in Figure A1, and the factors corresponding to them, J^* , $b_\pm \psi_\pm$ and F_\pm . We represent μ by a thin line and A by a thick line. As in Figure 1, the interaction between μ and A described by the transition matrix M , is represented by a shaded circle. Reversibility is included through the actions of the Hermitian or complex conjugates, J , M^\dagger , and F_j^* .

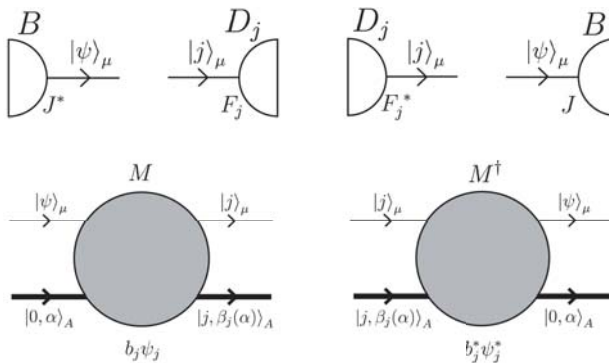


Figure A1. Schematic Feynman-diagram elements for the action of the source B , the transition matrix M and the sinks D_j ($j = \pm$) and their conjugates.

We use perturbation theory to compute the final-state density matrix,

$$S |0, \alpha\rangle_A \langle 0, \alpha| S^\dagger. \tag{A8}$$

We use the method of Nakanishi [20] to calculate this bilinear quantity directly rather than the state vector $S |0, \alpha\rangle_A$, simply because it makes normalization easy.

The diagrams of perturbation theory are shown in Figure A2. The zero-order no-change term is only an A -line corresponding to a contribution equal to 1 (Figure A2a). Figure A2b shows the diagram corresponding to that of Figure 1 with the source B and one sink D_j ($j = +, -$). The inverse of this diagram is that of Figure A2c. The two taken together into one diagram represents a reduction of the no-change component due to transitions to the other states (Figure A2d). This can be repeated

any number of times. All these diagrams leading back to the initial state (Figure A2e) contribute a geometrical series, representing the total no-change component of the final state,

$$1 - \sum_{j=+,-} J \psi_j^* b_j^* F_j^* F_j b_j \psi_j J^* + \left(\sum_{j=+,-} J \psi_j^* b_j^* F_j^* F_j b_j \psi_j J^* \right)^2 \pm \dots = \tag{A9}$$

$$\frac{1}{1 + (|F_+|^2 |\psi_+|^2 |b_+|^2 + |F_-|^2 |\psi_-|^2 |b_-|^2) |J|^2} = \frac{1}{1 + |J|^2 |F|^2 (|\psi_+|^2 e^{\Xi(\gamma - \frac{1}{2})} + |\psi_-|^2 e^{\Xi(-\gamma - \frac{1}{2})})}.$$

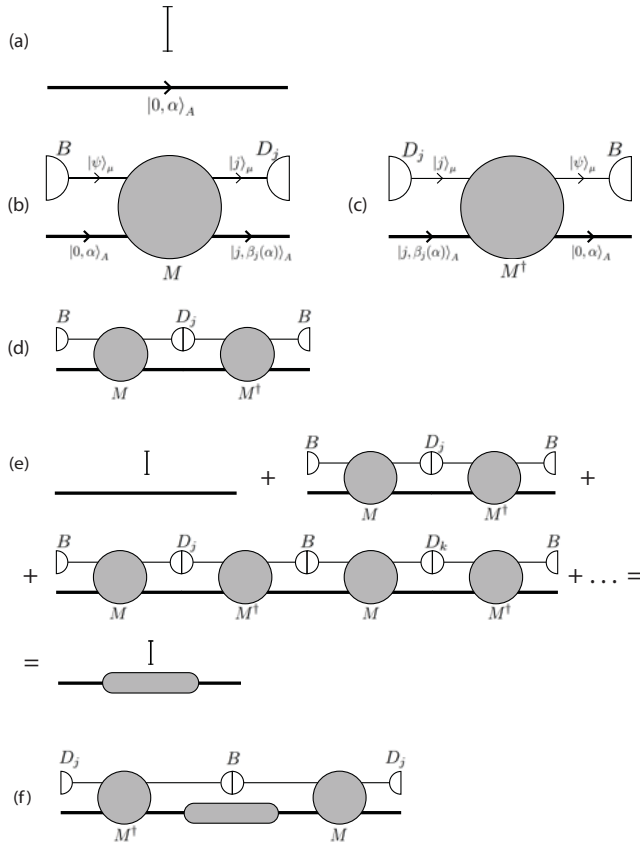


Figure A2. Schematic Feynman diagrams: (a) zero-order diagram for no change (the I-like sign above the A-line symbolizes “no μ -system”); (b) lowest order diagram for transition to a state with A marked by μ in the j state (see Figure 1); (c) inverse diagram of b; (d) diagrams b and c combined to a no-change correction; (e) summation over d repeated any number of times, i.e., summation of no-change diagrams to all orders; (f) the full perturbation expansion of the diagonal elements of the final-state density matrix with A marked by μ in the state $|j\rangle_\mu$.

Here we have used the expressions for the amplitudes in Equation (7) and given equal strength F to the two sinks D_+ and D_- . The total scattering probability, i.e., the probability of A being marked by μ is

$$\begin{aligned}
 & 1 - \frac{1}{1 + |J|^2|F|^2 \left(|\psi_+|^2 e^{\Xi(Y-\frac{1}{2})} + |\psi_-|^2 e^{\Xi(-Y-\frac{1}{2})} \right)} = \\
 & J\psi_+^* e^{\frac{1}{2}\Xi(Y-\frac{1}{2})} F^* \frac{1}{1 + |J|^2|F|^2 \left(|\psi_+|^2 e^{\Xi(Y-\frac{1}{2})} + |\psi_-|^2 e^{\Xi(-Y-\frac{1}{2})} \right)} F e^{\frac{1}{2}\Xi(Y-\frac{1}{2})} \psi_+ J^* + \quad (A10) \\
 & J\psi_-^* e^{\frac{1}{2}\Xi(-Y-\frac{1}{2})} F^* \frac{1}{1 + |J|^2|F|^2 \left(|\psi_+|^2 e^{\Xi(Y-\frac{1}{2})} + |\psi_-|^2 e^{\Xi(-Y-\frac{1}{2})} \right)} F e^{\frac{1}{2}\Xi(-Y-\frac{1}{2})} \psi_- J^* .
 \end{aligned}$$

The two terms on the right side of (A10) are the probabilities for the final states $|+, \beta_+(\alpha)\rangle_A$ and $|-, \beta_-(\alpha)\rangle_A$, corresponding to the diagrams of Figure A1f for the remaining diagonal elements of the density matrix. For large Ξ , the no-change contribution (A9) becomes negligible. The same is true for the non-diagonal elements of the density matrix. The diagonal terms for $+$ and $-$ in (A10) become

$$p_{\pm} = \frac{|\psi_{\pm}|^2 e^{\pm\Xi Y}}{|\psi_+|^2 e^{\Xi Y} + |\psi_-|^2 e^{-\Xi Y}} . \quad (A11)$$

For $Y = +1$, $p_+ = 1$ and the $+$ channel takes everything and for $Y = -1$, $p_- = 1$ and the $-$ channel takes everything. The norm is preserved, i.e., S is unitary. Reversibility is also clearly visible: J^* , M and F_{\pm} are active together with their conjugates that represent inverse processes.

Appendix C. Factorization of the Transition Amplitudes

We can think of the interaction between the small system μ and the measurement apparatus as an electromagnetic interaction with small energy and momentum transfer. In Quantum Electrodynamics (QED), it is described in terms of an exchange of soft photons. Emission and exchange of soft photons is an old and well-known example of factorizable processes in QED.

To show the factorization of soft photon exchange, we consider an outgoing electron (charge $-e$, mass m) with final momentum p , described by a spinor $\bar{u}(p)$ (we follow rather closely the conventions of Ref. [17]),

$$p^2 + m^2 = 0, \quad \bar{u}(p)(ip \cdot \gamma - m) = 0, \quad (A12)$$

after emitting two soft photons with momenta k_1, k_2 , and polarizations τ_1, τ_2 ,

$$\begin{aligned}
 & k_1^2 = k_2^2 = 0; \quad k_1 \cdot \tau_1 = k_2 \cdot \tau_2 = 0; \\
 & |\mathbf{k}_1|, |\mathbf{k}_2| \ll m .
 \end{aligned} \quad (A13)$$

In the evaluation of the Feynman diagram of Figure A3, the spinor $\bar{u}(p)$ for the outgoing electron of an original diagram (without soft photons) is replaced by an expression proportional to

$$\begin{aligned}
 & e^2 \bar{u}(p) \left[\tau_1 \cdot \gamma \frac{i(p+k_1) \cdot \gamma + m}{(p+k_1)^2 + m^2} \tau_2 \cdot \gamma + (1 \leftrightarrow 2) \right] \frac{i(p+k_1+k_2) \cdot \gamma + m}{(p+k_1+k_2)^2 + m^2} \approx \\
 & e^2 \frac{1}{2(p \cdot k_1 + p \cdot k_2)} \bar{u}(p) \left[\frac{\tau_1 \cdot \gamma (ip \cdot \gamma + m) \tau_2 \cdot \gamma (ip \cdot \gamma + m)}{2p \cdot k_1} + (1 \leftrightarrow 2) \right] = \quad (A14) \\
 & e^2 \frac{-p \cdot \tau_1 p \cdot \tau_2}{p \cdot k_1 + p \cdot k_2} \left(\frac{1}{p \cdot k_1} + \frac{1}{p \cdot k_2} \right) \bar{u}(p) = (s(k_1) \cdot \tau_1)(s(k_2) \cdot \tau_2) \bar{u}(p),
 \end{aligned}$$

where we have used the basic relation for the Dirac gamma matrices, $\gamma_{\mu\nu} + \gamma_{\nu\mu} = 2g_{\mu\nu}$, where $g_{\mu\nu}$ is the metric tensor. In (A14), $s_\mu(k)$ is the Fourier transform of the current density of a classical point charge $-e$ moving from $\mathbf{x} = 0$ at time zero with the velocity \mathbf{p}/p_0 ,

$$s_\mu(k) = -e \frac{ip_\mu}{p \cdot k} = -e \int_0^\infty dt \int d^3\mathbf{x} e^{i(\mathbf{k}\cdot\mathbf{x} - |\mathbf{k}|t)} \delta\left(\mathbf{x} - \frac{\mathbf{p}}{p_0}t\right) \frac{p_\mu}{p_0}. \tag{A15}$$

The contribution of the diagram that μ comes from is unchanged in the limit of small k_1, k_2 . Equation (A14) states that the emission of the two photons is described by one scalar emission factor for each photon. This can be extended to also include absorption.

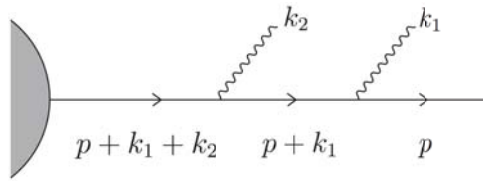


Figure A3. Feynman diagram for the emission of two soft photons.

The case of only one photon is, of course, similar and even simpler with just one emission factor. We took the example of two photons to show how the algebra gives the two factors also in this case. For the n -photon case one uses the algebraic identity

$$\sum_{(i_1 i_2 \dots i_n)} \frac{1}{a_{i_1}(a_{i_1} + a_{i_2}) \dots (a_{i_1} + a_{i_2} + \dots + a_{i_n})} = \frac{1}{a_1 a_2 \dots a_n}. \tag{A16}$$

Thus, we can think of the classical current density

$$j_\mu(k) = -e \delta\left(\mathbf{x} - \frac{\mathbf{p}}{p_0}t\right) \frac{p_\mu}{p_0} \tag{A17}$$

as representing the electron, i.e., the system μ as felt by other systems. μ can come as a very small wave-packet travelling along the x_1 -axis ($\mathbf{p} = (p_1, 0, 0)$) through a substance that can be ionized. Then we take A to be a thin cylinder of this substance around the path of the μ wave-packet.

It is convenient to consider A as consisting of a chain of N shorter cylinders A_1, A_2, \dots, A_N along the x_1 -axis with A_k defined by

$$\begin{aligned} x_1^{(0)} + \frac{k-1}{2}\Delta l &\leq x_1 \leq x_1^{(0)} + \frac{k+1}{2}\Delta l, \\ x_2^2 + x_3^2 &\leq \Delta r^2, \end{aligned} \tag{A18}$$

where Δl and Δr are small.

For our model, we can neglect the interaction between the small cylinders and we can consider μ to interact with A_k only during its passage, i.e., during the time interval

$$\frac{p_0}{p_1} \left(x_1^{(0)} + \frac{k-1}{2}\Delta l\right) < t \leq \frac{p_0}{p_1} \left(x_1^{(0)} + \frac{k+1}{2}\Delta l\right). \tag{A19}$$

Because of their independence, each of the cylinders acted on by μ via the current density (A17), contributes an independent factor to the total transition rate. In the mean, the factor from the μA_k -interaction should not change anything but in the single case, it can contribute an unknown factor close to one, as assumed in Equation (5). Thus, we have given here a rationale for this assumption.

References

1. Nauenberg, M. Does Quantum Mechanics Require A Conscious Observer? *J. Cosmol.* **2011**, *14*. Available online: <http://journalofcosmology.com/Consciousness139.html> (accessed on 26 August 2019).
2. Everett, H. "Relative State" Formulation of Quantum Mechanics. *Rev. Mod. Phys.* **1957**, *29*, 454. [[CrossRef](#)]
3. DeWitt, B.S. Quantum mechanics and reality. *Phys. Today* **1970**, *23*, 30–35. [[CrossRef](#)]
4. Gisin, N. Quantum measurements and stochastic processes. *Phys. Rev. Lett.* **1984**, *52*, 1657. [[CrossRef](#)]
5. Gisin, N.; Percival, I.C. The quantum-state diffusion model applied to open systems. *J. Phys. A Math. Gen.* **1992**, *25*, 5677–5691. [[CrossRef](#)]
6. Percival, I.C. Primary state diffusion. *Proc. R. Soc. A* **1994**, *447*, 189–209. [[CrossRef](#)]
7. Ghirardi, G.C.; Rimini, A.; Weber, T. Unified dynamics for microscopic and macroscopic systems. *Phys. Rev. D* **1986**, *34*, 470. [[CrossRef](#)] [[PubMed](#)]
8. Ghirardi, G.C.; Pearle, P.; Rimini, A. Markov processes in Hilbert space and continuous spontaneous localization of systems of identical particles. *Phys. Rev. A* **1990**, *42*, 78. [[CrossRef](#)] [[PubMed](#)]
9. Bohm, D. A suggested interpretation of the quantum theory in terms of "hidden" variables. I. *Phys. Rev.* **1952**, *85*, 166. [[CrossRef](#)]
10. Bell, J.S. Quantum Mechanics for Cosmologists. In *Speakable and Unsayable in Quantum Mechanics*; Cambridge University Press: Cambridge, UK, 2004.
11. Zeh, H.D. On the interpretation of measurement in quantum theory. *Found. Phys.* **1970**, *1*, 69–76. [[CrossRef](#)]
12. Zurek, W.H. Quantum theory of the classical: Quantum jumps, Born's Rule and objective classical reality via quantum Darwinism. *Philos. Trans. R. Soc. A* **2018**, *376*, 20180107. [[CrossRef](#)] [[PubMed](#)]
13. Rovelli, C. Relational quantum mechanics. *Int. J. Theor. Phys.* **1996**, *35*, 1637–1678. [[CrossRef](#)]
14. Zwirn, H. The measurement problem: Decoherence and convivial solipsism. *Found. Phys.* **2016**, *46*, 635–667. [[CrossRef](#)]
15. Eriksson, K.E. Measurement as soft final-state interaction with a stochastic system. *J. Phys. B At. Mol. Opt. Phys.* **2009**, *42*, 085001. [[CrossRef](#)]
16. Eriksson, K.E.; Cederwall, M.; Lindgren, K.; Sjöqvist, E. Bifurcation in Quantum Measurement. *arXiv* **2017**, arXiv:1708.01552v2.
17. Jauch, J.M.; Rohrlich, F. *The Theory of Photons and Electrons*; Addison-Wesley: Boston, MA, USA, 1955; pp. 163–167.
18. Schlosshauer, M. Decoherence, the measurement problem, and interpretations of quantum mechanics. *Rev. Mod. Phys.* **2005**, *76*, 1267–1305. [[CrossRef](#)]
19. Lindblad, G. On the generators of quantum dynamical semigroups. *Commun. Math. Phys.* **1976**, *48*, 119–130. [[CrossRef](#)]
20. Nakanishi, N. General theory of infrared divergence. *Prog. Theor. Phys.* **1958**, *19*, 159–168. [[CrossRef](#)]



© 2019 by the authors. Licensee MDPI, Basel, Switzerland. This article is an open access article distributed under the terms and conditions of the Creative Commons Attribution (CC BY) license (<http://creativecommons.org/licenses/by/4.0/>).

On the Rarefied Gas Experiments

Róbert Kovács ^{1,2,3} 

- ¹ Department of Energy Engineering, Faculty of Mechanical Engineering, Budapest University of Technology and Economics (BME), 1111 Budapest, Hungary; kovacs.robert@wigner.mta.hu
- ² Department of Theoretical Physics, Wigner Research Centre for Physics, Institute for Particle and Nuclear Physics, 1121 Budapest, Hungary
- ³ Montavid Thermodynamic Research Group, 1112 Budapest, Hungary

Received: 6 July 2019; Accepted: 22 July 2019; Published: 23 July 2019

Abstract: There are limits of validity of classical constitutive laws such as Fourier and Navier-Stokes equations. Phenomena beyond those limits have been experimentally found many decades ago. However, it is still not clear what theory would be appropriate to model different non-classical phenomena under different conditions considering either the low-temperature or composite material structure. In this paper, a modeling problem of rarefied gases is addressed. The discussion covers the mass density dependence of material parameters, the scaling properties of different theories and aspects of how to model an experiment. In the following, two frameworks and their properties are presented. One of them is the kinetic theory based Rational Extended Thermodynamics; the other one is the non-equilibrium thermodynamics with internal variables and current multipliers. In order to compare these theories, an experiment on sound speed in rarefied gases at high frequencies, performed by Rhodes, is analyzed in detail. It is shown that the density dependence of material parameters could have a severe impact on modeling capabilities and influences the scaling properties.

Keywords: rarefied gases; non-equilibrium thermodynamics; kinetic theory

1. Introduction

The classical material laws such as Fourier and Navier-Stokes are acceptable for tasks concerning homogeneous materials, dense gases, and far from low-temperatures (20 K). In the engineering practice, these constitutive equations are well-known and widely used. Nevertheless, there are situations where some generalizations must be applied. Such a case could occur on small (micro or nano) length scales, short time scales, near low-temperature or far from equilibrium.

It is easier to understand the origin of the present continuum model of non-equilibrium thermodynamics with internal variables (NET-IV) for rarefied gases together with its properties if a purely heat conduction problem is presented first, since the essential attributes are inherited. Moreover, the most visible differences are analogous in both cases, for instance, the available degrees of freedom, the structure of the equations and the interpretation of the parameters. All these differences originate at the roots of these approaches.

Considering only heat conduction, various forms of heat propagation are experimentally found [1–9]. These are called second sound and ballistic propagation [9–12]. Their modeling background is diverse, and one can find many extended heat conduction equations with many different interpretations in the literature [13–20]. One of them is related to the approach of Rational Extended Thermodynamics (RET) [9,21], it considers kinetic theory rigorously and uses phonon hydrodynamics to describe these deviations from Fourier's law [22,23]. Another approach uses non-equilibrium thermodynamics with internal variables and current multipliers (NET-IV) [12]. Both are tested on the same heat conduction experiment, and the latter one seems to be more effective [23].

The main difference between these two approaches is routed to the physics that lies behind the system of constitutive equations. Using kinetic theory, one always has to assume a priori a mechanism occurring between the particles and describe the interaction among them. On the other side, non-equilibrium thermodynamics is phenomenological, the derivation of constitutive equations does not require any assumption regarding the microstructure, which makes the model more general and, in parallel, offers more degrees of freedom by not restricting the coupling coefficients. In the kinetic theory, due to the prescribed interaction model, most of the coefficients can be calculated, and only a few of them have to be fitted to the experimental data. Although its mathematical structure is advantageous, it is symmetric hyperbolic [21,24], the fixed parameters lead to its weakness: e.g., in a previously mentioned heat conduction problem, one has to use at least 30 momentum equations with increasing tensorial order to obtain the ballistic propagation speed approximately. The approach of NET-IV can resolve this problem, also preserving the structure of momentum equation; however, in order to fit, it requires more parameters [12,22,23,25]. All these approaches have advantages and disadvantages, and their detailed comparison is presented in [26].

In the case of investigating room temperature non-Fourier phenomenon, the phonon picture is not applicable [25]. One advantage of NET-IV is that it is applicable and tested on room temperature experiments that show over-diffusive type non-Fourier heat propagation [27–29]. It makes the kinetic approach of heat conduction more challenging to apply for practical problems; however, there are situations where its predictive power is useful (e.g., estimating transport coefficients). Such a situation is related to the topic of rarefied gases [30]. In some senses, the behavior of a rarefied gas (i.e., a gas under low pressure) is analogous with a rarefied phonon gas that applied in case of heat conduction. The difference among them is the type of the particle and the interpretation of some physical quantities. In order to understand the analogy, the ballistic conduction must be defined.

Using phonon hydrodynamics, the ballistic heat conduction is interpreted as non-interacting particles that scatter on the boundary only, i.e., traveling through the material without any collision [9]. It is important to emphasize that the following Equations (1) and (2) describe not merely a ballistic phenomenon but together with the diffusion and second sound propagation modes. This assumption leads to the system of equations in one spatial dimension:

$$\begin{aligned} \partial_t e + c^2 \partial_x p &= 0, \\ \partial_t p + \frac{1}{3} \partial_x e + \partial_x N &= -\frac{1}{\tau_R} p, \\ \partial_t N + \frac{4}{15} c^2 \partial_x p &= -\left(\frac{1}{\tau_R} + \frac{1}{\tau_N}\right) N, \end{aligned} \tag{1}$$

where e being the energy density, p is momentum density, c stands for the Debye speed, τ_R and τ_N are the relaxation times referring to the resistive and normal processes [9], furthermore, ∂_t denotes the partial time derivative, applied for a rigid heat conductor. Here, N is the deviatoric part of the pressure tensor. In phonon hydrodynamics, it can be identified as a current density of the heat flux. The key aspect to include ballistic contributions into the modeling is achieving coupling between the heat flux and the pressure. This is one merit of this approach: such coupling was not realized in any other theories before. That was the motivation for the approach of NET-IV, this coupling is obtained using current multipliers [31], and the same structure can be reproduced [12,25]:

$$\begin{aligned} \rho c \partial_t T + \partial_x q &= 0, \\ \tau_q \partial_t q + q + \lambda \partial_x T + \kappa \partial_x Q &= 0, \\ \tau_Q \partial_t Q + Q + \kappa \partial_x q &= 0, \end{aligned} \tag{2}$$

where Q plays the role of N , q is the heat flux, c denotes the specific heat and the coefficient κ is not fixed on contrary to (1), this property allows to adjust the exact propagation speed using only

3 equations instead of 30. The properties of the models above are discussed deeply by Jou et al. [32], Alvarez et al. [33] and Guo et al. [34].

Despite the numerous differences between phonons and real molecules, the situation is similar for rarefied gases, at least at the level of entropy; Equation (3) does not contain restrictions about the type of the fluid, i.e., there is an “entropic equivalence” between them. Here, a gas under low pressure consists few enough particles to observe the ballistic contribution. In NET-IV, the starting point is the generalization of entropy density and its current:

$$s(e, \rho, q_i, \Pi_{ij}) = s_e(e, \rho) - \frac{m_1}{2} q_i q_i - \frac{m_2}{2} \Pi_{(ij)} \Pi_{(ij)} - \frac{m_3}{6} \Pi_{ii} \Pi_{jj},$$

$$J_i = (b_{(ij)} + b_{kk} \delta_{ij} / 3) q_j, \tag{3}$$

then exploiting the entropy production inequality of second law [12], one obtains a continuum model compatible with the kinetic theory to model rarefied gases [25,26,35]. Einstein’s summation convention is applied. Here Π_{ij} is an internal variable [36–38], it is identified as the viscous pressure, $\Pi_{ij} = P_{ij} - p \delta_{ij}$ with p being the hydrostatic pressure, in accordance with EIT [18,19]. This is the usual assumption in theories of Extended Thermodynamics, as a consequence of the compatibility with kinetic theory [21,32], it also includes Meixner’s theory [39], the first extension of Navier-Stokes equation. Besides, b_{ij} is called Nyíri-multiplier (or current multiplier) [31] which permits obtaining coupling between the heat flux and the pressure. Furthermore, the form of entropy flux (3) is compatible with the one proposed by Sellitto et al. [40], where the gradient of heat flux acts as a multiplier. Since the proper description requires the separation of deviatoric and spherical parts, in Equation (3) $\langle \rangle$ denotes the traceless part of the pressure. Equation (3) presents the same generalization as used for modeling complex heat conduction processes that include diffusive and wave propagation modes together, thus, hereinafter it is called *non-local generalization* of entropy and its current density [25]. The linearized-generalized Navier-Stokes-Fourier system reads in one dimension [25]:

$$\begin{aligned} \tau_q \partial_t q + q + \lambda \partial_x T - \alpha_{21} \partial_x \Pi_s - \beta_{21} \partial_x \Pi_d &= 0, \\ \tau_d \partial_t \Pi_d + \Pi_d + \nu \partial_x v + \beta_{12} \partial_x q &= 0, \\ \tau_s \partial_t \Pi_s + \Pi_s + \eta \partial_x v + \alpha_{12} \partial_x q &= 0, \end{aligned} \tag{4}$$

where the lower indices d and s denote the deviatoric and spherical parts, respectively. The η is the bulk viscosity, ν denotes the shear viscosity, α_{ab}, β_{ab} ($a, b = 1, 2$) are the coupling parameters between the heat flux and the pressure and τ_m ($m = q, d, s$) are the relaxation times, here the coupling parameters and the relaxation times are to be fit. This structure is equivalent to the 1D linearized version model from RET [41–43]:

$$\begin{aligned} \tau_q \partial_t q + q + \lambda \partial_x T - R T_0 \tau_q \partial_x \Pi_d + R T_0 \tau_q \partial_x \Pi_s &= 0, \\ \tau_d \partial_t \Pi_d + \Pi_d + 2\nu \partial_x v - \frac{2\tau_d}{1 + c_v^*} \partial_x q &= 0, \\ \tau_s \partial_t \Pi_s + \Pi_s + \eta \partial_x v + \frac{\tau_s (2c_v^* - 3)}{3c_v^* (1 + c_v^*)} \partial_x q &= 0, \end{aligned} \tag{5}$$

with R being the gas constant and c_v^* denotes the dimensionless specific heat: $c_v^* = c_v / R$. As it is apparent, only the relaxation times are free parameters, all the other coefficients are fixed. It is interesting to note that the system (5) is derived by considering a doubled hierarchy of balance equations [24,44]. The reason behind that fact is related to the more degrees of freedom within polyatomic gases [26]. It is also important to note that it is not the only way for the kinetic theory: Lebon and Clout derived a possible generalization using gradient terms as new variables [45] to

model nonlocal phenomena. In order to obtain a complete (closed) system of equations, beside the constitutive equations above, one has to use the balance laws as well:

$$\begin{aligned} \partial_t \rho + \rho_0 \partial_x v &= 0, \\ \rho_0 \partial_t v + \partial_x \Pi_d + \partial_x \Pi_s + RT_0 \partial_x \rho + R \rho_0 \partial_x T &= 0, \\ \rho_0 c \partial_t T + \partial_x q + R \rho_0 T_0 \partial_x v &= 0, \end{aligned} \tag{6}$$

i.e., the mass, momentum and energy balances, respectively.

It is worth mentioning the earlier works of Lebon and Clout [45] and Carrasi and Morro [46,47] where a similar comparison is performed. In these papers, other experiments are analyzed that are conducted by Meyer and Sessler [48], which slightly differ from the following one.

Before discussing the experimental observations about rarefied gases, one must define what a rarefied gas is. According to Klimontovich, a density parameter ε should be small for rarefied gases: $\varepsilon \ll 1$. It expresses the ratio of the occupied volume by the molecules and the overall available volume. Using the air properties at atmospheric pressure and room temperature, it turns out that $\varepsilon \approx 10^{-4}$ [49]. In other words, air at 10 atm is also rarefied or at least close to a rarefied state. Eventually this definition is not appropriate as it takes the volume corrections only into account, leaving the Knudsen number out of sight. The validity limit of the classical transport equations can be given more appropriately using the Knudsen number since it includes the mean free path as a characteristic quantity of a process. Above $Kn \approx 0.05 - 0.1$ the generalizations of the Navier-Stokes-Fourier equations must be applied [30,35].

In the following, the particular experimental observations of Rhodes are presented. That experiment highlights two essential aspects which are not independent of each other, namely, the density dependence of material parameters and the frequency/pressure (ω/p) scaling properties of the RET and NET-IV models. The discussion aims to present the necessary requirements of obtaining ω/p -dependence from continuum point of view. At the end, that measurement is evaluated using the framework of NET-IV and compared to the approach of RET.

2. Experiments

As in the case of heat conduction [23], the experimental results are considered as a benchmark problem in order to test the validity and feasibility of the corresponding generalized model. Here, one measurement performed by Rhodes [50] is discussed in detail. There are many other data in the literature [51–54], but this one is going to be sufficient to present all the necessary conclusions and difficulties arising in that field, i.e., how the scaling properties appear, the interpretation of the experiments and more importantly, the role of the material parameters.

A sonic interferometer [55] is used to measure the sound speed for various frequency-pressure ratios [50], see Figure 1 for typical data. The interferometer is placed in a dewar to maintain a constant temperature within.

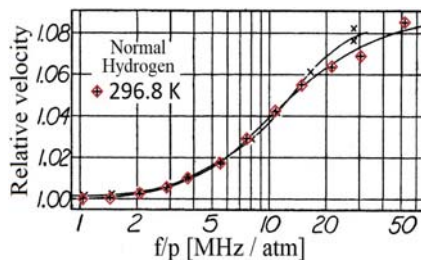


Figure 1. Speed of sound measurement performed by Rhodes [50]. The vertical axis denotes the relative speed of sound, i.e., v/v_0 , where v_0 is the speed of sound related to the normal state. The original data can be found in [50]. The relevant points are emphasized by red squares.

It has to be emphasized that the frequency was constant as well in the experiments [50], i.e., the pressure is varied over the whole interval. More appropriately, it was the density that changed during the experiment when the constant temperature has maintained. In Figure 1, the results related to normal Hydrogen is presented. The measurement is also performed using pure para-Hydrogen and the 50–50 mixture of para-ortho Hydrogen [50]. Now choosing the curve from Figure 1 corresponding to 296.8 K. Before making any advancement with the extended models, two essential aspects must be discussed. The first one is to investigate the density dependence of material parameters. Then, one can calculate the dispersion relation for the relating model (4)–(6) or (5) and (6) to model the experiment and analyze the frequency-pressure dependency, too.

2.1. Density Dependence of Material Parameters

Despite the fact that the experimental data are recorded as a function of ω/p only, it is also emphasized in the related paper of Rhodes [50] that the frequency was constant all along the measurement in an isothermal environment. It means that the pressure is varied by changing the density of the gas only. That is, changing the state of the gas from normal (or dense) state to a rarefied one must reflect the role of density dependence of material parameters.

Indeed, this is an efficient way to demonstrate the validity region of the classical Navier-Stokes-Fourier equations. As the experiment shows, some effects become essential when the gas reaches its rarefied state. Density-dependent material coefficients could represent it: some of them make the related memory and nonlocal effects (couplings) negligible for dense states and worthwhile to account in rarefied states while the others change accordingly. This is a natural expectation from theoretical point of view.

Considering the RET approach of Arima et al. [43], one can notice the following:

- the viscosities are constant: $\nu = p_0 \tau_d$ for shear viscosity and $\eta \sim p_0 \tau_s$ for the bulk part,
- the thermal conductivity is also constant: $\lambda \sim c p_0 \tau_q$ (in which c being the specific heat),
- as a consequence of the above, the relaxation times are inversely proportional with mass density: $\tau \sim \frac{1}{\rho}$.

All the other parameters are fixed and do not depend on the mass density in any way. It is important to emphasize that the essential material parameters used in their analysis are constant for very different pressures, like 10^3 or 10^5 Pa. These viscosities are derived on kinetic theory considerations (see, e.g., [56–58]) and are independent of the mass density. Since it is a theoretical value, in the following it is referred to be “physical” or theoretical quantity. It is needed to be underlined that only the “effective” or apparent properties are measurable which may differ from the theoretical ones. As Michalis et al. [59] draw the attention to the “effective” viscosity, the theoretical one must be corrected for rarefied gas flows as a function of the Knudsen number. These corrections are devoted to facilitating the phenomenological descriptions and can be compared to the above-mentioned measurements [59–63].

As the measured effective viscosity shows mass dependence, it requires corrections in both directions: from the rarefied state to the extremely dense states (up to the magnitude of 10^3 MPa). One example is the Enskog-type correction [63–65]. It is in good agreement with particular experiments that are devoted to measuring the density dependence of shear viscosity for dense states [64,66–68]. These measurements do not aim to investigate low-pressure behavior. Extrapolating the “dense data” to zero, they show the presence of non-zero viscosities at zero density (see Figure 2 for details) [56,60,66,69].

On the other hand, the measurements of Itterbeek et al. [70–72] demonstrate decreasing viscosity by decreasing the pressure. It can be only piecewise linear, its steepness changes drastically at very low pressures (1–10 Pa), and the viscosity tends to zero (Figure 3). However, it is extremely difficult to perform viscosity measurements at such a rarefied state. The outcome of the experiment depends on the size of the apparatus and could influence the results. Furthermore, evaluating such

viscosity measurement that corresponds to high Kn number, the classical Navier-Stokes theory may be insufficient and a non-local theory should be used. So to say, there could be some uncertainty regarding the values of the viscosities. From practical point of view, the density dependence seems to be natural and the measurements of Itterbeek et al. also strengthen this expectation: at zero density, there is no viscosity. From a theoretical point of view, this is contradictory to the kinetic theory in the sense of the non-zero value for viscosity in the zero-density limit. Beskok and Karniadakis [73], to overcome that contradiction, suggested a correction that is inversely proportional with the Knudsen number. The correction of the “physical” viscosity is improved by Roohi and Darbandi [74], too.

From a practical point of view again, these effective quantities are essential for modeling, for instance see [59,75–79]. In these papers, generalized constitutive laws are proposed in which apparent quantities play a central role and are used as being the coefficients in the constitutive equations, this is the case also in NET-IV. These referred problems (rheology, non-Newtonian fluids, biological materials) demonstrates that the apparent transport coefficients can depend on various quantities, especially in complex materials. Since the theoretical coefficients differ from the apparent one, at least in the sense of density dependence, it could influence the scaling properties of a model. It is discussed in the following.

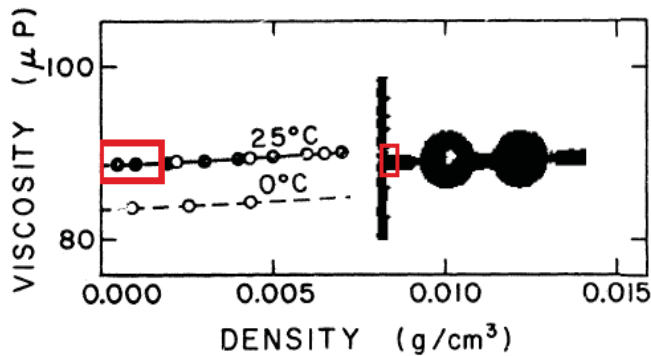


Figure 2. Density dependence of viscosity for dense gases when the non-zero viscosity at zero density appears. The original measurements can be found in [66]. Here, the red boxes show the region of interest together with the extrapolation to zero density.

p mm	$10^7 \cdot \eta$ or $10^7 \cdot \eta'$
1 Atm	889
0,0211	69,1
0,01042	39,3
0,00529	23,3
0,00267	12,0

Figure 3. Pressure dependence of viscosity for rarefied gases at room temperature. The original data can be found in [72] which is only partially depicted here.

For the sake of complete comparison with the work of Arima et al., the same assumptions are used, i.e.,

- both viscosities and the thermal conductivity are constant:
 $\nu = 8.82 \times 10^{-6}$ Pas, $\eta = 326 \times 10^{-6}$ Pas and $\lambda = 0.182$ W/(mK), respectively.
- all relaxation times and the coupling coefficients have $1/\rho$ dependence.

These follow from a scaling requirement which is discussed in the next section.

2.2. Frequency-Pressure Dependence

It is stated frequently in the early experimental papers [51–53] that the behavior of a gas depends on the ratio of frequency and pressure alone. From the point of view of kinetic theory, this scaling property is natural and follows from the Boltzmann equation.

However, it is not that straightforward from a continuum point of view. Although this scaling is correct based on the experimental data [50], it requires constant transport coefficients, $1/\rho$ dependence in the new parameters (relaxation times and coupling coefficients) and ideal gas state equation. These assumptions work for the corresponding evaluations; it could not be valid for an extensive pressure (or density, accordingly) domain, e.g., from 10 Pa to 10^8 Pa as the apparent (It is worth to note again that the continuum models consist apparent (or measurable) coefficients in the constitutive equations.) viscosities and the thermal conductivity do depend on the pressure. Moreover, it is not clear how that scaling would appear using a more general equation of state.

Furthermore, it would be worth investigating the scaling of relaxation times as the particle-wall interaction starts to dominate the process instead of the particle-particle collisions. In this kind of process, the characteristics of relaxation times are changed and thus changing the scaling properties of the equations. This could be the validity limit of the pure $1/\rho$ dependence. For example, in the experiments of Meyer and Sessler the lower pressure limit is around 0.2 Pa in which such particle-wall contribution can be especially important to consider.

This scaling property can be easily demonstrated for the classical Navier-Stokes-Fourier model by calculating the dispersion relation using the previous assumptions. Then, there no one will find terms containing the frequency ω and the pressure p separately, as follows.

Assuming the common $e^{i(\omega t - kx)}$ plane wave solution of the system (7) with the usual wave number k and frequency ω ,

$$\begin{aligned} \partial_t \rho + \rho_0 \partial_x v &= 0, \\ \rho_0 \partial_t v + \partial_x \Pi_d + \partial_x \Pi_s + RT_0 \partial_x \rho + R \rho_0 \partial_x T &= 0, \\ \rho_0 c_V \partial_t T + \partial_x q + R \rho_0 T_0 \partial_x v &= 0, \\ q + \lambda \partial_x T &= 0, \\ \Pi_d + \nu \partial_x v &= 0, \\ \Pi_s + \eta \partial_x v &= 0, \end{aligned} \tag{7}$$

and omitting the detailed derivation, one obtains the following expression for phase velocity $v_{ph} = \frac{\omega}{k}$:

$$\begin{aligned} v_{ph}^2 &= \frac{cRT\rho^2 + R^2T\rho^2 + ic\eta\rho\omega + i\lambda\rho\omega + ic\nu\rho\omega}{2c\rho^2} + \\ &+ i \frac{\sqrt{\rho^2 \left(-4c\lambda\omega(-iRT\rho + (\eta + \nu)\omega) + (iR^2T\rho - \lambda\omega + c(iRT\rho - (\eta + \nu)\omega))^2 \right)}}{2c\rho^2}. \end{aligned} \tag{8}$$

Expanding all the terms within Equation (8), the $v_{ph} = v_{ph}(\omega/p)$ dependence becomes visible and all the experimental data can be evaluated without calculating the pressure (or the mass density) independently from the frequency. In the case of the generalized NSF model, the situation is the same, and the previous assumptions ensure such scaling. Here, the final remark is made from an experimental point of view: the frequency and the pressure are separately controlled and should be documented in this way. Then, in a continuum model, the pressure dependence in any parameter could be implemented without any problem, and the model would be free from assumptions that may be made unconsciously. Moreover, it could extend the validity region of this modeling approach.

2.3. Evaluations, Comparisons and Conclusions

First, let us consider the results of Arima et al. [24,43], see Figure 4 for details. There are some important remarks on their evaluation method:

1. Dimensionless frequency $\Omega = \tau_d \omega$ is used instead of ω/p , moreover, $p\tau_d \omega/p = v\omega/p$ hence the shear viscosity ν is used to rescale the experimental data. Moreover, the papers [24,43] do not reflect the fact that the frequency was constant. It could be confusing hence it hides that the mass density ρ is the real independent variable in the equations in which all new coefficients (relaxation times and coupling parameters) depend on ρ .
2. Regarding the temperature, 295.15 K is used instead of 296.8 K. It is seemingly a small difference; however, when one attempts to calculate the mass density from the data ω/p , it leads to a different value, i.e., slightly inaccurate the data in [24]. As a consequence, even the speed of sound is slightly inaccurate that used for vertical scale.
3. In [24,43], only certain ratios of relaxation times are fitted. One has to know the pressure in order to determine their values.
4. One single parameter set is used to fit the data from papers [50,53,80] (Figure 4). The relevant data is the following: $\tau_q/\tau_d = 1.46$, $\tau_s/\tau_d = 144$, since the coupling coefficients are also proportional with the relaxation times. It is apparent from Figure 4 that for other measurements, even on the same material, these ratios may be different.

Figure 4 demonstrates that kinetic theory can model the behavior of the gas in the rarefied state.

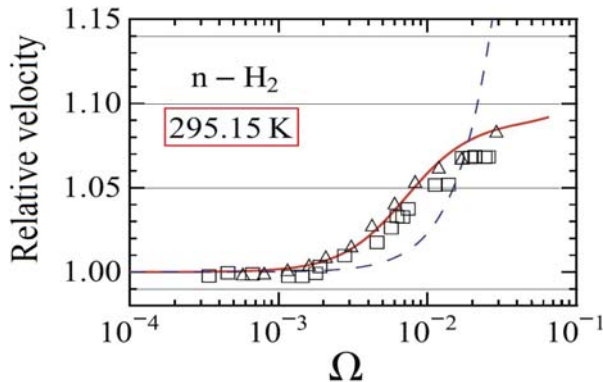


Figure 4. Calculations of Arima et al. [24]. The solid red line shows the prediction, the squares and triangles are referring to different experimental data; here, the triangles represent the data from Rhodes [50]. The dashed line shows the behavior of the Navier-Stokes-Fourier equations.

Here, using the NET-IV continuum model, only the experiment related to $T = 296.8$ K is considered for demonstrational reasons. It is not intended to evaluate the complete series of measurements. In Figure 5, two horizontal scales are used that intend to indicate the one-to-one correspondence between the ω/p and ρ . It is always possible if the frequency and the temperature are known. Although the fitting procedure is conducted by hand, it is clear that the NET-IV model is also applicable to these problems. However, it is more difficult to do due to more degrees of freedom. Tables 1 and 2 show the corresponding values of each parameter. For simplicity, in the fitting procedure the ratio of relaxation times was constrained to be the same as for RET, i.e., $\tau_q/\tau_d = 1.46$, $\tau_s/\tau_d = 144$.

Table 1. Fitted relaxation time coefficients for continuum model.

$\tau_q = \frac{t_1}{\rho}, t_1 = \left[\frac{\text{kg}\cdot\text{s}}{\text{m}^3} \right]$	$\tau_d = \frac{t_2}{\rho}, t_2 = \left[\frac{\text{kg}\cdot\text{s}}{\text{m}^3} \right]$	$\tau_s = \frac{t_3}{\rho}, t_3 = \left[\frac{\text{kg}\cdot\text{s}}{\text{m}^3} \right]$	τ_q/τ_d	τ_s/τ_d
4.526×10^{-9}	3.1×10^{-9}	4.464×10^{-7}	1.46	144

Table 2. Fitted coupling coefficients for continuum model.

$\alpha_{12} = \frac{a_{12}}{\rho}, a_{12} = \left[\frac{\text{kg}\cdot\text{s}}{\text{m}^3} \right]$	$\beta_{12} = \frac{b_{12}}{\rho}, b_{12} = \left[\frac{\text{kg}\cdot\text{s}}{\text{m}^3} \right]$	$\alpha_{21} = \frac{a_{21}}{\rho}, a_{21} = \left[\frac{\text{kg}}{\text{m}\cdot\text{s}} \right]$	$\beta_{21} = \frac{b_{21}}{\rho}, b_{21} = \left[\frac{\text{kg}}{\text{m}\cdot\text{s}} \right]$
1.7×10^{-6}	1.27×10^{-6}	1.3×10^{-4}	1.55×10^{-5}

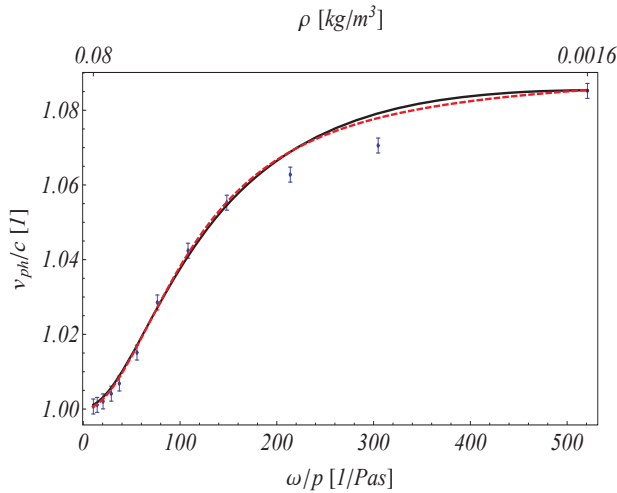


Figure 5. Evaluation using NET-IV (thick black line). The pressure starts at 1 atm and decreases to 2000 Pa, $\omega = 1$ MHz. Error bars are placed for each measurement point to indicate the uncertainty of digitalizing data, its magnitude is ± 2.5 m/s. The red dashed line shows the results of Arima et al. [24].

3. Discussion

The models originated from RET and NET-IV are briefly introduced and tested on a particular experiment performed by Rhodes. It is apparent from the experimental data that the rarefaction in a Hydrogen gas shows substantial deviation from its dense state. Here, the speed of sound data can be evaluated without any obstacles in NET-IV as well, but this evaluation highlights some crucial aspects.

First, we note the difference between the theoretical and measured properties which has great importance in kinetic theory. In contrast, a continuum model does not propose this distinction, it is not possible to calculate the “physical” (theoretical) coefficient without a detailed micromechanism. Moreover, especially from practical point of view, the NET-IV model contains the “effective” (measurable) quantities which have density dependence as well, beside the temperature, according to the referred literature. Since the continuum approach does consist of the measurable transport coefficients, it keeps the continuum model on a more general level that is not restricted specifically, in contrast to the kinetic theory. In the present experimental evaluation, constant viscosities and thermal conductivity are used in order to keep the model compatible with the kinetic theory.

Second, it is advantageous if all the data are given in the experiment; the frequency-pressure ratio could be insufficient, especially when the effective transport coefficients are not constant respect to the pressure. In continuum theory, it does matter what is changed: the frequency, the pressure, or both. In that sense, it is confusing to use dimensionless frequency, especially when all the necessary data are

given for the appropriate scale. Besides that fact, the application of dimensionless quantities is still valid, but their use makes it a bit more difficult to interpret the experimental data. Moreover, in the end, even the kinetic approach requires the knowledge about the pressure in order to evaluate the relaxation times and the coupling coefficients.

Moreover, it is also shown that besides the frequency/pressure scaling of experimental data, it is not necessarily obtained in the dispersion relations of a continuum model, merely by restrictive assumptions of constant coefficients. However, it is worth noting that if every experimental data are given appropriately, that is, the frequency and pressure are given separately, then the experimental data become evaluable even if the ω/p scaling is not visible in the dispersion relations. Furthermore, recalling the experimental data of Itterbeek and Gracki et al. in which the viscosity depends on the mass density, this is clear that its inclusion into the models would strongly influence the scaling properties as well. Thus, one question remains: which transport property is important from the aspect of the scaling, the theoretical one or the measurable one?

The difference between the presented approaches originates in the preassumptions. Using kinetic theory, a detailed interaction is assumed, and it restricts some degrees of freedom. On the other hand, in NET-IV, it is not necessary to make any preassumption regarding the type of the fluid, while in kinetic theory it is fixed as a first step, and the derived model such as Equation (5) will be valid only for this restricted case, in the price of the number of free coefficients. As mentioned in the introduction, one of the main difficulties is the fitting of free parameters in the model of NET-IV (4), that is, 7 coefficients are to be fitted instead of 3 that presented by Equation (5). It can be reduced if one adopts some knowledge from the kinetic approach and applies in the continuum model, such as the ratio of relaxation times. This disadvantage could be an advantage if the number of equations is still enough to describe a three-dimensional process on the contrary to the kinetic theory where the momentum expansion generates a large system of equations for a more general situation, for instance in the low temperature heat conduction problems.

As a final remark, it is essential to realize that these approaches extend each other from different directions. While NET-IV keeps the models as general as possible, RET builds a detailed one, with much more knowledge about the coefficients. Although the underlying physical picture is different, the resulting system of equations can be compatible with each other.

Funding: This research was funded by National Research, Development and Innovation Office—NKFIH K116197, K124366 and KH130378. The research reported in this paper was also supported by the Higher Education Excellence Program of the Ministry of Human Capacities in the frame of Nanotechnology research area of Budapest University of Technology and Economics (BME FIKP-NANO).

Acknowledgments: The author is thankful to Henning Struchtrup and Péter Ván for valuable discussions.

Conflicts of Interest: The author declares no conflict of interest.

References

1. Chester, M. Second sound in solids. *Phys. Rev.* **1963**, *131*, 2013–2015. [[CrossRef](#)]
2. Guyer, R.A.; Krumhansl, J.A. Thermal Conductivity, Second Sound, and Phonon Hydrodynamic Phenomena in Nonmetallic Crystals. *Phys. Rev.* **1966**, *148*, 778–788. [[CrossRef](#)]
3. Jackson, H.E.; Walker, C.T.; McNelly, T.F. Second sound in NaF. *Phys. Rev. Lett.* **1970**, *25*, 26–28. [[CrossRef](#)]
4. Rogers, S.J. Transport of heat and approach to second sound in some isotropically pure alkali-halide crystals. *Phys. Rev. B* **1971**, *3*, 1440. [[CrossRef](#)]
5. Narayanamurti, V.; Dynes, R.C. Observation of second sound in bismuth. *Phys. Rev. Lett.* **1972**, *28*, 1461–1465. [[CrossRef](#)]
6. Gyarmati, I. On the wave approach of thermodynamics and some problems of non-linear theories. *J. Non-Equilib. Thermodyn.* **1977**, *2*, 233–260. [[CrossRef](#)]
7. Joseph, D.D.; Preziosi, L. Heat waves. *Rev. Mod. Phys.* **1989**, *61*, 41. [[CrossRef](#)]
8. Joseph, D.D.; Preziosi, L. Addendum to the paper on heat waves. *Rev. Mod. Phys.* **1990**, *62*, 375–391. [[CrossRef](#)]

9. Dreyer, W.; Struchtrup, H. Heat pulse experiments revisited. *Contin. Mech. Thermodyn.* **1993**, *5*, 3–50. [[CrossRef](#)]
10. McNelly, T.F.; Rogers, S.J.; Channin, D.J.; Rollefson, R.J.; Goubau, W.M.; Schmidt, G.E.; Krumhansl, J.A.; Pohl, R.O. Heat pulses in NaF: Onset of second sound. *Phys. Rev. Lett.* **1970**, *24*, 100–102. [[CrossRef](#)]
11. McNelly, T.F. Second Sound and Anharmonic Processes in Isotopically Pure Alkali-Halides. Ph.D. Thesis, Cornell University, Ithaca, NY, USA, 1974.
12. Kovács, R.; Ván, P. Generalized heat conduction in heat pulse experiments. *Int. J. Heat Mass Transf.* **2015**, *83*, 613–620. [[CrossRef](#)]
13. Ván, P. Weakly nonlocal irreversible thermodynamics—The Guyer-Krumhansl and the Cahn-Hilliard equations. *Phys. Lett. A* **2001**, *290*, 88–92. [[CrossRef](#)]
14. Ván, P.; Fülöp, T. Universality in heat conduction theory—Weakly nonlocal thermodynamics. *Annalen der Physik (Berlin)* **2012**, *524*, 470–478. [[CrossRef](#)]
15. Chen, G. Ballistic-diffusive heat-conduction equations. *Phys. Rev. Lett.* **2001**, *86*, 2297–2300. [[CrossRef](#)]
16. Cimmelli, V.A. Different thermodynamic theories and different heat conduction laws. *J. Non-Equilib. Thermodyn.* **2009**, *34*, 299–333. [[CrossRef](#)]
17. Ván, P. Theories and heat pulse experiments of non-Fourier heat conduction. *Commun. Appl. Ind. Math.* **2016**, *7*, 150–166. [[CrossRef](#)]
18. Jou, D.; Casas-Vázquez, J.; Lebon, G. *Extended Irreversible Thermodynamics*, 4th ed.; Springer: Berlin, Germany, 2010.
19. Sellitto, A.; Cimmelli, V.A.; Jou, D. *Mesoscopic Theories of Heat Transport in Nanosystems*; Springer: Berlin, Germany, 2016.
20. Szücs, M.; Fülöp, T. Kluitenberg-Verhás rheology of solids in the GENERIC framework. *arXiv* **2019**, arXiv:1812.07052.
21. Müller, I.; Ruggeri, T. *Rational Extended Thermodynamics*; Springer: Berlin, Germany, 1998.
22. Kovács, R.; Ván, P. Models of Ballistic Propagation of Heat at Low Temperatures. *Int. J. Thermophys.* **2016**, *37*, 95. [[CrossRef](#)]
23. Kovács, R.; Ván, P. Second sound and ballistic heat conduction: NaF experiments revisited. *Int. J. Heat Mass Transf.* **2018**, *117*, 682–690. [[CrossRef](#)]
24. Ruggeri, T.; Sugiyama, M. *Rational Extended Thermodynamics Beyond the Monatomic Gas*; Springer: Berlin, Germany, 2015.
25. Kovács, R. Heat Conduction beyond Fourier's Law: Theoretical Predictions and Experimental Validation. Ph.D. Thesis, Budapest University of Technology and Economics (BME), Budapest, Hungary, 2017.
26. Kovács, R.; Madjarević, D.; Simić, S.; Ván, P. Theories of rarefied gases. *arXiv* **2018**, arXiv:1812.10355.
27. Both, S.; Czél, B.; Fülöp, T.; Gróf, G.; Gyenis, Á.; Kovács, R.; Ván, P.; Verhás, J. Deviation from the Fourier law in room-temperature heat pulse experiments. *J. Non-Equilib. Thermodyn.* **2016**, *41*, 41–48. [[CrossRef](#)]
28. Ván, P.; Berezovski, A.; Fülöp, T.; Gróf, G.; Kovács, R.; Lovas, Á.; Verhás, J. Guyer-Krumhansl-type heat conduction at room temperature. *EPL* **2017**, *118*, 50005. [[CrossRef](#)]
29. Fülöp, T.; Kovács, R.; Lovas, Á.; Rieth, Á.; Fodor, T.; Szücs, M.; Ván, P.; Gróf, G. Emergence of non-Fourier hierarchies. *Entropy* **2018**, *20*, 832. [[CrossRef](#)]
30. Struchtrup, H. *Macroscopic Transport Equations for Rarefied Gas Flows*; Springer: Berlin, Germany, 2005.
31. Nyíri, B. On the entropy current. *J. Non-Equilib. Thermodyn.* **1991**, *16*, 179–186. [[CrossRef](#)]
32. Jou, D.; Casas-Vázquez, J.; Lebon, G. Extended Irreversible Thermodynamics. *Rep. Prog. Phys.* **1988**, *51*, 1105. [[CrossRef](#)]
33. Alvarez, F.X.; Jou, D.; Sellitto, A. Phonon hydrodynamics and phonon-boundary scattering in nanosystems. *J. Appl. Phys.* **2009**, *105*, 014317. [[CrossRef](#)]
34. Guo, Y.; Wang, M. Phonon hydrodynamics and its applications in nanoscale heat transport. *Phys. Rep.* **2015**, *595*, 1–44. [[CrossRef](#)]
35. Struchtrup, H. Resonance in rarefied gases. *Contin. Mech. Thermodyn.* **2012**, *24*, 361–376. [[CrossRef](#)]
36. Berezovski, A.; Ván, P. Microinertia and internal variables. *arXiv* **2015**, arXiv:1504.03485.
37. Berezovski, A.; Ván, P. *Internal Variables in Thermoelasticity*; Springer: Basel, Switzerland, 2017.
38. Verhás, J. *Thermodynamics and Rheology*; Springer: Dordrecht, The Netherlands, 1997.
39. Meixner, J. Absorption und Dispersion des Schalles in Gasen mit Chemisch Reagierenden und Anregbaren Komponenten. I. Teil. *Annalen der Physik* **1943**, *435*, 470–487. (In German) [[CrossRef](#)]

40. Sellitto, A.; Cimmelli, V.A.; Jou, D. Entropy flux and anomalous axial heat transport at the nanoscale. *Phys. Rev. B* **2013**, *87*, 054302. [[CrossRef](#)]
41. Arima, T.; Taniguchi, S.; Ruggeri, T.; Sugiyama, M. Extended thermodynamics of dense gases. *Contin. Mech. Thermodyn.* **2012**, *24*, 271–292. [[CrossRef](#)]
42. Arima, T.; Taniguchi, S.; Ruggeri, T.; Sugiyama, M. Extended thermodynamics of real gases with dynamic pressure: An extension of Meixner’s theory. *Phys. Lett. A* **2012**, *376*, 2799–2803. [[CrossRef](#)]
43. Arima, T.; Taniguchi, S.; Ruggeri, T.; Sugiyama, M. Dispersion relation for sound in rarefied polyatomic gases based on extended thermodynamics. *Contin. Mech. Thermodyn.* **2013**, *25*, 727–737. [[CrossRef](#)]
44. Pavić, M.; Ruggeri, T.; Simić, S. Maximum entropy principle for rarefied polyatomic gases. *Phys. A Stat. Mech. Appl.* **2013**, *392*, 1302–1317. [[CrossRef](#)]
45. Lebon, G.; Cloot, A. Propagation of ultrasonic sound waves in dissipative dilute gases and extended irreversible thermodynamics. *Wave Motion* **1989**, *11*, 23–32. [[CrossRef](#)]
46. Carrasi, M.; Morro, A. A modified Navier-Stokes equation, and its consequences on sound dispersion. *Il Nuovo Cimento B* **1972**, *9*, 321–343. [[CrossRef](#)]
47. Carrasi, M.; Morro, A. Some remarks about dispersion and absorption of sound in monatomic rarefied gases. *Il Nuovo Cimento B* **1973**, *13*, 281–289. [[CrossRef](#)]
48. Meyer, E.; Sessler, G. Schallausbreitung in gasen bei hohen frequenzen und sehr niedrigen drucken. *Zeitschrift für Physik* **1957**, *149*, 15–39. (In German) [[CrossRef](#)]
49. Klimontovich, Y.L. *Statistical Theory of Open Systems: A Unified Approach to Kinetic Description of Processes in Active Systems*; Springer: Dordrecht, The Netherlands, 1995.
50. Rhodes, J.E., Jr. The velocity of sound in hydrogen when rotational degrees of freedom fail to be excited. *Phys. Rev.* **1946**, *70*, 932. [[CrossRef](#)]
51. Sette, D.; Busala, A.; Hubbard, J.C. Energy transfer by collisions in vapors of chlorinated methanes. *J. Chem. Phys.* **1955**, *23*, 787–793. [[CrossRef](#)]
52. Greenspan, M. Propagation of sound in five monatomic gases. *J. Acoust. Soc. Am.* **1956**, *28*, 644–648. [[CrossRef](#)]
53. Sluijter, C.G.; Knaap, H.F.P.; Beenakker, J.J.M. Determination of rotational relaxation times of hydrogen isotopes by sound absorption measurements at low temperatures I. *Physica* **1964**, *30*, 745–762. [[CrossRef](#)]
54. Sluijter, C.G.; Knaap, H.F.P.; Beenakker, J.J.M. Determination of rotational relaxation times of hydrogen isotopes by sound absorption measurements at low temperatures II. *Physica* **1965**, *31*, 915–940. [[CrossRef](#)]
55. Stewart, J.L. A variable path ultrasonic interferometer for the four megacycle region with some measurements on air, co₂, and h₂. *Rev. Sci. Instrum.* **1946**, *17*, 59–65. [[CrossRef](#)] [[PubMed](#)]
56. Truesdell, C.; Muncaster, R.G. *Fundamentals of Maxwell’s Kinetic Theory of a Simple Monatomic Gas: Treated as a Branch of Rational Mechanics*; Academic Press: Cambridge, MA, USA, 1980; Volume 83.
57. Pollard, W.G.; Present, R.D. On gaseous self-diffusion in long capillary tubes. *Phys. Rev.* **1948**, *73*, 762. [[CrossRef](#)]
58. Chapman, S.; Cowling, T. *The Mathematical Theory of Non-uniform Gases*, 3rd ed.; Cambridge University Press: New York, NY, USA, 1970.
59. Michalis, V.K.; Kalarakis, A.N.; Skouras, E.D.; Burganos, V.N. Rarefaction effects on gas viscosity in the Knudsen transition regime. *Microfluid. Nanofluidics* **2010**, *9*, 847–853. [[CrossRef](#)]
60. Cohen, Y.; Sandler, S.I. The viscosity and thermal conductivity of simple dense gases. *Ind. Eng. Chem. Fundam.* **1980**, *19*, 186–188. [[CrossRef](#)]
61. van der Gulik, P.S.; Trappeniers, N.J. The viscosity of argon at high densities. *Phys. A Stat. Mech. Appl.* **1986**, *135*, 1–20. [[CrossRef](#)]
62. van der Gulik, P.S.; Trappeniers, N.J. Application of Enskog theory on the viscosity of argon. *Physica B + C* **1986**, *139*, 137–139. [[CrossRef](#)]
63. van der Gulik, P.S.; ten Seldam, C.A. Density dependence of the viscosity of some noble gases. *Int. J. Thermophys.* **2002**, *23*, 15–26. [[CrossRef](#)]
64. Dymond, J.H. Corrections to the Enskog theory for viscosity and thermal conductivity. *Physica B* **1987**, *144*, 267–276. [[CrossRef](#)]
65. Umla, R.; Vesovic, V. Viscosity of liquids—Enskog-2 σ model. *Fluid Phase Equilib.* **2014**, *372*, 34–42. [[CrossRef](#)]
66. Gracki, J.A.; Flynn, G.P.; Ross, J. *Viscosity of Nitrogen, Helium, Hydrogen, and Argon from –100 to 25 c up to 150–250 Atmospheres*; Project SQUID Technical Report; Purdue University: Lafayette, IN, USA, 1969; 33p.

67. Gracki, J.A.; Flynn, G.P.; Ross, J. Viscosity of Nitrogen, Helium, Hydrogen, and Argon from -100 to 25 c up to 150 – 250 atm. *J. Chem. Phys.* **1969**, *9*, 3856–3863. [[CrossRef](#)]
68. Haynes, W.M. Viscosity of gaseous and liquid argon. *Physica* **1973**, *67*, 440–470. [[CrossRef](#)]
69. Liboff, R.L. *Kinetic Theory: Classical, Quantum, and Relativistic Descriptions*; Springer Science & Business Media: Basel, Switzerland, 2003.
70. van Itterbeek, A.; Keesom, W.H. Measurements on the viscosity of helium gas between 293 and 1.6 k. *Physica* **1938**, *5*, 257–269. [[CrossRef](#)]
71. van Itterbeek, A.; Claes, A. Measurements on the viscosity of hydrogen-and deuterium gas between 293 K and 14 K. *Physica* **1938**, *5*, 938–944. [[CrossRef](#)]
72. van Itterbeek, A.; van Paemel, O. Measurements on the viscosity of gases for low pressures at room temperature and at low temperatures. *Physica* **1940**, *7*, 273–283. [[CrossRef](#)]
73. Beskok, A.; Karniadakis, G.E. Report: A model for flows in channels, pipes, and ducts at micro and nano scales. *Microscale Thermophys. Eng.* **1999**, *3*, 43–77.
74. Roohi, E.; Darbandi, M. Extending the Navier–Stokes solutions to transition regime in two-dimensional micro-and nanochannel flows using information preservation scheme. *Phys. Fluids* **2009**, *21*, 082001. [[CrossRef](#)]
75. Galindo-Rosales, F.J.; Rubio-Hernández, F.J.; Sevilla, A. An apparent viscosity function for shear thickening fluids. *J. Non-Newton. Fluid Mech.* **2011**, *166*, 321–325. [[CrossRef](#)]
76. Møller, P.C.F.; Fall, A.; Bonn, D. Origin of apparent viscosity in yield stress fluids below yielding. *Europhys. Lett.* **2009**, *87*, 38004. [[CrossRef](#)]
77. Falls, A.H.; Musters, J.J.; Ratulowski, J. The apparent viscosity of foams in homogeneous bead packs. *SPE Reserv. Eng.* **1989**, *4*, 155–164. [[CrossRef](#)]
78. Lipowsky, H.H.; Usami, S.; Chien, S. In vivo measurements of “apparent viscosity” and microvessel hematocrit in the mesentery of the cat. *Microvasc. Res.* **1980**, *19*, 297–319. [[CrossRef](#)]
79. Metzner, A.B.; Otto, R.E. Agitation of non-Newtonian fluids. *AIChE J.* **1957**, *3*, 3–10. [[CrossRef](#)]
80. Winter, T.G.; Hill, G.L. High-temperature ultrasonic measurements of rotational relaxation in hydrogen, deuterium, nitrogen, and oxygen. *J. Acoust. Soc. Am.* **1967**, *42*, 848–858. [[CrossRef](#)]



© 2019 by the author. Licensee MDPI, Basel, Switzerland. This article is an open access article distributed under the terms and conditions of the Creative Commons Attribution (CC BY) license (<http://creativecommons.org/licenses/by/4.0/>).

A Note on the Entropy Force in Kinetic Theory and Black Holes

Rudolf A. Treumann ^{1,†} and Wolfgang Baumjohann ^{2,*,†} 

¹ International Space Science Institute, 3012 Bern, Switzerland

² Space Research Institute, Austrian Academy of Sciences, Schmiedlstr. 6, 8042 Graz, Austria

* Correspondence: Wolfgang.Baumjohann@oeaw.ac.at

† These authors contributed equally to this work.

Received: 2 June 2019; Accepted: 19 July 2019; Published: 23 July 2019

Abstract: The entropy force is the collective effect of inhomogeneity in disorder in a statistical many particle system. We demonstrate its presumable effect on one particular astrophysical object, the black hole. We then derive the kinetic equations of a large system of particles including the entropy force. It adds a collective therefore integral term to the Klimontovich equation for the evolution of the one-particle distribution function. Its integral character transforms the basic one particle kinetic equation into an integro-differential equation already on the elementary level, showing that not only the microscopic forces but the hole system reacts to its evolution of its probability distribution in a holistic way. It also causes a collisionless dissipative term which however is small in the inverse particle number and thus negligible. However it contributes an entropic collisional dissipation term. The latter is defined via the particle correlations but lacks any singularities and thus is large scale. It allows also for the derivation of a kinetic equation for the entropy density in phase space. This turns out to be of same structure as the equation for the phase space density. The entropy density determines itself holistically via the integral entropy force thus providing a self-controlled evolution of entropy in phase space.

Keywords: entropy force; non-equilibrium phenomena; kinetic theory; entropic phase space density; black hole entropy

1. Introduction: Entropy Force

About thirty years ago, Prigogine [1] attempted a microscopic theory of entropy assuming that, by some quantum process, seeds of entropy could be generated. Such a hypothetical process would, in the early universe, possibly lay down the direction of time. Unfortunately, so far, such microscopic sources of entropy have not been confirmed. It seems that they can hardly be expected because quantum uncertainty itself is a stochastic process, which by its own nature does not contain any direction. It is hard to believe that it could lead to entropy production if not aided by some kind of dissipative interaction. Entropy is a thermodynamic concept, which by itself requires an underlying dynamics, which allows for the presence of many states that a system consisting of many subsystems, components, particles would be able to occupy.

More recently, it has been speculated [2] that that kind of a mesoscopic entropy in quantum string theory could cause gravity to emerge from the action of a quantum entropic force as a gradient of entropy generated in string interactions, intended to provide a physical basis for the so-called modified Newtonian gravity, which proposes that Newton's law should be corrected on the large scales to eliminate the problem of dark matter in astronomy.

From a completely different point of view, the idea of an entropy force has been picked up in the discussion of maximum entropy methods in prediction theory [3,4] in open systems where the probabilistic version of entropy depends on space and time, propagates into the future

and, thus, has a finite gradient in space and time, which is interpreted as force. It apparently is capable of allowing, based on maximization of entropy, predicting the time evolution of the system, an interesting and possibly far-reaching predictive concept. In a sufficiently small closed system, it necessarily must describe the evolution of entropy towards a finite thermal state of maximum entropy. Recently, entropy forces have also been applied to molecular dynamics in proteins ([5] and the references therein). Spatial smallness is required by causality to enable synchronization. Therefore, the concept applies to the universe on the cosmological timescale only in order to allow for homogenization of entropy. On any local scale, the entropy produced in the classical system represents a localized excess in entropy. If not artificially confined, this excess tends to expand and affect its environment. This necessarily generates a local entropy force, a classical force that should not be mixed up with the above-mentioned entropic force in string systems. This force follows from the first law in thermodynamics:

$$dE = TdS - PdV \quad (1)$$

which relates the three different forms of energy E , pressure PV , and entropy TS . Gradients in energy, pressure, and temperature are known to be forces, and the gradient of volume causes dispersion, flows, and forces, for instance in charged systems.

In a similar vein, a gradient in entropy corresponds to a collective macroscopic effect as the entropy tends to expand and maximize. This is a purely macroscopic effect indeed because, similar to density/volume and pressure, the entropy S is defined only for macroscopic systems, consisting of a large number of subsystems, to which finite temperature and density can be assigned and which occupy a finite volume. In the first law, it is only the energy E that maintains its meaning also in the microscopic world down to only one particle, to which assigning temperature makes no sense. The entropy potential $U = TS$ indeed is not just a thermodynamic potential; it is also a real potential always being positive and thus repulsive. The entropy force is then given as its gradient:

$$\mathbf{F} = -\nabla U \quad (2)$$

as usually taken negative. It consist of two parts, a thermal force $-\nabla T$, which is of no interest here, and the genuine entropy force:

$$\mathbf{F}_S = -T\nabla S \quad (3)$$

This might look trivial; however, it is not, as we will demonstrate below with a particular example: the black hole.

However, before proceeding, we recall that, since both T and S are positive definite, the entropy force is repulsive in the direction negative to the gradient of entropy. This means that an accumulation of entropy at some location, if not artificially confined to a box, will act outward. Adopting an interpretation of entropy as disorder, which by no means is generally justified, thus implies that disorder tends to infect its external region. It has the tendency to expand.

With temperature T in energy units, the entropy S has no dimension. Moreover, the product of temperature and entropy is a scalar function with the dimension of a potential. For scalar temperature, i.e., at temperature isotropy, S is also a scalar. Under conditions of anisotropic temperature, the inverse temperature becomes a vector [6], and thus, S becomes a vector as well (more generally, both become tensors). In the interest of simplicity, we do not consider this case in the following.

This entropy force does not depend on particle mass or charge, at least not explicitly. Mass is contained in temperature and energy, but there is no explicit reference to it in the definition of the entropy force. Thus, for a given temperature, all particles independent of their properties will be subject to the same entropy force. In this sense, the entropy force is a general mechanical force seeking to restore smoothness in disorder on a higher level of disorder, completely independent of which kind of particles have contributed to the inhomogeneity in disorder.

By its nature, the above entropy force is a long-range force. It does not compete with the Coulomb force on the short scales. From the first law, one realizes that the main force it competes with is the

pressure gradient. Both are proportional to the temperature, which thus drops out when comparing the forces. Both are proportional to the density gradient. Thus, in the presence of changing volume, the entropy force adds to or diminishes the effect of the pressure force.

2. Entropy Force of Schwarzschild Black Holes

Let us turn to our example, the Schwarzschild black hole, which we chose for demonstration because of its simplicity and cleanness compared to Kerr or charged Nordstrom black holes. Black holes are known to carry entropy [7–12]. More correctly, since the interior of the black hole is not accessible, it is the black hole horizon that carries an entropy. This came as a surprise, as it implies that the horizon possesses a temperature and therefore must be considered as a macrosystem, which occupies a large number of states. Microscopically, this puzzle has not been resolved until today, even though a large number of attempts have been put forward to elucidate the internal structure of the horizon (see [13–17] and several others). Such considerations were based on the Bekenstein–Hawking entropy and the Hawking radiation of a black hole [11], which is attributed to its finite entropy and thus finite temperature. It implies the existence of a thermodynamic for the black hole horizon with the implication that the horizon physics involves a very large number of states that can be occupied. Jacobson [15] extended this concept to horizons in general in order to develop a thermodynamics of gravitational horizons from which he found that Einstein’s gravitational field equations formally play the role of equations of state. This concept was reviewed and extended subsequently by Padmanabhan [16] to speculate about the general importance of horizon physics in general relativity and cosmology, suggesting that all the physics is holographically contained in the physics of horizons.

Schwarzschild black holes are in the first place classical objects. However, their entropy includes the quantum nature of matter at the horizon (cf., e.g., [13]), which is induced by the sharpness of the horizon and indicates that black holes are not purely classical. Let us ask what the entropy force related to the presence of the horizon would be.

2.1. Schwarzschild Constant

A Schwarzschild black hole of mass M has energy Mc^2 , radius $R_S = 2GM/c^2$, and spherical surface $A_{BH} = 4\pi R_S^2$. Forming the ratio of the total black hole energy and the Schwarzschild radius yields:

$$F_S = Mc^2/R_S = c^4/2G = 6.053 \times 10^{43} \text{ N} \tag{4}$$

a constant that has the dimension of a force and that we call the Schwarzschild constant. This is a universal constant, whose value is independent of any property of the black hole, a force. This force is the Planck force, which so far has not been given any physical meaning. We prefer to call it the Schwarzschild constant as the black hole is the only place where it naturally arises.

2.2. Horizon Entropy Force

The entropy of the black hole horizon is the (dimensionless) Bekenstein–Hawking entropy:

$$S_{BH} = \frac{A_{BH}}{4\lambda_P^2} = \frac{\pi R_S^2 c^3}{G\hbar} \tag{5}$$

with λ_P the Planck length, and its corresponding black-body radiation temperature is the Hawking temperature:

$$T^{BH} = k_B T_H = \hbar c^3/8\pi GM \tag{6}$$

here given in energy units. This yields trivially the Bekenstein–Hawking energy $E_{BH} = T^{BH} S_{BH} = \frac{1}{2} Mc^2$ of the horizon, just half the black hole energy. For a classical black hole, the horizon has no width, suggesting an infinite gradient when crossing it. In order to obtain the force, the relevant distance

taken for the gradient is the diameter $2R_S$ of the black hole, yielding for the modulus of the outward directed entropy force:

$$F_S^{BH} \sim \frac{T^{BH} S_{BH}}{2R_S} = \frac{c^4}{8G} = \frac{F_S}{4} \approx 1.5 \times 10^{43} \text{ N} \tag{7}$$

a quarter of the Schwarzschild constant. A more precise calculation would correct for the numerical factor, which, however, is of order $O(1)$. Formally, the Schwarzschild constant, and thus also the entropy force at the horizon, is in fact a very strong force. Its presence, if real, at the horizon is rather surprising. It suggests that the physics of what happens inside the black hole is not really well enough understood.

Forming the ratio of the gravitational force $F_G^{BH} = -GmM/R_S^2$ any particle of mass m experiences when approaching and touching the black hole horizon to this horizon entropy force, one obtains:

$$\left| F_G^{BH} / F_S^{BH} \right| \sim m/M \tag{8}$$

For any massive black hole and any normal mass particle, this is a small number. A light particle $m \ll M$ will barely overcome this repulsion when hitting the horizon. To overcome it, it requires the collision of two black holes of nearly equal mass $M_1 \sim M_2$, which would make the ratio $m/M \rightarrow M_1/M_2 \approx 1$. Collisions of such nearly-equal mass black holes have only recently been detected by the spectacular observation of gravitational waves.

At its horizon, the entropy force of a massive black hole $M \gg m$ compensates by far for the black hole’s gravitational attraction on m . This is a consequence of the enormous sharpness of the entropy gradient at the horizon where the entropy is restricted to the surface of the horizon only, whose width is not precisely given, but as generally assumed, is of the order of a few Planck lengths λ_p only. This force is remarkable only at the horizon itself when the mass m gets into contact with the horizon. It will not be susceptible at some larger finite distance.

This follows from the fact that there is no known classical entropy field that would allow the entropy force to extend a distance ahead of the black hole into the surrounding space and is conjectured from the complete absence of any radial dependence of the force outside the horizon. In this picture, the entropy gradient is felt only locally across the horizon of the black hole when the particle touches it, an instant that is never seen or experienced by an external observer for whom the time the particle approaches the horizon stretches out to infinity. The particle, however, does in fact experience the presence of the black hole and, assuming that it remains intact having survived the enormous attraction during its inward spiraling motion, in its proper frame at proper time, really touches the horizon and wants to cross it. Shortly before this instant, however, the horizon entropy comes into play and stops the particle.

The gravitational force on the particle of mass m (assuming it retains its mass till reaching the horizon, which is certainly not the case) would overcome the entropic force still only at a small fraction of the radius given by:

$$\frac{\Delta r}{R_S} \approx \left(\frac{M_\odot}{M} \right)^{\frac{1}{2}} \left(\frac{m}{M_\odot} \right)^{\frac{1}{2}} \approx 3 \times 10^{-28} \left(\frac{M_\odot}{M} \right)^{\frac{1}{2}} \tag{9}$$

where on the right, we assumed a proton. For instance, this distance for a proton and a $M = 10^8 M_\odot$ massive black hole is of the order of only $\Delta r \sim 10^{-23}$ m, deep inside the submicroscopic domain, though ten orders of magnitude larger than the Planck length. If it applies, then it would cause accumulation of matter in a film of roughly this width only.

The classical picture does not inform about the microscopic physics going on when this happens. Elucidating the real physics requires a quantum electrodynamic calculation for instance along the paths drawn by Hawking when calculating the black-body black hole radiation. Referring to Hawking’s results implies that the horizon will be surrounded by a dilute and thin radial dust film of newly- and

continuously-created virtual particles, which sustain and support the weak Hawking radiation when tunneling into reality. The radial extension of this dust film implies a softening of the radial entropy gradient corresponding to a finite radial extension of the action region of the entropy force. It would be this radial domain where the light particle in its inward spiraling motion becomes trapped and retarded and is ultimately stopped and prevented from entering the interior of the black hole.

2.3. Body Entropy

What happens to the entropy inside the black hole would be important to know (cf. [18] for a discussion of Hawking radiation inside black hole geometry) in order to resolve the puzzle. It is rather improbable that the entropy would be constant inside the black hole, as this would require that the interior is in thermal equilibrium, which it is certainly not when being under the conditions of collapsing matter under gravitational attraction. One might speculate that towards deeper inside, the entropy decreases with decreasing radius, because the surface decreases as $\sim(r/R_S)^2$. Assigning a Hawking temperature to each shell of such a radius, the corresponding Hawking temperature would increase only as $\sim R_S/r$. Thus any entropy-force potential should decrease towards the interior like $\sim r/R_S$. The outer black hole horizon becomes the black hole shell of maximum entropy, the radius where the black hole entropy maximizes. The interior entropy force, the gradient of the potential, remains constant throughout the entire interior volume of the black hole with the exclusion of the singularity.

Notably, this entropy force points towards the interior of the hole, i.e., towards the singularity. It thus adds to the already existing gravitational acceleration being felt throughout the entire interior. By pointing inside towards decreasing radius r , it would push any existing massive particle that made it across the horizon into the singularity up in energy. This probably means that classically, no massive particle can make it across the horizon. It can only be non-massive radiation that crosses inward: photons and gluons, the massless bosons of electrodynamics and chromodynamics. Whether massive particles like electrons and quarks can indeed tunnel across the horizon remains a question that cannot be answered in the realm of classical physics.

Admittedly, these considerations are rather speculative as long as the evolution of entropy with increasing radial distance from the horizon towards inside and also outside the black hole has not been microscopically inferred. In any case, the question of the horizon representing a sharp surface remains a question that probably only quantum gravity can give an ultimate answer to, as it must proceed on scales close to the Planck scale λ_P . This is not our concern here.

2.4. Visibility and Matter Digestion

Naked isolated black holes are invisible except for their weak and so far inaccessible Hawking radiation. The question why black holes, which are embedded into surrounding matter, when accreting become visible at all is comparably easy to answer. Any mass flow approaching the horizon before encounter feels the gravitational field of the black hole, spirals in, accelerates, heats up, becomes partially transformed into radiation, and starts radiating violently. General relativity indicates that this process stretches time to infinity. Hence, even though the matter starts as material particles that cannot be digested by the black hole, because matter cannot pass the horizon due to the barrier the classical entropic force provides for massive particles, the emitted radiation is visible for long. The latter is a well-known fact, and though radiation from accreting black hole suspects has been observed for decades already, the observational proof has only very recently been given when a particular black hole signature could be resolved in radio emission.

During inward spiraling, the matter irradiates, which happens for all the matter that consists of much smaller mass particles (gaseous clouds, dust, stars) than the black hole. The total mass of the matter that hits the horizon at each instant is much less than M . The radiation produced in this process may be considered isotropic because there is no remarkable beaming until the matter becomes charged during gravitational compression, heating, and ionization. It then via a dynamo process generates its

proper magnetic field, which tangentially surrounds the black hole horizon and funnels the irreducible to radiation charged particles into two approximately symmetric jets. This self-generated magnetic field provides the outflow channel for the escape of light not irradiated charged matter, which the entropy force rejects from crossing the horizon. Matter accreted by a massive black hole does not arrive at the very horizon as matter, but as charge and massless radiation: mostly photons, possibly gluons, depending on the strength of the gravitational force (i.e., on the mass M of the black hole whether or not it would be large enough to overcome gluon confinement, which is rather unbelievable).

The fraction of radiative energy that hits the black hole and gets trapped consists of photons. These are massless and do not feel the entropy force when encountering the horizon, because the entropy force acts on finite mass particles only. The photons feel, however, the gravitational black hole potential, which is acting on their energy and thus gravitationally deflects their orbits. The photon paths become spirally warped until they ultimately hit the horizon. When this happens, the photons make it across the horizon and enter the interior of the black hole. Looked at from the outside, this takes infinitely long again. It is an open question as to what happens to them inside the horizon, whether or not they collapse, and whether a singularity forms at all if only photons are available. We do not ponder about those interesting questions here.

The implication is that the mass influx into the hole proceeds via irradiation of matter as radiative inflow, not as matter inflow. The black hole is fed by photons. Feeding a black hole with small portions of matter in this view proceeds via transformation into radiation. Those parts of matter that do not transform into radiation, protons and the required neutralizing electrons, become expelled along the newly-formed magnetic funnels into space in the form of jets before touching the horizon. The jets either disperse in interaction with distant matter or become part of cosmic radiation. The process of how radiation may tunnel across the horizon is answered by the quantum electrodynamics of this process including the positive entropy potential drop at the horizon the radiation passes when hitting the black hole, which however barely affects the uncharged and massless photons.

Another question concerns the merging of two equal mass massive black holes. This case is of substantial interest because it has been observed in the first detections of gravitational radiation. If there is just a small mass difference, then probably the two almost equally-strong forces would produce a deformation of the horizons at contact, causing a bubble to evolve, like in the encounter of two soap bubbles. Merging of the horizons takes place at the circumference where the gradients of the entropy become tangential. The holes would start here to merge until the horizon encompasses both holes, with a trapped bubble forming in its common interior and thus becoming invisible to the external observer.

Finally, what happens when asking for the mysterious planckions, Planck particles of mass $M \sim 10^{-8}$ kg ($\sim 10^{19}$ GeV), which may have been created in the Big Bang and are believed to be Planck scale black holes? According to Hawking radiation theory, they should have evaporated in a Planck time of $\sim 10^{-43}$ s already after production, though it is not clear whether at the Planck scale, one can speak at all of black holes, as inside the planckion, quantum gravity necessarily comes into play, and Hawking's quantum electrodynamical calculations should become invalid. Looked at from the outside, a planckion is its own horizon and thus is fuzzy because its radius and diameter equal spatial uncertainty. Assuming that one still could speak about their surface, entropy, and entropy force, their entropy would be of the order of $S \sim O(1)$, while the entropy force would remain huge, equal to the Schwarzschild constant, outrunning the gravitational attraction force. Does this mean that planckions would neither radiate, nor be able to merge, keeping one another at a distance and in larger numbers causing some crystal-like texture? In this case, they could have survived (cf., e.g., [19] for contras) since the Big Bang and accumulated in agglomerations like clusters of galaxies where they could well serve (see [20] for pros) as a dark matter candidate.

3. Microscopic Phase-Space Density and the Entropy Force

So far, we just discussed the effect of the entropy force on a particular object: Schwarzschild black holes in astrophysics. We now turn to the general kinetic problem of the microscopic evolution of the particle distribution in many-particle physics. We restrict solely to classical systems, i.e., to systems that are described on the microscopic level by the classical Liouville equation, respectively its Klimontovich [21] equivalent in Equation (12) given below, and its hydrodynamic generalization [22].

Liouville’s equation describes the evolution of the microscopic phase space density in N -dimensional phase space. On the classical elementary level of indistinguishable point charges, which have some properties like mass m_a , possibly some charge e of different sign, and are distributed over a spatial volume V with volume element d^3q and the momentum volume of element d^3p can be described alternatively [21,22] by an exact known phase space density:

$$\begin{aligned} \mathcal{N}_a^m(\mathbf{p}, \mathbf{q}, t) &= \sum_{i=1}^{N_a} \delta(\mathbf{p} - \mathbf{p}_{ai}(t)) \delta(\mathbf{q} - \mathbf{q}_{ai}(t)) \\ &\equiv \sum_{i=1}^{N_a} \delta(\mathbf{x} - \mathbf{x}_{ai}(t)) \end{aligned} \tag{10}$$

which simply counts the number of particles of sort a in the entire $6D$ -phase space volume, such that it is normalized as:

$$N_a = \int d^3p d^3q \mathcal{N}_a^m(\mathbf{p}, \mathbf{q}, t) \tag{11}$$

For a constant particle number, the time dependence is implicit in the particle trajectories $\mathbf{p}_{ai}(t)$, $\mathbf{q}_{ai}(t)$ such that integration has to be performed along all of them. One may note that the microscopic phase space density \mathcal{N}_a^m is otherwise dimensionless. This is seen from the definition of the delta-functions, which in the integration over phase space simply count numbers, which of course means that the normalization to space and momentum is implicit to them. Later, we will make the normalization more explicit, as this will be required by reference to the entropy.

Since the assumption is that the particles are classical, then in the absence of any particle sources or losses, the particle number in phase space is conserved along all the dynamical trajectories of the particles under their mutual, as well as external forces. In this case, the continuity equation of the particles, i.e., the microscopic Liouville equation in the N_a -particle $6D$ -phase space [21], reads simply:

$$\dot{\mathcal{N}}_a^m \equiv \frac{\partial \mathcal{N}_a^m}{\partial t} + \frac{\mathbf{p}}{m_a} \cdot \nabla_{\mathbf{q}} \mathcal{N}_a^m + \frac{d\mathbf{p}}{dt} \cdot \frac{\partial \mathcal{N}_a^m}{\partial \mathbf{p}} = 0 \tag{12}$$

Of course, here, $\dot{\mathbf{p}} = \mathbf{F}$ is the total force that acts on the particles at their location $\mathbf{q} = \mathbf{q}_{ai}(t)$ and thus on the phase space density, and the two last terms together constitute the Poisson bracket [...] in the Liouville equation, which in N_a -phase space, the $6D$ -phase space that within, the N_a particles perform their trajectories, is a tautology.

The entropy force can be compared with other more conventional forces. Let, for simplicity, the total force $\mathbf{F} = \mathbf{F}_Q + \mathbf{F}_S$ be the sum of the entropy force and of another potential force $\mathbf{F}_Q = -\nabla_{\mathbf{q}} U$, where $U(\mathbf{q}, t)$ is the force potential. The entropy force just adds the potential $TS(\mathbf{q}, t)$ to the force potential U . Note that the entropy-force potential is always positive, as already made use of above, because there are neither negative temperatures [23] (The absence of negative temperatures is immediately clear from the definition of the temperature T as proportional to the mean ensemble averaged square of the momentum fluctuations $T \sim \langle (\delta \mathbf{p})^2 \rangle$ of all particles in the volume, which clearly, is a positive definite quantity. Negative temperatures would require imaginary momenta or particle mass. There are no candidates for such particles, though experiments of neutrino oscillations provide negative mean square masses, which, however, are interpreted differently.), nor are there negative entropies. Clearly, for strong forces acting on the particles and weak entropy gradients, the entropy force is negligible. This might be the usual case. On the other hand, if on the large scale the

inter-particle forces compensate, the entropy force will remain because there is no obvious counterpart that could compensate it. For instance, when dealing with electrostatic interactions only in the absence of any external fields and forces, the microscopic force $\mathbf{F}_Q^m(\mathbf{q}, t) = \sum_a e_a \mathcal{E}^m(\mathbf{q}, t)$ is the Coulomb force acting on the charges $e_a = ae$ with $a = +, -$ in the microscopic electrostatic field $\mathcal{E}^m(\mathbf{q}, t)$ obeying Maxwell–Poisson’s equations:

$$\nabla_q \cdot \mathcal{E}^m = \frac{1}{\epsilon_0} \sum_a \rho_{ae}^m(\mathbf{q}, t), \quad \mathcal{E}^m = -\nabla_q \Phi_e^m(\mathbf{q}, t) \tag{13}$$

with electrostatic potential Φ_e^m , and thus, $U = \sum_a e_a \Phi_e^m$. On the microscopic level in phase space, the microscopic electric space charge (not the charge density) of species a is:

$$\rho_{ae}^m(\mathbf{q}, t) = e_a \int d^3p \mathcal{N}_a^m(\mathbf{p}, \mathbf{q}, t), \quad \int d^3q \rho_{ae}^m = e_a N_a \tag{14}$$

It simply counts all charges in the total volume not relating them to the spatial volume V_a yet. Summing over all species a , the total space charge is obtained. On average, it will be zero. The charges are moving, and there is a microscopic current:

$$\mathbf{j}_{ae}^m(\mathbf{q}, t) = \frac{e_a}{m_a} \int d^3p \mathbf{p} \mathcal{N}_a^m(\mathbf{p}, \mathbf{q}, t) = e_a \mathbf{v}_a(\mathbf{q}, t) N_a \tag{15}$$

with $\mathbf{v}_a(\mathbf{q}, t)$ the average velocity of particles in group a . It gives rise to an internal magnetic field, which, in the electrostatic approximation, is relativistically small and is thus neglected (e.g., [21]), though this is not completely correct, because in a linear theory of fluctuations, it should be taken into account.

Electrostatic interactions have been the subject of exhaustive investigations in the literature. Here, they serve only as another force field against which the entropy force can be compared. The striking difference is that for the entropy force, no field is generated because there is no entropy charge comparable to e_a and, hence, no singularity that would act as the source of the entropy field. In other words, the entropy field is, in contrast to the electric field, not related to field equations and thus lacks a field theory. Disorder lacks any elementary source not being a field, at least in classical physics.

The entropy of a system entering the first law of total energy conservation is an integral quantity. In order to refer to it on the elementary level of the microscopic kinetic equation in $6D$ -phase space, one has to return to its microscopic definition as the phase space average of the probability distribution.

It is convenient to define an entropy phase space density by referring to Gibbs–Boltzmann’s definition of entropy through the probability density. Entropy density will then be obtained by integrating out the momentum space coordinates in the usual way. In the definition of the phase space density of entropy, we will at this point not yet make the assumption that the phase space volume is constant, but include the spatial dependence as well. This is advantageous because it allows making use of phase space densities. Integrating out the volume can be done at a later stage. With this in mind, the “microscopic Boltzmann entropy phase-space density” of species a becomes (A number of other definitions or generalizations of entropy different from Boltzmann–Gibbs have been put forward in the near past [24–30], the physical, not the statistical meaning of which is not entirely clear. Though the theory could be extended to include those, we will neither refer to, nor use them in this note.):

$$S_{aB}^m(\mathbf{p}, \mathbf{q}, t) = -\log \mathcal{N}_a^m(\mathbf{p}, \mathbf{q}, t), \quad \mathcal{N}_a^m = \mathcal{N}_a^m / N_a \tag{16}$$

where the phase space density has been normalized to the total number N_a of particles of species a . This makes the argument of the logarithm smaller than one, of which the negative sign takes care. A definition like this leans on Boltzmann’s proposal. It is incomplete on the microscopic level because the entropy is a collective quantity, which is obtained by integrating over momentum space with the

microscopic phase space density \mathcal{N}_a as the weight. One thus has as microscopic N -particle entropy phase-space density in (\mathbf{p}, \mathbf{q}) -space:

$$S_a^m(\mathbf{p}, \mathbf{q}, t) = -\mathcal{N}_a^m(\mathbf{p}, \mathbf{q}, t) \log \mathcal{N}_a^m(\mathbf{p}, \mathbf{q}, t) \tag{17}$$

This microscopic phase-space density of the entropy is not the entropy itself, which is a function solely of the space coordinates. The N_a -particle entropy of sort a is explicitly obtained by the integration of (17) over the entire momentum phase space:

$$\begin{aligned} S_a^m(\mathbf{q}, t) &= \int d^3 p \mathcal{S}_a^m(\mathbf{q}, \mathbf{p}, t) \\ &\equiv \int d^3 p' d^3 q' \delta(\mathbf{q} - \mathbf{q}') \mathcal{S}_a^m(\mathbf{q}', \mathbf{p}', t) \end{aligned} \tag{18}$$

and is always positive, as is easily seen from the definition of the microscopic phase space density, a positive quantity, and the above choice of entropy. Summing over all particle species a then gives the total entropy. Moreover, because information is transported via some field, for instance the electromagnetic field, the time under the integral in Equation (17) is the retarded time $t^R = t - |\mathbf{q} - \mathbf{q}'|/c$ where c is the velocity of signal/information transport between the particles at locations \mathbf{q} and \mathbf{q}' in the real-space subspace of the $6D$ -phase space [31,32]. In conventional kinetic theory, retardation is neglected because c is the velocity of light, and the distances between particles are usually less than ct . This is also assumed in the following.

There is a direct correspondence between this real space microscopic entropy density and the real space charge density $\rho^m(\mathbf{q}, t)$. Both enter the force term via taking the spatial gradient. The difference is that for the electric charge density, this step passes through the electric field \mathcal{E}^m , which is generated by the space charges. Repeated again, for the entropy, there is no such field, nor field equation in classical physics. Entropy is not a charge of some entity and thus does not generate a field. Taking its spatial gradient directly provides the force that acts on the particle at location \mathbf{q} .

4. Kinetic Equation with Entropy Force

The entropy force acting on species a is the negative gradient of Equation (18). This leads to a repulsive force, independent of any charge. It adds to the potential U in Klimontovich's equation. Thus, taking it into account in Equation (12), it becomes clear that it does not affect the particle number and thus does not imply any important change in the microscopic N_a -particle phase space density \mathcal{N}_a^m . The main interest is in its effect on the one-particle kinetic phase space distribution function $f_a(\mathbf{x}, t)$. This is defined through the ensemble-averaged N_a -particle phase space density:

$$\frac{N_a}{V_a} f_a(\mathbf{x}, t) = \langle \mathcal{N}_a^m(\mathbf{x}, t) \rangle \tag{19}$$

where $\langle \dots \rangle$ indicates the ensemble average, and explicitly for the one-particle distribution:

$$f_a(\mathbf{x}_{a1}, t) = V_a \int f_N d^6 \mathbf{x}_{a2} \dots d^6 \mathbf{x}_{aN_a} \prod_{b \neq a} d^6 \mathbf{x}_{b1} \dots d^6 \mathbf{x}_{bN_b} \tag{20}$$

$$\langle \mathcal{N}_a^m(\mathbf{x}, t) \rangle = N_a \int \delta(\mathbf{x} - \mathbf{x}_{a1}) f_N \prod_a d^6 \mathbf{x}_{a1} \dots d^6 \mathbf{x}_{aN_a} \tag{21}$$

with $V_a \equiv V$ the spatial volume occupied by the indistinguishable particle sort a . f_N is the N -particle distribution function, and the integration is with respect to all indistinguishable particles $N - 1$, but one, the particle with coordinates \mathbf{x}_{a1} , as has been defined by Klimontovich [21]. In fact, the distribution function f_N is not explicitly given. It can be resolved on the way of sequentially stepping up the ladder from the one-particle distribution function to higher order distribution functions, which depend on one, two, three, or more indistinguishable particles.

Before proceeding to rewriting the Klimontovich Equation (12), it is necessary to investigate what happens to the entropy when performing the ensemble average implied in the former equations. We do actually not need the entropy itself, rather its spatial gradient, i.e., we need the spatial gradient of the entropy-phase space density (17). For this, we have:

$$-\nabla_{\mathbf{q}} S_a^m = \left(1 + \log \mathcal{N}_a^m\right) \nabla_{\mathbf{q}} \mathcal{N}_a^m \tag{22}$$

The entropy force is the integral of the gradient of Equation (18) over the primed phase space:

$$\begin{aligned} \mathbf{F}_S^a(\mathbf{q}, t) &= T \nabla_{\mathbf{q}} \int d^3 p' d^3 q' \delta(\mathbf{q} - \mathbf{q}') \times \\ &\times \mathcal{N}_a^m(\mathbf{p}', \mathbf{q}', t) \log \mathcal{N}_a^m(\mathbf{p}', \mathbf{q}', t) \end{aligned} \tag{23}$$

Reduction of the entropy-force term in Klimontovich’s equation requires performing the ensemble average of the term:

$$\mathbf{F}_S^a(\mathbf{q}, t) \cdot \frac{\partial}{\partial \mathbf{p}} \mathcal{N}_a^m(\mathbf{q}, \mathbf{p}, t) \tag{24}$$

In order to do so, we need to consider different groups of particles such that:

$$\begin{aligned} \mathbf{F}_S(\mathbf{q}, t) &= T \sum_b \nabla_{\mathbf{q}} \int d^3 p' d^3 q' \delta(\mathbf{q} - \mathbf{q}') \times \\ &\times \mathcal{N}_b^m(\mathbf{p}', \mathbf{q}', t) \log \mathcal{N}_b^m(\mathbf{p}', \mathbf{q}', t) \end{aligned} \tag{25}$$

This produces formally the entropy force contribution to the Klimontovich equation:

$$\begin{aligned} \mathbf{F}_S \cdot \frac{\partial}{\partial \mathbf{p}} \mathcal{N}_a^m &= T \nabla_{\mathbf{q}} \sum_b \int d^3 p' d^3 q' \delta(\mathbf{q} - \mathbf{q}') \cdot \\ &\cdot \frac{\partial}{\partial \mathbf{p}} \left\langle \mathcal{N}_a^m(\mathbf{p}, \mathbf{q}, t) \mathcal{N}_b^m(\mathbf{p}', \mathbf{q}', t) \log \mathcal{N}_b^m(\mathbf{p}', \mathbf{q}', t) \right\rangle \end{aligned} \tag{26}$$

where $\langle \dots \rangle$ indicates the ensemble average, and we have used Equation (22). The momentum differentiation affects only terms containing the phase space density. This leads to the appearance of the logarithmic term on the right and introduces a third-order correlation term. The $(N - 1)$ -particle ensemble-averaged term provides problems because it contains the logarithm of the phase space density. In a somewhat severe approximation, we may assume that the logarithm is a slowly-varying function. Its argument is smaller than one such that it can be expanded, which yields:

$$\begin{aligned} &\left\langle \mathcal{N}_a^m(\mathbf{p}, \mathbf{q}, t) \mathcal{N}_b^m(\mathbf{p}', \mathbf{q}', t) \log \mathcal{N}_b^m(\mathbf{p}', \mathbf{q}', t) \right\rangle \\ &\approx \left\langle \mathcal{N}_a^m(\mathbf{p}, \mathbf{q}, t) \mathcal{N}_b^m(\mathbf{p}', \mathbf{q}', t) \left(\mathcal{N}_b^m(\mathbf{p}', \mathbf{q}', t) - 1 \right) \right\rangle \end{aligned} \tag{27}$$

This generates the ensemble-averaged Klimontovich equation:

$$\begin{aligned} \frac{\partial \langle \mathcal{N}_a^m \rangle}{\partial t} &+ \frac{\mathbf{p}}{m_a} \cdot \nabla_{\mathbf{q}} \langle \mathcal{N}_a^m \rangle - T \nabla_{\mathbf{q}} \sum_{b \neq a} \int d^3 x' \delta(\mathbf{q} - \mathbf{q}') \\ &\cdot \frac{\partial}{\partial \mathbf{p}} \left\langle \mathcal{N}_a^m(\mathbf{x}, t) \mathcal{N}_b^m(\mathbf{x}', t) \right\rangle = - \left\langle C_a^S(\mathbf{x}, t) \right\rangle \end{aligned} \tag{28}$$

The average purely entropic collision term on the right collects the third-order correlations:

$$\begin{aligned} \langle \mathcal{C}_a^S(\mathbf{x}, t) \rangle &= T \nabla_q \sum_{b \neq a} \int d^6 x' \delta(\mathbf{q} - \mathbf{q}') \\ &\cdot \frac{\partial}{\partial \mathbf{p}} \langle \mathcal{N}_a^m(\mathbf{x}, t) \mathcal{N}_b^m(\mathbf{x}', t) \mathcal{N}_b^m(\mathbf{x}', t) \rangle \end{aligned}$$

In these expressions, we have, for simplicity of writing, only included the entropy force term. One trivially adds the microscopic Coulomb or any other force term to this if required (Note, however, that adding the microscopic gravitational force causes problems because it remains uncompensated (As in any kinetic theory, this is an important difference between gravitation and any other force. It implies that in kinetic theory gravitation can only be included consistently in a general relativistic quantum gravitation where gravitation is balanced by quantum fluctuations.)). The entropy force term resembles the latter, but lacks a charge singularity. This is replaced by the spatial derivative of the delta-function, which appears under the integral.

The main difference is that already on this very basic level, the presence of the entropy force contributes a purely entropic dissipative term $\langle \mathcal{C}_a^S(\mathbf{x}, t) \rangle$, which has been transferred to the right in the above expression. This term arises due to the generation of entropy in the system. It is a three-particle correlation term, as will become clear below. It is caused by the logarithm in the entropy, the continuous growth of entropy in a many-particle system. Whether it can be neglected as being of higher order is a subtle question. It causes collisionless dissipation in the presence of entropy. Since this effect is non-collisional, when neglecting particle collisions, one must take care whether its neglect is allowed. Below, we show that, however, dissipation is proportional to the inverse particle number N_a^{-1} and can in most cases for very large numbers of particles be neglected.

The next step in this theory is to relate the last equation to the one-particle distribution function defined in Equation (19). Following Klimontovich [21], this is achieved via considering the fluctuations:

$$\delta \mathcal{N}_a^m(\mathbf{x}, t) = \mathcal{N}_a^m(\mathbf{x}, t) - \langle \mathcal{N}_a^m(\mathbf{x}, t) \rangle \tag{29}$$

When ensemble-averaged, these deviations from the mean phase-space density vanish, and we have:

$$\begin{aligned} \langle \mathcal{N}_a^m(\mathbf{x}, t) \mathcal{N}_b^m(\mathbf{x}', t) \rangle &= \langle \mathcal{N}_a^m(\mathbf{x}, t) \rangle \langle \mathcal{N}_b^m(\mathbf{x}', t) \rangle \\ &+ \langle \delta \mathcal{N}_a^m(\mathbf{x}, t) \delta \mathcal{N}_b^m(\mathbf{x}', t) \rangle \end{aligned} \tag{30}$$

We can now make use of the definition of the one-particle distribution function $f_a(\mathbf{x}, t)$ by Klimontovich [21]. Define the particle density $n_a = N_a/V_a$ to obtain:

$$\begin{aligned} \langle \mathcal{N}_a^m(\mathbf{x}, t) \mathcal{N}_b^m(\mathbf{x}', t) \rangle &= n_a n_b \left[f_a(\mathbf{x}, t) f_b(\mathbf{x}', t) \right. \\ &\left. + g_{ab}(\mathbf{x}, \mathbf{x}', t) \right] + \delta_{ab} \delta(\mathbf{x} - \mathbf{x}') n_a f_a(\mathbf{x}, t) \end{aligned} \tag{31}$$

Here, $g_{ab}(\mathbf{x}, \mathbf{x}', t)$ is the two-particle correlation function, which results from the ensemble-averaged product of the fluctuations $\delta \mathcal{N}^m$ of the phase space density in the last term on the right in Equation (30). The three terms in the expression (31) are of the same structure as in the ordinary one-particle kinetic theory [21]. One may note that the last term, which is linear in the distribution function, simply becomes absorbed in the convective term in the kinetic equation. In non-relativistic, theory it just causes a translation. We can immediately write down the one-particle kinetic equation including the entropy force. One must, however, take care of to which terms the gradient and momentum operations apply. This yields the result:

$$\begin{aligned} & \frac{\partial f_a}{\partial t} + \frac{\mathbf{p}}{m_a} \cdot \nabla_{\mathbf{q}} f_a - T \nabla_{\mathbf{q}}^b \sum_b n_b \int d^6 x' \\ & \times \delta(\mathbf{q} - \mathbf{q}') \cdot \frac{\partial}{\partial \mathbf{p}} [f_a(\mathbf{x}, t) f_b(\mathbf{x}', t)] = \left(\mathcal{G}_{ab}^{S(\mathbf{x}, t)} - \langle \mathcal{C}_a^{S(\mathbf{x}, t)} \rangle \right) (\mathbf{x}, t) \end{aligned} \tag{32}$$

which, when integrating over the primed spatial coordinate, simplifies to:

$$\begin{aligned} & \frac{\partial f_a}{\partial t} + \frac{\mathbf{p}}{m_a} \cdot \nabla_{\mathbf{q}} f_a - T \frac{\partial}{\partial \mathbf{p}} f_a(\mathbf{q}, \mathbf{p}, t) \\ & \cdot \nabla_{\mathbf{q}} \sum_b n_b \int d^3 p' f_b(\mathbf{q}, \mathbf{p}', t) = \left(\mathcal{G}_{ab}^{S(\mathbf{x}, t)} - \langle \mathcal{C}_a^{S(\mathbf{x}, t)} \rangle \right) (\mathbf{x}, t) \end{aligned} \tag{33}$$

In this expression on the right, the term \mathcal{G}_{ab} results from the two-particle correlation term $g_{ab}(\mathbf{x}, \mathbf{x}', t)$. It corresponds to what in kinetic theory is understood as direct particle collisions. The last expression contains the integral over the primed momentum space. Only the distribution f_b depends on this integration. It is therefore convenient to define the number density ρ_a of species a as:

$$\rho_a(\mathbf{q}, t) = n_a \int d^3 p f_a(\mathbf{q}, \mathbf{p}, t) \tag{34}$$

and the last expression just includes the global entropy force term:

$$\begin{aligned} & \frac{\partial f_a}{\partial t} + \frac{\mathbf{p}}{m_a} \cdot \nabla_{\mathbf{q}} f_a - T \left(\nabla_{\mathbf{q}} \sum_b \rho_b(\mathbf{q}, t) \right) \cdot \frac{\partial f_a}{\partial \mathbf{p}} \\ & = \left(\mathcal{G}_{ab}^{S(\mathbf{x}, t)} - \langle \mathcal{C}_a^{S(\mathbf{x}, t)} \rangle \right) (\mathbf{x}, t) \end{aligned} \tag{35}$$

The sum is over all particle components, implying the total number density. Thus, the entropy force term simply adds to any other potential force term in the kinetic equation. This is true already to first order in the expansion of the logarithmic term in the definition of the entropy. In the case of charged particles, such a force is the Coulomb force or the Lorentz force, when including magnetic fields. The difference is, however, that this force term does not depend on charge while acting on the microscopic particle phase space distribution. It resembles the gravitational force, but does not contain its inverse square dependence on the inter-particle distance. This is advantageous as it releases from the necessity of compensation. On the other hand, the new force term introduces another non-linearity contained in the density, which itself is the integral of the distribution function.

The entropy force resembles a pressure force on the kinetic level. With zero right-hand side in the kinetic equation, it conserves particle number. This is a rather simple result, which, of course, could have been anticipated, without reference to any complicated derivation from first principles as done here, by adding a macroscopic entropy force to the force terms.

The ensemble-averaged term $\langle \mathcal{C}_a^S \rangle$ is a purely entropic lowest order (in the smallness of \mathcal{N}_a^{m}) dissipation term for which, in conventional kinetic theory, no equivalence arises. This term is, however, small and thus negligible, as will be shown in the next section.

In the collisionless kinetic theory of forces between particles, any non-collisional dissipation term caused by particle interactions via their fields yields correlations, which can be neglected, respectively discussed away by comparing dissipation and collisionless scales. The entropic dissipation term instead remains because it is not caused by particle collisions, nor wave-particle interactions. There is no entropy source field that leads to the correlations between particles. Rather, it is the inhomogeneity in the macroscopic disorder that is responsible for the fluctuations and the appearance of the dissipative entropic correlations between the fluctuations leading to the dissipation term. Hence, this term remains

even under completely collisionless conditions. Once disorder exhibits spatial structure, it will always be present. In the next section, we provide the explicit versions of these two terms.

5. Dissipative Terms

In order to complete the theory, one needs to express the two dissipative terms in the final kinetic Equation (32). The collision term \mathcal{G}_{ab} is of the same structure as the Coulomb collision term [21,33]. It adds to the latter:

$$\mathcal{G}_{ab}^S = T \sum_b n_b \nabla_{\mathbf{q}} \cdot \int d^6 x' \delta(\mathbf{q} - \mathbf{q}') \frac{\partial}{\partial \mathbf{p}} g_{ab}(\mathbf{x}, \mathbf{x}', t) \tag{36}$$

In the particular case that the correlation g_{ab} does not contain any singularity, this expression has no singularity at $\mathbf{q} = \mathbf{q}'$ other than that in the derivative of the delta-function, which replaces $\mathbf{q}' \rightarrow \mathbf{q}$ in the correlation function g_{ab} when the integration is carried out. The remaining expression becomes:

$$\mathcal{G}_{ab}^S(\mathbf{q}, \mathbf{p}, t) = T \frac{\partial}{\partial \mathbf{p}} \cdot \sum_b n_b \int d^3 p' \nabla_{\mathbf{q}} g_{ab}(\mathbf{q}, \mathbf{p}, \mathbf{p}', t) \tag{37}$$

The presence of the entropy force thus contributes to the collision term via the particle correlation function. Clearly, due to the strong Coulomb force at short distances, the particle interaction on the short scales is dominated by the Coulomb force. However, at distances larger than the Coulomb collision length, the entropic collisional interaction remains. In a charge collisionless plasma, for instance, the Coulomb term causes charge screening felt inside the Debye sphere and eliminates the microscopic electric field between the charges on scales larger than the Debye length λ_D . On such scales, entropic dissipation might enter the scene. Since it is proportional to temperature T and also number density ρ , it has the character of a collisional contribution of the pressure in the inhomogeneities of the entropy.

One may take notice that the spatial gradient operator can be taken out of the integral in the last expression. This allows writing:

$$\mathcal{G}_{ab}^S(\mathbf{q}, \mathbf{p}, t) = T \nabla_{\mathbf{q}} \cdot \frac{\partial}{\partial \mathbf{p}} G_a^S(\mathbf{q}, \mathbf{p}, t) \tag{38}$$

where we introduced the entropic correlation integral:

$$G_a^S(\mathbf{q}, \mathbf{p}, t) = \sum_b n_b \int d^3 p' g_{ab}(\mathbf{q}, \mathbf{p}, \mathbf{p}', t) \tag{39}$$

We will return to the discussion of this correlation integral below, because it contains the most interesting effect introduced by the entropy force.

In general, the correlation will contain contributions from the forces that depend on local charges. This leads from the field equations to singularities in the correlation function, as the example of the Coulomb force suggests. The simplified form of the correlation term in the dissipation function retains the form in Equation (36) and must be explicitly spelled out. Exchanging the derivatives, this can be written as:

$$\mathcal{G}_{ab}^S = T \frac{\partial}{\partial \mathbf{p}} \cdot \sum_b n_b \nabla_{\mathbf{q}} \int d^6 x' \delta(\mathbf{q} - \mathbf{q}') g_{ab}(\mathbf{x}, \mathbf{x}', t) \tag{40}$$

Let us now turn to the remaining term $\langle \mathcal{C}_a^S \rangle$. From Equations (27) and (28), one realizes that it contains the product of three microscopic phase space densities before taking the ensemble average. This complicates its calculation. In analogy to Equations (30) and (31), it requires the introduction of higher order correlations. Formally, this is quite simple as it has been pioneered by Klimontovich [21]

how one would have to deal with it in this case. We need the third-order ensemble average, which becomes in the same way as (31):

$$\begin{aligned} \langle \mathcal{N}_a^m \mathcal{N}_b^m \mathcal{N}_c^m \rangle &= n_a n_b n_c f_{abc}(\mathbf{x}, \mathbf{x}', \mathbf{x}'') \\ &+ \delta_{ab} n_a n_c \delta(\mathbf{x} - \mathbf{x}') f_{ac}(\mathbf{x}, \mathbf{x}'') \\ &+ \delta_{ac} n_a n_b \delta(\mathbf{x} - \mathbf{x}'') f_{ab}(\mathbf{x}, \mathbf{x}') \\ &+ \delta_{bc} n_a n_c \delta(\mathbf{x}' - \mathbf{x}'') f_{ac}(\mathbf{x}, \mathbf{x}'') \\ &+ \delta_{ab} \delta_{bc} \delta(\mathbf{x} - \mathbf{x}') \delta(\mathbf{x} - \mathbf{x}'') f_a(\mathbf{x}) \end{aligned} \tag{41}$$

For convenience, we dropped the common variable t . The two- and three-particle distribution functions f_{ab} , f_{abc} read:

$$\begin{aligned} f_{ab}(\mathbf{x}, \mathbf{x}') &= f_a(\mathbf{x}) f_b(\mathbf{x}') + g_{ab}(\mathbf{x}, \mathbf{x}') \\ f_{abc}(\mathbf{x}, \mathbf{x}', \mathbf{x}'') &= f_a(\mathbf{x}) f_b(\mathbf{x}') f_c(\mathbf{x}'') \\ &+ f_a(\mathbf{x}) g_{bc}(\mathbf{x}', \mathbf{x}'') + f_b(\mathbf{x}') g_{ac}(\mathbf{x}, \mathbf{x}'') \\ &+ f_c(\mathbf{x}'') g_{ab}(\mathbf{x}, \mathbf{x}') + g_{abc}(\mathbf{x}, \mathbf{x}', \mathbf{x}'') \end{aligned} \tag{42}$$

With their help, the dissipation function can be constructed. However, its structure simplifies substantially because in our case, on the left in the first line in Equation (41), the microscopic phase space densities of index b and c are identical, and only the f_{ab} contributes. Hence, the ensemble average becomes:

$$\langle \mathcal{N}_a^m \mathcal{N}_b^m \mathcal{N}_c^m \delta_{bc} \delta(\mathbf{x}' - \mathbf{x}'') \rangle = n_a n_b f_{ab}(\mathbf{x}, \mathbf{x}') \frac{1}{N_b} \tag{43}$$

Therefore, only the two-particle distribution function f_{ab} would be relevant in the determination of the dissipative term, i.e., in the first line in Equation (42). This is, however, the same as what we already used in Equation (31). To this result, one has to apply the operation of space and momentum differentiation. Hence, the collisionless dissipative term contributed by the entropy force is of the same kind as the collision term \mathcal{G}_{ab}^S it contributes, though being of a different sign. In other words, the two terms would cancel to first order if there were not the normalization to particle number N_b . Since $N_b \approx N_a \gg 1$, we find that the collisionless dissipation due to the entropy force $\langle \mathcal{C}_a^S \rangle \ll \mathcal{G}_{ab}^S$ is small and can be neglected in comparison with the entropic collision term.

Thus, it is the collisional correlation term $\mathcal{G}_{ab}^S(\mathbf{x}, t)$ (37) that is retained as a long-range collisional dissipation introduced by the presence of the entropy force. It adds to the Coulomb collisions and might become important on the large scales much larger than the Debye scale or any other inter-particle interaction scale. this important result suggests that the entropic dissipation is a mesoscale, respectively macro effect. We should, however, point out here that we are still dealing with a non-relativistic theory. At large scales, transport and propagation of information, respectively entropy, cannot be neglected anymore, and the theory has to given a covariant relativistic formulation.

6. Kinetic Equation for Fluctuations

The remaining problem is the behavior of fluctuations. These are defined as deviations in the one-particle phase space distribution f_a from its mean “equilibrium” value \bar{f}_a as:

$$\delta f_a = f_a - \bar{f}_a, \quad \overline{\delta f_a} = 0 \tag{44}$$

The evolution equation of the fluctuations is obtained from Equation (33) via subtracting the averaged kinetic equation:

$$\begin{aligned} & \frac{\partial \bar{f}_a}{\partial t} + \frac{\mathbf{p}}{m_a} \cdot \nabla_{\mathbf{q}} \bar{f}_a - T \sum_b n_b \int d^3 p' \times \\ & \times \nabla_{\mathbf{q}}^b \cdot \frac{\partial}{\partial \mathbf{p}} \left[\bar{f}_a(\mathbf{q}, \mathbf{p}, t) \bar{f}_b(\mathbf{q}, \mathbf{p}', t) + \overline{\delta f_a \delta f_b} \right] = \overline{\mathcal{G}_{ab}^S} \end{aligned} \tag{45}$$

The mean collision term on the right contains all the contributions of the correlations of the mean and fluctuating quantities. Being interested only in linear fluctuations and assuming that the collisions are weak enough to not contribute to the evolution of fluctuations, we drop this term in the following. Subtracting from the complete kinetic equation, the fluctuations obey the non-collisional equation:

$$\begin{aligned} & \frac{\partial \delta f_a}{\partial t} + \frac{\mathbf{p}}{m_a} \cdot \nabla_{\mathbf{q}} \delta f_a - T \sum_b n_b \int d^3 p' \\ & \times \nabla_{\mathbf{q}}^b \cdot \frac{\partial}{\partial \mathbf{p}} \left[\delta f_a(\mathbf{q}, \mathbf{p}, t) \bar{f}_b(\mathbf{q}, \mathbf{p}', t) \right] = \\ & T \sum_b n_b \int d^3 p' \nabla_{\mathbf{q}}^b \cdot \frac{\partial}{\partial \mathbf{p}} \left[\bar{f}_a(\mathbf{q}, \mathbf{p}, t) \delta f_b(\mathbf{q}, \mathbf{p}', t) - \overline{\delta f_a \delta f_b} \right] \end{aligned} \tag{46}$$

This expression still contains the average $\overline{\delta f_a \delta f_b}$ of the squared fluctuations. If this is a constant on the fluctuation time scale, then the equation can be rescaled. In linear theory, it would be neglected to first order and taken into account to second order in a quasi-linear approach.

Again, carrying out the integration with respect to \mathbf{p}' , the last expression simplifies to:

$$\begin{aligned} & \frac{\partial \delta f_a}{\partial t} + \frac{\mathbf{p}}{m_a} \cdot \nabla_{\mathbf{q}} \delta f_a - T \frac{\partial \delta f_a}{\partial \mathbf{p}} \cdot \nabla_{\mathbf{q}} \left(\sum_b \bar{\rho}_b(\mathbf{q}, t) \right) \\ & = T \sum_{b \neq a} n_b \int d^3 p' \nabla_{\mathbf{q}}^b \cdot \frac{\partial}{\partial \mathbf{p}} \left[\bar{f}_a(\mathbf{x}, t) \delta f_b(\mathbf{q}, \mathbf{p}', t) - \overline{\delta f_a \delta f_b} \right] \end{aligned} \tag{47}$$

where in the term on the right-hand side, we retained the fluctuation in the distribution function, not replacing it with the density fluctuation $\delta \rho_b(\mathbf{q}, t)$ for the obvious reason that this is an equation for the fluctuations in the distribution function itself. The term on the right couples all fluctuations in the different particle components $b \neq a$ to \bar{f}_a .

The linear theory is still complicated by the fact that it contains the sum over the particle correlations. Here, one must include all particles contained in the medium. Moreover, we have written here only those terms that result from the inclusion of the entropy force. To these terms, one must add the electromagnetic force terms. Since the electromagnetic and entropy forces superimpose, this does not produce any additional mixing, but simply adds those common and well-known terms that take care of the electromagnetic interactions. In this sense, the formal theory is complete. The ranges of the two different forces acting on the particle populations are vastly different because the entropy force is a collective force, which does not originate from any elementary charge. There is no singularity of the entropy that could give rise to an entropy field. The search for such singularities is outside classical physics.

7. Evolution of Entropic Phase Space Density

Having defined the entropic phase space density in Equation (17), the question arises how it possibly evolves in phase space. Since the entropy is given as the phase space integral with respect to the entropic phase space density, an always positive quantity, this question is not senseless. Once knowing its evolution, the entropy can be calculated by integration. Moreover, if an equation for the phase space density can be obtained, its entropic momentum should yield an evolution equation for the entropy, which, essentially, in the long-term limit should be the fundamental thermodynamic laws, while in

the short term, it should give the evolution equation of entropy with time. In order to construct the entropic phase space equation, we multiply Equation (12) by $-\log \mathcal{N}_a^m$ to obtain:

$$\partial_t \mathcal{S}_a^m + [\mathcal{H}_{N_a}, \mathcal{S}_a^m] - \left\{ \partial_t \mathcal{N}_a^m + [\mathcal{H}_{N_a}, \mathcal{N}_a^m] \right\} = 0 \tag{48}$$

The term in the braces vanishes identically, yielding ultimately:

$$\partial_t \mathcal{S}_a^m + [\mathcal{H}_{N_a}, \mathcal{S}_a^m] = 0 \tag{49}$$

We thus find the almost trivial result that the microscopic entropic phase-space density \mathcal{S}_a^m itself satisfies the Liouville equation, i.e., the continuity equation for the entropic phase space density in the phase space. It thus evolves in the microscopic particle phase space like a dissipationless fluid. This is just another expression for the fact that (classically), there are no microscopic sources of entropy, nor is there any entropic field. Entropy is just disorder in the particles.

However, the microscopic entropic density in phase space is not entirely independent of any disorder. It acts back on itself via the integral entropy force term contained in the above Hamiltonian \mathcal{H}_{N_a} . It provides an entropy potential contribution $U_S = TS$ to the Hamiltonian with S , the momentum space integral of the entropy phase space density $\mathcal{S}_a^m \{ \mathcal{N}_a^m \}$, which itself is a function of the phase space density \mathcal{N}_a^m . Though the structure of the kinetic equation for the entropy density \mathcal{S}_a^m remains the same as that of the phase space density \mathcal{N}_a^m , both containing the entropy force term and becoming integro-differential equations, the phase space density is determined by the integral entropy density through the entropy force. This force is obtained by adding up all contributions over all phase space. This shows that both the kinetic equation for the particle density and the kinetic equation for the entropy density in phase space must be solved together as both are intimately related.

One can interpret this result in the way that the holographic reaction of the integral entropy on the evolution of the phase space density of the entropy appears like an elementary entropy source. This is not unsatisfactory, because it can hardly be expected that a microscopic source of entropy would exist as there are no entropy charges and no entropy fields in the world, at least not classically. Instead, the elementary source arises from the non-linear self-interaction of the entropy. This is a rather important conclusion in that, presumably, little will be changed when including quantum effects in a quantum mechanical treatment, making the transition to quantum statistical mechanics.

8. Discussion and Conclusions

In this note, we included the force that an inhomogeneous entropy might exert on the dynamics of particles in phase space. This is not an obvious step. It is a purely collective effect. So far, any such force has not yet been included in the dynamics of large numbers of particles and kinetic theory.

Collective effects of this kind are known from ponderomotive forces and pressure forces. However, the inclusion of a separate ponderomotive force or a pressure force on the microscopic level is not necessary. Ponderomotive forces are taken care of by the interaction of the electromagnetic field with the particles. They arise from correlations. Similarly, the pressure force, which is directly proportional to the gradient of the particle density on any level, is already included in the evolution of the phase space density.

The entropy force is different in the sense that it is not obvious that it is given by the gradient of density. The entropy force takes care of the chaotic disorder that is produced by the dynamics itself. Neither the pressure, nor the temperature account for it. Entropy is a function of the phase space density, not its moment like pressure and temperature. It is the cause of chaotic expansion of the phase space in the course of the dynamics. It therefore gives rise to a collective effect felt on the level of the microscopic phase space density. In many processes, this effect may be very small and negligible. This will depend on scales. Elucidating those effects requires investigation of particular cases. The present work presents the theory on which such attempts must be based.

We derived the basic kinetic equation for the one particle phase space density including the global entropy force. Since this force is a global integral one, it has no microscopic source, while it affects the dynamics of the one-particle phase space density through the interaction Hamiltonian. This gives rise to the construction of a kinetic equation for the entropic phase space density, which turns out to be of similar structure, like the Liouville (Klimontovich) equation for the phase space density. There is, however, a fundamental difference in that the entropic kinetic equation is self-referential. It determines the dynamics of the entropy density in phase space by reference to the integrated entropy of the entire system itself. This is a very important finding because it shows that the entropy density in phase space evolves holographically. It is determined by itself. It takes care of its own evolution, which in addition depends on the evolution of the matter phase space density. This can be interpreted as a self-regulation of the evolution of entropy on the microscopic level, which takes care of the total produced entropy. According to this finding, any many-particle system that in the course of its dynamics generates entropy in an inhomogeneous and time-dependent way is subject to the entropy that controls its own evolution. This we feel is the most important insight we arrived at in our analysis. Entropy generates and controls itself in this highly nonlinear way already on the microscopic level of phase space density. We conjecture that these properties remain when including quantum effects in kinetic theory on the microscopic quantum level without the need to introduce a seed source of entropy.

In order to demonstrate an effect, we in the introductory part of this note treated the astrophysical example of a Schwarzschild black hole. This led us to the definition of the Schwarzschild constant, a universal constant, which is essentially the Planck force, which so far had been formally postulated without finding a physical interpretation. Its meaning lies in the Schwarzschild constant as the entropy force at the black hole horizon. Some of its implications we have discussed briefly. The entropy force at the horizon, being independent of charge, is of only one sign. It causes a repulsive force. This is similar to the gravitational force, though counteracting it. It thus in large space may compete with the gravitational attraction, where it may become kind of an anti-gravity. Investigation of its effect on the universal expansion might also be of interest, as also the role it may play in primordial black holes and planckions, which may have been generated in the early universe, the Big Bang, and if surviving, possibly due to the anti-gravity action of the entropy force, could provide all or part of the mysterious dark matter on the scales of clusters of galaxies.

Author Contributions: Conceptualization, W.B. and R.T., formal analysis, R.T., writing—review and editing, W.B. and R.T.

Funding: This research received no external funding.

Acknowledgments: This work was part of a Visiting Scientist Programme at the International Space Science Institute (ISSI) Bern. The interest of the ISSI Directorate is acknowledged, as is in particular the friendly hospitality of the ISSI staff. Thanks are directed to the ISSI system administrator Saliba F. Saliba for technical support and to the librarians Andrea Fischer and Irmela Schweizer for access to the library and literature.

Conflicts of Interest: The authors declare no conflict of interest.

References

1. Prigogine, I. *From Being to Becoming. Time and Complexity in the Physical Sciences*; Freeman: New York, NJ, USA, 1980.
2. Verlinde, E. On the origin of gravity and the laws of Newton. *J. High Energy Phys. JHEP* **2011**, 2011, 29. [[CrossRef](#)]
3. Kappen, H.J. Comment: Causal entropic forces. *arXiv* **2013**, arXiv:1312.4185.
4. Wissner-Gross, A.D.; Freer, C.E. Causal entropy forces. *Phys. Rev. Lett.* **2013**, *110*, 168702. *OhysRevLett*.110.168702. [[CrossRef](#)] [[PubMed](#)]
5. Keul, N.D.; Oruganty, K.; Bergman, E.T.S.; Beattie, N.R.; McDonald, W.E.; Kadirvelraj, R.; Gross, M.L.; Phillips, R.S.; Harvey, S.C.; Wood, Z.A. The entropic force generated by intrinsically disordered segments tunes protein function. *Nature* **2018**, *563*, 584–588. [[CrossRef](#)] [[PubMed](#)]
6. Nakamura, T.K. Relativistic equilibrium distribution by relative entropy maximization. *Europhys. Lett. EPL* **2009**, *88*, 40009. [[CrossRef](#)]

7. Bardeen, J.M.; Carter, B.; Hawking, S.W. The four laws of black hole mechanics. *Commun. Math. Phys.* **1973**, *31*, 161–170. [[CrossRef](#)]
8. Bekenstein, J.D. Black holes and entropy. *Phys. Rev. D* **1973**, *7*, 2333–2346. [[CrossRef](#)]
9. Bekenstein, J.D. Black holes and the second law. *Nuovo Cim. Lett.* **1972**, *4*, 737–740. [[CrossRef](#)]
10. Hawking, S.W. Gravitational radiation from colliding black holes. *Phys. Rev. Lett.* **1971**, *21*, 1344–1346. [[CrossRef](#)]
11. Hawking, S.W. Particle creation by black holes. *Comm. Math. Phys.* **1975**, *43*, 199–220. [[CrossRef](#)]
12. Hawking, S. Black holes and thermodynamics. *Phys. Rev. D* **1976**, *13*, 191–197. [[CrossRef](#)]
13. Brout, R.; Massar, S.; Parentani, R.; Spindel, P. A primer for black hole quantum physics. *Phys. Rep.* **1995**, *260*, 329–446. [[CrossRef](#)]
14. Doran, R.; Lobo, F.S.N.; Crawford, P. Interior of a Schwarzschild black hole revisited. *Found. Phys.* **2008**, *38*, 160–187. [[CrossRef](#)]
15. Jacobson, T. Thermodynamics of spacetime: The Einstein equation of state. *Phys. Rev. Lett.* **1995**, *75*, 1260–1263. [[CrossRef](#)] [[PubMed](#)]
16. Padmanabhan, T. Thermodynamical aspects of gravity: New insights. *Rep. Progr. Phys.* **2009**, *73*, 6901. [[CrossRef](#)]
17. Taylor, P.L.; Tabachnik, J. Entropic forces—Making the connection between mechanics and thermodynamics in an exactly soluble model. *Eur. J. Phys.* **2013**, *34*, 729. [[CrossRef](#)]
18. Hamilton, A.J.S. Hawking radiation inside a Schwarzschild black hole. *Gen. Relat. Gravit.* **2018**, *50*, 50. [[CrossRef](#)]
19. Carr, B.; Kühnel, F.; Sandstad, M. Primordial black holes and dark matter. *Phys. Rev. D* **2016**, *94*, 083504. [[CrossRef](#)]
20. Garny, M.; McCullen, S.; Sloth, M.S. Planckian interacting massive particles as dark matter. *Phys. Rev. Lett.* **2016**, *116*, 10302. [[CrossRef](#)]
21. Klimontovich, Y.L. *The Statistical Theory of Non-Equilibrium Processes in a Plasma*; The MIT Press: Cambridge, MA, USA, 1967.
22. Gerasimenko, V.I.; Shtyuk, V.O.; Zagorodny, A.G. Hydrodynamic equations for microscopic phase densities. *Centr. Eur. J. Phys.* **2011**, *9*, 71–77. [[CrossRef](#)]
23. Dunkel, J.; Hilbert, S. Consistent thermostatics forbids negative absolute temperatures. *Nat. Phys.* **2014**, *10*, 67–69. [[CrossRef](#)]
24. Rényi, A. *Probability Theory*; North-Holland Publ. Comp.: Amsterdam, The Netherlands, 1970.
25. Tsallis, C. Possible generalization of Boltzmann-Gibbs statistics. *J. Stat. Phys.* **1988**, *52*, 479–487. [[CrossRef](#)]
26. Treumann, R.A. Kinetic theoretical foundation of Lorentzian statistical mechanics. *Phys. Scr.* **1999**, *59*, 19–26. [[CrossRef](#)]
27. Treumann, R.A.; Jaroschek, C.H.; Scholer, M. Stationary plasma states far from equilibrium. *Phys. Plasmas* **2004**, *11*, 1317–1325. [[CrossRef](#)]
28. Treumann, R.A.; Jaroschek, C.H. Gibbsian theory of power-law distributions. *Phys. Rev. Lett.* **2008**, *100*, 155005. [[CrossRef](#)] [[PubMed](#)]
29. Treumann, R.A.; Baumjohann, W. Beyond Gibbs-Boltzmann-Shannon: General entropies—The Gibbs-Lorentzian example. *Front. Phys.* **2014**, *2*, 49. [[CrossRef](#)]
30. Wehrl, A. General properties of entropy. *Rev. Mod. Phys.* **1978**, *50*, 221–260. [[CrossRef](#)]
31. Wheeler, J.A.; Feynman, R.P. Interaction with the absorber as the mechanism of radiation. *Rev. Mod. Phys.* **1945**, *17*, 157–161. [[CrossRef](#)]
32. Wheeler, J.A.; Feynman, R.P. Classical electrodynamics in terms of direct interparticle action. *Rev. Mod. Phys.* **1949**, *21*, 425–433. [[CrossRef](#)]
33. Treumann, R.A.; Baumjohann, W. Causal kinetic equation of non-equilibrium plasmas. *Ann. Geophys.* **2017**, *35*, 683–690. [[CrossRef](#)]



Dynamic Maximum Entropy Reduction

Václav Klika ^{1,*}, Michal Pavelka ² , Petr Vágrner ^{2,3} and Miroslav Grmela ⁴

¹ Department of Mathematics—FNSPE, Czech Technical University, Trojanova 13, 12000 Prague, Czech Republic

² Mathematical Institute, Faculty of Mathematics and Physics, Charles University, Sokolovská 83, 18675 Prague, Czech Republic

³ Weierstrass Institute, Mohrenstrasse 39, 10117 Berlin, Germany

⁴ École Polytechnique de Montréal, C.P.6079 suc. Centre-ville, Montréal, QC H3C3A7, Canada

* Correspondence: vaclav.klika@jfifi.cvut.cz

Received: 28 June 2019; Accepted: 19 July 2019; Published: 22 July 2019



Abstract: Any physical system can be regarded on different levels of description varying by how detailed the description is. We propose a method called Dynamic MaxEnt (DynMaxEnt) that provides a passage from the more detailed evolution equations to equations for the less detailed state variables. The method is based on explicit recognition of the state and conjugate variables, which can relax towards the respective quasi-equilibria in different ways. Detailed state variables are reduced using the usual principle of maximum entropy (MaxEnt), whereas relaxation of conjugate variables guarantees that the reduced equations are closed. Moreover, an infinite chain of consecutive DynMaxEnt approximations can be constructed. The method is demonstrated on a particle with friction, complex fluids (equipped with conformation and Reynolds stress tensors), hyperbolic heat conduction and magnetohydrodynamics.

Keywords: model reduction; non-equilibrium thermodynamics; MaxEnt; dynamic MaxEnt; complex fluids; heat conduction; Ohm's law

1. Introduction

The problem of model reduction is ubiquitous in physics and mathematics. Consider a system (physical or mathematical) that can be regarded on two levels of description, upper (more detailed level) and lower (less detailed). The state variables on the lower level contain less information than state variables on the upper level. A projection from the upper level to the lower level is necessary to state the problem of model reduction correctly. Assume, moreover, that dynamics of the state variables on the upper level is granted, but one wishes to see evolution of the lower variables. The reason can be for instance the complexity of the detailed evolution, availability of experimental observations or simplicity of the lower description. A reduction of dynamics from the upper level to the lower (less detailed) level is called model reduction.

There is no general model reduction technique applicable to all systems. However, many physically based (we do not focus on formal mathematical expansion methods although we make a certain comparison below) methods have been developed, such as the Chapman–Enskog expansion [1] or other series expansions [2], projector operator techniques [3,4], or the method of natural projector, invariant slow manifolds, entropic scalar product and Ehrenfest reduction [5–8]. A common feature of the reduction techniques is the recognition of entropy, since entropy (measuring unavailable information) grows during the passage from the more detailed level to the less detailed. In particular, states on the higher level corresponding to maximum entropy are referred to as the quasi-equilibrium manifold. This manifold is constructed by maximization of entropy on the upper level while knowing

the result of the projection of the state variables to the lower level. This is the principle of Maximum Entropy (MaxEnt), see e.g., [9,10].

Apart from the relations between state variables on the two levels of description, it is necessary to find relations between vector fields generating evolution on the two levels. Indeed, evolution equations on the higher level can be seen as a motion along a given vector field (following arrows of the field) while the corresponding vector field on the lower level is to be found. For instance, in the Ehrenfest reduction, the vector field on the higher level is first prolonged by Taylor series and subsequently projected to the lower level, using MaxEnt, and closed. See [7] for various geometric techniques on how to obtain the vector field on the lower level of description.

Our approach is different. First, we recognize not only the state variables, but also conjugate variables as independent quantities, being motivated by the formulation of thermodynamics in contact geometry [11–13]. Eventually, conjugate variables become related to the state variables through derivatives of a thermodynamic potential (e.g., energy or entropy), but they are considered independent from direct variables in contact formulation and exhibit evolution towards that relation while approaching a given level. State variables between the levels can be related by MaxEnt as in [7,9,14], but conjugate variables can be exploited to find the approximation of the vector field on the higher level of description such that evolution on the lower level becomes closed while extracting key features (“measured” by entropy potential) of the upper level dynamics. In other words, the vector field on the lower level becomes tangent to the quasi-equilibrium manifold, see [15] or [14]. We refer to this method as Dynamic MaxEnt (DynMaxEnt).

Novelty of this paper lies in the following points: (i) The DynMaxEnt is introduced in the energetic representation, which simplifies the calculations, (ii) a chain or higher order DynMaxEnt approximations is identified, (iii) DynMaxEnt is compared to asymptotic expansions and (iv) it is applied to a reduction of various complex continuum dynamics to classical irreversible thermodynamics (conformation tensor, Reynolds stress, hyperbolic heat conduction and magnetohydrodynamics).

In Section 2, we first recall the usual (static) Maximum Entropy principle (MaxEnt). In Section 3, we introduce the method of Dynamic MaxEnt, which serves as a reduction from the more detailed evolution equations to less detailed, and then we demonstrate it on damped particle dynamics. In Section 4, we use the DynMaxEnt method for reduction of dynamics of complex fluids, hyperbolic heat conduction and electromagnetohydrodynamics to the Navier–Stokes–Fourier system and magnetohydrodynamics. Finally, in Section 5, we present a geometric motivation for the DynMaxEnt method in the framework of contact geometry.

2. Static MaxEnt

As a thorough understanding of (static) maximum entropy (MaxEnt) method is required, we shall recapitulate its key steps, what it means and what it provides.

Let us denote the state variables on the more microscopic level as $x \in \mathcal{M}$, \mathcal{M} being the manifold (often vector space) of the state variables, with conjugate variables x^* via entropy $\uparrow S$. Furthermore, let us assume that there is a projection that relates two sets of variables $x \in \mathcal{M}$, $y \in \mathcal{N}$ via $\pi(x) = y$ where the latter corresponds to the more macroscopic level of description. The static MaxEnt provides an inverse mapping $\tilde{x}(y)$ such that $\tilde{x}(y)$ is the point of preimage $\pi^{-1}(y)$ with the highest entropy. This determines a manifold in \mathcal{M} , the MaxEnt manifold $\tilde{\mathcal{M}}$.

The inverse mapping can be achieved by maximization of entropy while keeping the constraint that $\pi(x) = y$, i.e., by the method of Lagrange multipliers. More geometrically, it can be also done via two consecutive Legendre transformations which together correspond to maximisation with a constraint $y = \pi(x)$ [14,16]. In particular, as a first step, one obtains a relation $\tilde{x}(y^*)$ from solving

$$\mathbf{0} = \partial_x \underbrace{\left(-\uparrow S(x) + \langle y^*, \pi(x) \rangle \right)}_{\uparrow \phi} \tag{1}$$

while the lower conjugate entropy is $\downarrow S^*(\mathbf{y}^*) = \uparrow \phi(\tilde{\mathbf{x}}(\mathbf{y}^*), \mathbf{y}^*)$. Note that this (actually generalized) Legendre transformation can not be inverted.

Next, Legendre transformation of the lower conjugate entropy provides lower entropy and a relation $\tilde{\mathbf{y}}^*(\mathbf{y})$:

$$\mathbf{0} = \partial_{\mathbf{y}^*} \underbrace{\left(-\downarrow S^*(\mathbf{y}^*) + \langle \mathbf{y}, \mathbf{y}^* \rangle \right)}_{\downarrow \phi^*}, \tag{2}$$

which solution yields $\tilde{\mathbf{y}}^*(\mathbf{y})$ and $\downarrow S(\mathbf{y}) = \downarrow \phi^*(\mathbf{y}, \tilde{\mathbf{y}}^*(\mathbf{y}))$. Finally, the “inverse” mapping to the projection $\mathbf{y} = \pi(\mathbf{x})$ is $\mathbf{x} = \tilde{\mathbf{x}}(\tilde{\mathbf{y}}^*(\mathbf{y})) := \pi^{-1}(\mathbf{y})$. Note that it is now evident that π^{-1} is not a one-to-one mapping but rather a mapping identifying the most probable (with respect to the lower entropy) set of values of the microscale variable \mathbf{x} that correspond to a given macroscale state \mathbf{y} . We shall refer to this method as MaxEnt and see Figure 1 for a summary of the method.

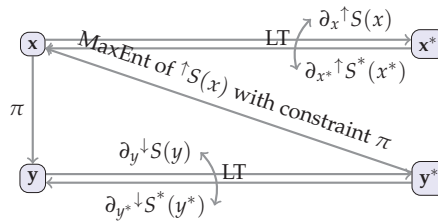


Figure 1. A summary of static MaxEnt highlighting relations between state variables on the higher level and the lower level of description and their conjugates. MaxEnt provides lower entropy $\downarrow S(\mathbf{y})$ and a relation $\mathbf{x} = \pi^{-1}(\mathbf{y})$ from composition of $\tilde{\mathbf{x}}(\mathbf{y}^*)$ and $\tilde{\mathbf{y}}^*(\mathbf{y})$. LT denotes a relation via Legendre transformation, π stands for a projection from the microscale to the macroscale variables and by an arrow we depict a mapping (written above or below the arrow) that relates the variables in the connected nodes.

3. Dynamic MaxEnt

A form of the Dynamic MaxEnt reduction first appeared in [15] in the context of contact geometry. Here, we further develop DynMaxEnt using the energetic representation, which simplifies the procedure so that reductions, for example, from complex fluid dynamics to Navier–Stokes equation and from hyperbolic heat conduction to the Fourier law are carried out easily. Moreover, we generalize the method to an infinite chain of consecutive approximations.

The key idea behind dynamic MaxEnt is to treat conjugate variables \mathbf{x}^\dagger as independent quantities ensuring invariance of the quasi-equilibrium manifold. This step is motivated by contact geometry, where conjugate variables are indeed granted independence and evolve towards the corresponding Gibbs–Legendre manifold, see Section 6.1.

3.1. First Order DynMaxEnt Reduction

Here, we propose an extension to the static version of MaxEnt (This extension is based on our previous work in [14]; however, we clarify, extend and elaborate on this method in this article.), which provides in addition to the lower entropy $\downarrow S(\mathbf{y})$ and the inverse projection $\pi^{-1}(\mathbf{y})$ the dynamics on the lower level, i.e., reduced evolution equations.

Assuming the evolution on the more microscopic (higher) level can be expressed as

$$\dot{\mathbf{x}}^i = V^i(\mathbf{x}, \mathbf{x}^\dagger), \tag{3}$$

where \mathbf{x}^\dagger are conjugate variables which can be eventually identified with derivatives of energy (being the choice in this paper or e.g., [17–19]), entropy or another thermodynamic potential. Let us denote the

yet unspecified functional by $\uparrow\Phi$, i.e., $x_i^\dagger = \uparrow\Phi_{x_i}$. Components of the right-hand side of the evolution equations V^i can be interpreted as elements of a vector field on the manifold of state variables \mathcal{M} , $\mathbf{x} \in \mathcal{M}$. With the inverse relation (we shall use simply $\bar{\mathbf{x}}(\mathbf{y})$ instead of $\pi^{-1}(\mathbf{y})$ hereafter) at hand, which enslaves the microscale state variables \mathbf{x} in terms of the macroscale (or reduced) variables \mathbf{y} , we may evaluate the more detailed evolution equations on the MaxEnt manifold as

$$\dot{x}^i = \frac{\partial \bar{x}^i}{\partial y^a} \dot{y}^a = V^i \left(\bar{\mathbf{x}}(\mathbf{y}), \mathbf{x}^\dagger = \mathbf{y}^\dagger \cdot \frac{\partial \pi}{\partial \mathbf{x}} \Big|_{\bar{\mathbf{x}}(\mathbf{y})} \right), \tag{4}$$

noting that

$$\frac{\partial \uparrow\Phi(\bar{\mathbf{x}}(\pi(\mathbf{x})))}{\partial x^i} \Big|_{\bar{\mathbf{x}}(\mathbf{y})} = \frac{\partial \uparrow\Phi}{\partial \mathbf{y}} \cdot \frac{\partial \pi}{\partial \mathbf{x}} \Big|_{\bar{\mathbf{x}}(\mathbf{y})} \tag{5}$$

for $\downarrow\Phi(\mathbf{y}) = \uparrow\Phi(\bar{\mathbf{x}}(\mathbf{y}))$. By projection π , we obtain the reduced equations

$$\dot{y}^a = \frac{\partial \pi^a}{\partial x^i} \Big|_{\bar{\mathbf{x}}(\mathbf{y})} \dot{x}^i = \frac{\partial \pi^a}{\partial x^i} \Big|_{\bar{\mathbf{x}}(\mathbf{y})} V^i \left(\bar{\mathbf{x}}(\mathbf{y}), \mathbf{x}^\dagger = \mathbf{y}^\dagger \cdot \frac{\partial \pi}{\partial \mathbf{x}} \Big|_{\bar{\mathbf{x}}(\mathbf{y})} \right), \tag{6}$$

where it should be noted that the reduced equations have to live on the lower level. To this end, a relation $\bar{\mathbf{x}}^\dagger(\mathbf{y}, \mathbf{y}^\dagger)$ has to be identified. By comparing these last two evolution equations, it follows that

$$\frac{\partial \bar{x}^i}{\partial y^a} \frac{\partial \pi^a}{\partial x^j} \Big|_{\bar{\mathbf{x}}(\mathbf{y})} V^j \left(\bar{\mathbf{x}}(\mathbf{y}), \mathbf{x}^\dagger = \mathbf{y}^\dagger \cdot \frac{\partial \pi}{\partial \mathbf{x}} \Big|_{\bar{\mathbf{x}}(\mathbf{y})} \right) = V^i(\bar{\mathbf{x}}(\mathbf{y}), \mathbf{x}^\dagger(\mathbf{y}, \mathbf{y}^\dagger)), \tag{7}$$

which is a consistency condition entailing relations among conjugate variables $\bar{\mathbf{x}}^\dagger(\mathbf{y}, \mathbf{y}^\dagger)$. Without this condition, the evolution (4) would leave the manifold of MaxEnt states $\bar{\mathbf{x}}(\mathbf{y})$, the vector field would be sticking out of the MaxEnt manifold \mathcal{M} . Condition (7) is actually an equation for \mathbf{x}^\dagger , the solution of which will be denoted by $\bar{\mathbf{x}}^\dagger(\mathbf{y}, \mathbf{y}^\dagger)$. After substitution into Equation (6), we obtain the reduced evolution equations for \mathbf{y} , which is the result of the first order DynMaxEnt reduction.

The first order DynMaxEnt reduction can be summarized as the sequence

$$\mathbf{y} \xrightarrow{\text{MaxEnt}} \bar{\mathbf{x}}(\mathbf{y}) \xrightarrow{\text{Equation (7)}} \bar{\mathbf{x}}^\dagger(\mathbf{y}, \mathbf{y}^\dagger), \tag{8}$$

which ends up in a closed system of equations for the reduced state variables \mathbf{y} . The lower level potential follows from the projection as $\downarrow\Phi(\mathbf{y}) = \uparrow\Phi(\bar{\mathbf{x}}(\mathbf{y}))$.

Note, however, that the link tying \mathbf{x} and \mathbf{x}^\dagger was broken because $\bar{\mathbf{x}}^\dagger$ was determined by solving Equation (7) instead of differentiating the potential $\uparrow\Phi$ with respect to \mathbf{x} at $\bar{\mathbf{x}}(\mathbf{y})$. This leads to the higher order DynMaxEnt reduction.

3.2. Higher Order DynMaxEnt

From the first order DynMaxEnt, we have acquired independent relations among direct and conjugate variables, $\bar{\mathbf{x}}(\mathbf{y})$ and $\bar{\mathbf{x}}^\dagger(\mathbf{y}, \mathbf{y}^\dagger)$, but at the same time direct and conjugate variables are linked via the potential $\uparrow\Phi$. This entails that these two relations cannot be independent and some of the relations have to be violated.

There are two possible remedies of this situation both being iterative: (i) to correct the upper entropy so that the MaxEnt value is indeed a conjugate to the identified relation $\bar{\mathbf{x}}^\dagger(\mathbf{y}, \mathbf{y}^\dagger)$ on the lower level; however, this change in entropy means that MaxEnt has to be recalculated including everything that follows as well and the situation repeats itself; (ii) to correct the MaxEnt value of the direct variable so that the direct and conjugate values are now in line with the upper entropy evaluated on the lower level; however, this again modifies the dependent evolution equations on the lower level, in turn the value of upper conjugate variables and the situation repeats.

Although the former correction, the correction of the upper entropy, might seem natural, it turns out that it cannot be a general approach as the corrected entropy would fail to meet the requirement of being an even function with respect to time reversal when the reduced state variables change parity during the transition to a lower level, see Appendix A.1. We shall now develop the latter approach in detail (forming a possibly infinite chain of corrections) and compare it with asymptotic methods for upscaling evolution equations.

To repair the link between \mathbf{x} and \mathbf{x}^\dagger , which remained broken after the first order DynMaxEnt reduction, an additional correction of the state variables \mathbf{x} is required,

$$\left. \frac{\partial^\dagger \Phi}{\partial \mathbf{x}} \right|_{\bar{\mathbf{x}}^{(2)}} = \bar{\mathbf{x}}^\dagger(\mathbf{y}, \mathbf{y}^\dagger). \tag{9}$$

The solution to this equation gives the second iteration of the value of the state variable, $\bar{\mathbf{x}}^{(2)}(\mathbf{y}, \mathbf{y}^\dagger)$.

However, is the consistency condition (7) satisfied at $\bar{\mathbf{x}}^{(2)}$? Not in general. Therefore, the condition can be regarded as an equation for the second-order iteration of \mathbf{x}^\dagger , $\bar{\mathbf{x}}^{\dagger(2)}$. This iterative chain can be summarized as

$$\mathbf{y} \xrightarrow{\text{MaxEnt}} \bar{\mathbf{x}}(\mathbf{y}) \xrightarrow{\text{Equation (7)}} \bar{\mathbf{x}}^\dagger(\mathbf{y}, \mathbf{y}^\dagger) \xrightarrow{\text{Equation (9)}} \bar{\mathbf{x}}^{(2)}(\mathbf{y}, \mathbf{y}^\dagger) \xrightarrow{\text{Equation (7)}} \bar{\mathbf{x}}^{\dagger(2)}(\mathbf{y}, \mathbf{y}^\dagger) \rightarrow \dots, \tag{10}$$

which can continue indefinitely. We have thus found an infinite chain of DynMaxEnt reduction, which leads to evolution equations for the reduced state variables \mathbf{y} in a closed form. Note that the lower potential corresponds to the chosen step k in the infinite chain of DynMaxEnt as $\downarrow\Phi^{(k)}(\mathbf{y}) = \uparrow\Phi(\bar{\mathbf{x}}^{(k)}(\mathbf{y}))$.

It is now apparent that any correction in this infinite chain of DynMaxEnt reduction leads to another correction as any of the adaptations, be it in direct or conjugate variables or even entropy, yield new disparity. Where should one end the iteration and what is the best choice of a method generating evolution equations on the lower level of description while retaining the thermodynamic structure and knowledge of the equations?

First, it should be mentioned that the aim of dynamic MaxEnt is to arrive at reasonable evolution equations for a specified level of description. We conjecture that the static MaxEnt value of direct variables $\bar{\mathbf{x}}(\mathbf{y})$ is the best choice as it corresponds to the most probable, least biased relation [20] between direct lower and upper state variables. The conjugate variables then follow from the requirement of the dynamics being such that it does not drive the system away from the MaxEnt values of the direct variables, i.e., $\bar{\mathbf{x}}^\dagger(\mathbf{y}, \mathbf{y}^\dagger)$. Finally, the lower potential is chosen as the first correction $\downarrow\Phi^{(2)}(\mathbf{y}) = \uparrow\Phi(\bar{\mathbf{x}}^{(2)}(\mathbf{y}))$. The reason is twofold: (i) a correction of the lower entropy neither affects the static MaxEnt value nor does it explicitly change the evolution equations that are given in terms of direct and conjugate variables (it affects them indirectly via a resulting change of the relation of conjugate to direct variables); (ii) the corrected entropy is more tightly linked to the evolution equations rather than to the static MaxEnt which we aim to extend. Additionally, as we shall see below, in the special case of projection corresponding to relaxation of fast variables, the $\downarrow S$ entropy is simply the upper entropy but where all the effects of fast variables are neglected while the correction $\downarrow S^{(2)}$ includes additional (typically non-local) effects resulting from this transition between levels.

In short, direct state variables are set-up in such a way that their most probable value (with given information about the system comprised in entropy) is always kept on the lower level (although it might evolve with the evolution of the lower state variables). The choice of conjugate variables entails persistence of the direct variables exactly on their most probable values. Lower entropy corresponds to the set-up of conjugate rather than direct variables, which contain some non-trivial effects due to the transition of scales.

3.3. Prototype Example—Damped Particle

Let us now demonstrate the DynMaxEnt reduction on a prototype example—damped particle in a potential field. The state variables represent position, momentum and entropy of the particle, $\mathbf{x} = (\mathbf{r}, \mathbf{p}, s)$, and momentum is considered as the fast variable, which is to be reduced, i.e., $y = (\mathbf{r}, s)$. The projection to the lower (less detailed) level is thus $\pi : (\mathbf{r}, \mathbf{p}, s) \rightarrow (\mathbf{r}, s)$.

The more detailed evolution equations are ([14], Ch 5.3.1)

$$\dot{\mathbf{r}} = \mathbf{p}^\dagger, \tag{11a}$$

$$\dot{\mathbf{p}} = -\mathbf{r}^\dagger - \frac{1}{\tau} \frac{\mathbf{p}^\dagger}{s^\dagger}, \tag{11b}$$

$$\dot{s} = \frac{1}{\tau} \left(\frac{\mathbf{p}^\dagger}{s^\dagger} \right)^2, \tag{11c}$$

where x^\dagger can be interpreted as conjugates with respect to energy

$$\uparrow e = \frac{\mathbf{p}^2}{2m} + V(\mathbf{r}) + \varepsilon(s), \tag{12}$$

consisting of kinetic energy, potential energy and internal energy. The evolution equations represent Hamilton canonical equations (for \mathbf{r} and \mathbf{p}) equipped with friction in \mathbf{p} and entropy production, c.f. [21]. Total energy is conserved by the evolution equations, $\dot{e} = \mathbf{r}^\dagger \dot{\mathbf{r}} + \mathbf{p}^\dagger \dot{\mathbf{p}} + s^\dagger \dot{s} = 0$.

3.3.1. First Order DynMaxEnt

From relation (12), it follows that entropy on the higher level reads

$$\uparrow s = s \left(e - \frac{\mathbf{p}^2}{2m} - V(\mathbf{r}) \right), \tag{13}$$

$s(\bullet)$ being the inverse function to $\varepsilon(\bullet)$. Entropy attains maximum (for a given energy and position) at $\bar{\mathbf{p}} = 0$, which is the MaxEnt value of momentum.

The consistency condition (7) becomes in this particular case

$$\begin{pmatrix} 1 & 0 \\ 0 & 0 \\ 0 & 1 \end{pmatrix} \cdot \begin{pmatrix} 1 & 0 & 0 \\ 0 & 0 & 1 \end{pmatrix} \cdot \begin{pmatrix} \mathbf{p}^\dagger \\ -\mathbf{r}^\dagger - \frac{1}{\tau} \frac{\mathbf{p}^\dagger}{s^\dagger} \\ \frac{1}{\tau} \left(\frac{\mathbf{p}^\dagger}{s^\dagger} \right)^2 \end{pmatrix} = \begin{pmatrix} \mathbf{p}^\dagger \\ -\mathbf{r}^\dagger - \frac{1}{\tau} \frac{\mathbf{p}^\dagger}{s^\dagger} \\ \frac{1}{\tau} \left(\frac{\mathbf{p}^\dagger}{s^\dagger} \right)^2 \end{pmatrix}, \tag{14}$$

which can be simplified to

$$0 = -\mathbf{r}^\dagger - \frac{1}{\tau} \frac{\mathbf{p}^\dagger}{s^\dagger}. \tag{15}$$

The solution to this equation is the first iteration of the conjugate momentum, $\bar{\mathbf{p}}^\dagger = -\tau s^\dagger \mathbf{r}^\dagger$. Plugging this back into the evolution equations leads to

$$\dot{\mathbf{r}} = -\tau s^\dagger \mathbf{r}^\dagger, \tag{16a}$$

$$\dot{s} = \tau (\mathbf{r}^\dagger)^2. \tag{16b}$$

These are the reduced equations obtained by the first order DynMaxEnt procedure. The \dagger symbols denote derivative of a yet unspecified energy on the lower level of description $\downarrow e(\mathbf{r}, s)$. Note that the energy is again conserved and that entropy is produced. To make the reduced evolution equations closed, we should identify the lower energy $\downarrow e$ as the MaxEnt value of the higher-level energy,

$$\downarrow e = \uparrow e(\mathbf{r}, \bar{\mathbf{p}}, s) = V(\mathbf{r}) + \varepsilon(s). \tag{17}$$

Equations (16) then gain an explicit form manifesting that the particle tends to the minimum of the potential V while producing entropy.

3.3.2. Second Order DynMaxEnt

By solving equation (14), we have actually broken the link between \mathbf{p} and \mathbf{p}^\dagger , namely $\mathbf{p}^\dagger \neq \partial^\dagger e / \partial \mathbf{p}$. To recover that link, we have to find a new value of \mathbf{p} that corresponds to the obtained $\tilde{\mathbf{p}}^\dagger$,

$$\frac{\tilde{\mathbf{p}}^{(2)}}{m} = \left. \frac{\partial^\dagger e}{\partial \mathbf{p}} \right|_{\tilde{\mathbf{p}}^{(2)}} = -\tau \frac{\partial^\dagger e}{\partial s} \frac{\partial^\dagger e}{\partial \mathbf{r}} = -\tau \frac{\partial \varepsilon}{\partial s} \frac{\partial V}{\partial \mathbf{r}}. \tag{18}$$

Plugging this new value of \mathbf{p} into energy ${}^\dagger e$ gives a new energy on the lower level,

$$\downarrow e^{(2)} = \frac{m}{2} \left(\tau \frac{\partial \varepsilon}{\partial s} \frac{\partial V}{\partial \mathbf{r}} \right)^2 + V(\mathbf{r}) + \varepsilon(s), \tag{19}$$

which can be seen as a weakly nonlocal correction of the MaxEnt lower energy $\downarrow e$.

Once the link between \mathbf{p} and \mathbf{p}^\dagger through derivative of energy (Legendre transformation) has been recovered by updating $\tilde{\mathbf{p}}$ to $\tilde{\mathbf{p}}^{(2)}$, condition (14) no longer holds. To satisfy the condition, we have to find a new value of the conjugate momentum by solving (assuming that $\tau \partial \varepsilon / \partial s = \zeta = \text{const}$ for simplicity)

$$\begin{aligned} \dot{\tilde{\mathbf{p}}}^{(2)} &= -m\zeta \frac{\partial^2 V}{\partial \mathbf{r}^2} \dot{\mathbf{r}} = -m\zeta \frac{\partial^2 V}{\partial \mathbf{r}^2} \tilde{\mathbf{p}}^{+(2)} \\ &= -\mathbf{r}^\dagger - \frac{1}{\zeta} \tilde{\mathbf{p}}^{+(2)} = -\frac{\partial V}{\partial \mathbf{r}} - \frac{1}{\zeta} \tilde{\mathbf{p}}^{+(2)}. \end{aligned} \tag{20}$$

The solution to this equation is

$$\tilde{\mathbf{p}}^{+(2)} = \frac{-\zeta \frac{\partial V}{\partial \mathbf{r}}}{1 - m\zeta^2 \frac{\partial^2 V}{\partial \mathbf{r}^2}} \sim -\zeta \frac{\partial V}{\partial \mathbf{r}} - m\zeta^3 \frac{\partial V}{\partial \mathbf{r}^2} + O(\zeta)^5. \tag{21}$$

The latter contribution is obviously of the second order in the relaxation time τ while the former contribution is identical to the \mathbf{p}^\dagger found above. This second-order correction of conjugate momentum can be plugged back into the equations for $\dot{\mathbf{r}}$ and \dot{s} to obtain

$$\dot{\mathbf{r}} = \frac{-\zeta \frac{\partial V}{\partial \mathbf{r}}}{1 - m\zeta^2 \frac{\partial^2 V}{\partial \mathbf{r}^2}}, \tag{22a}$$

$$\dot{s} = \frac{\zeta}{s^\dagger} \frac{\left(\frac{\partial V}{\partial \mathbf{r}} \right)^2}{\left(1 - m\zeta^2 \frac{\partial^2 V}{\partial \mathbf{r}^2} \right)^2}, \tag{22b}$$

which is the second-order DynMaxEnt reduction. It is instructive to compare asymptotic expansion of the evolution equations for small τ / ζ with DynMaxEnt.

Note that the singularity suggested by this second order DynMaxEnt is not physically relevant but rather an invitation to a higher order as Equation (20) reveals—independence of $\mathbf{p}^{+(2)}$ and $\partial_{\mathbf{r}} V = 0$. In addition, if $\tau \ll 1$, i.e., $\zeta \ll 1$ is small, DynMaxEnt generates a converging sequence of evolution laws where there is no blow-up. Hence, when the parameter ζ or τ is not small, the “corrections” stemming from higher order DynMaxEnt might be large and significant. Hence, as we shall further explore below, the higher order corrections seem to be mainly relevant when a small parameter is present.

3.3.3. Damped Particle by Asymptotic Expansions

A hallmark example of the usage of asymptotic expansions in statistical physics is the Chapman–Enskog expansion in kinetic theory [2,22].

In general, the two approaches, asymptotic expansion vs. Dynamic MaxEnt, are very different concepts of obtaining description of a system on a coarser level. The asymptotic analysis (such as the method of multiple scales, homogenisation, regular and singular perturbation methods or boundary layer analysis) does not explicitly assess the lower level of description or what exactly does the asymptotic approximation represents, but, from intuition and the dimensionless form of the evolution equations, one can use the presence of a small parameter to relate two levels of description (more precisely, two different spatial or temporal scales). The number of state variables and evolution equations are typically not changed (although in Chapman–Enskog analysis, evolution equations for several moments of the distribution function somewhat naturally appear) and a suitable choice of the form of expansion series allows a nested problem formulation on the coarser level by sequentially solving each asymptotic order. Note, however, that there is not a unique way to include the small parameter in spatial scaling, etc.

Dynamic MaxEnt, on the other hand, uses projections to the lower level of description (e.g., by relaxation of fast variables). In particular, the number of evolution equations (state variables) can be very different on the two levels in contrast to asymptotic analysis.

Let us compare the asymptotic method of solution with the Dynamic MaxEnt method on the simple problem of a damped particle where the dimensionless parameter $1/\tau$ measures the ratio of the reversible and irreversible evolution. Typically, the timescale of relaxation of dissipative processes is much shorter than the remaining evolution, hence $\tau \ll 1$. The solution to the problem can be searched in the form of asymptotic expansions

$$\mathbf{p} = \mathbf{p}_0 + \tau \mathbf{p}_1 + \tau^2 \mathbf{p}_2 + O(\tau^3), \quad \mathbf{r} = \mathbf{r}_0 + \tau \mathbf{r}_1 + O(\tau^2), \quad s = s_0 + \tau s_1 + O(\tau^2) \quad (23)$$

and the conjugate \mathbf{r}^\dagger variable has the following expansion

$$\mathbf{r}^\dagger = V_{\mathbf{r}}(\mathbf{r}_0 + \tau \mathbf{r}_1 + \tau^2 \mathbf{r}_2) = V_{\mathbf{r}}(\mathbf{r}_0) + \tau \mathbf{r}_1 V_{\mathbf{r}}(\mathbf{r}_0) + O(\tau^2).$$

Noting that $\mathbf{p}^\dagger = \mathbf{p}/m$, the leading order solution is

$$\tau^{-1} : \quad \mathbf{p}_0 = 0,$$

while the first subleading order gives

$$\tau^0 : \quad \mathbf{p}_1 = -ms^\dagger V_{\mathbf{r}}(\mathbf{r}_0), \quad \dot{\mathbf{r}}_0 = \frac{\mathbf{p}_0}{m} = 0.$$

Therefore, \mathbf{p}_1 is independent of time and the second subleading order reads

$$\mathbf{p}_2 = -ms^\dagger V_{\mathbf{r}\mathbf{r}}(\mathbf{r}_0) \mathbf{r}_1 - ms^\dagger \dot{\mathbf{p}}_1 = -ms^\dagger V_{\mathbf{r}\mathbf{r}}(\mathbf{r}_0) \mathbf{r}_1, \quad \dot{\mathbf{r}}_1 = \frac{\mathbf{p}_1}{m} = -s^\dagger V_{\mathbf{r}}(\mathbf{r}_0), \quad (24)$$

while, finally, $\dot{\mathbf{r}}_2 = \mathbf{p}_2/m$. In summary, the reduced evolution up to the second order can be characterised by the following set of equations:

$$\dot{\mathbf{r}}_0 = 0, \quad \dot{\mathbf{r}}_1 = -s^\dagger V_{\mathbf{r}}(\mathbf{r}_0), \quad \dot{\mathbf{r}}_2 = -s^\dagger V_{\mathbf{r}\mathbf{r}}(\mathbf{r}_0) \mathbf{r}_1. \quad (25)$$

From the first subleading order, one could estimate that perhaps $\mathbf{p}_0 = 0$, $\mathbf{p}_1 = -ms^\dagger \mathbf{r}^\dagger$ and thus $\dot{\mathbf{r}} = -\tau ms^\dagger \mathbf{r}^\dagger$. We can now straightforwardly verify this by using the asymptotic expansions (23).

Hence, indeed, we have $\mathbf{p} = -\tau m s^\dagger \mathbf{r}^\dagger$ while the remaining equations can be written in the following way:

$$\dot{\mathbf{r}} = -\tau s^\dagger \mathbf{r}^\dagger, \tag{26a}$$

$$\dot{s} = \tau \left(\mathbf{r}^\dagger\right)^2, \tag{26b}$$

which means that the particle tends to the minimum of the potential $V(\mathbf{r})$. These equations are in line with Equations (16), obtained by DynMaxEnt. Additionally, the leading order solution in the asymptotic method corresponds to MaxEnt $\tilde{\mathbf{x}}(\mathbf{y})$ value (as in the Chapman–Enskog solution to the Boltzmann equation where the leading order solution corresponding to vanishing collision term is the local Maxwell distribution).

Note that we proposed the DynMaxEnt method to be the first order in state variables (both direct and conjugate) accompanied by the second order lower energy $\downarrow e^{(2)}$. In particular, if we now compare the lower evolution equations from the asymptotic (26) and dynamic MaxEnt (16), we observe that they are identical with the exception stemming from the correction of the lower energy (conjugates in the lower evolution equations are always with respect to the lower energy). Furthermore, the comparison of the asymptotic solution \mathbf{p} , Equation (24), and of the dynamic MaxEnt result reveals that: (i) the structure of dynamic MaxEnt iteration resembles asymptotic expansion for a small parameter τ ; (ii) the leading order solutions are the same, however, the subleading terms differ.

3.3.4. Relation to GENERIC

Evolution equations for the damped particle (11) can be seen as a particular realization of the General Equation for Non-Equilibrium Reversible-Irreversible Coupling (GENERIC) [4,14,23,24], with the following building blocks

$$\mathbf{L} = \begin{pmatrix} 0 & 1 & 0 \\ -1 & 0 & 0 \\ 0 & 0 & 0 \end{pmatrix} \quad \text{and} \quad \Xi(\mathbf{p}) = \frac{1}{2} \frac{1}{\tau} (\mathbf{p}^*)^2, \tag{27}$$

where the former expression defines a Poisson bivector while the latter dissipation potential (Irreversible evolution generated by a dissipation potential is also called gradient dynamics. It is in tight relation to the Steepest Entropy Ascent [25,26], which is essentially equivalent to the formulation of GENERIC with dissipative brackets [4].). The dissipation potential is naturally formulated in terms of \mathbf{p}^* , which can be interpreted as derivative of entropy. The evolution equation consists of reversible part $\mathbf{L} \cdot dE$ and irreversible $\Xi_{\mathbf{p}^*}|_{\mathbf{p}^*=s_{\mathbf{p}}}$. In order to use only derivative w.r.t. energy, we recall the relation among the two representations $\mathbf{p}^* = -\mathbf{p}^\dagger/s^\dagger$, see [14,27] for more details (Indeed, on the Gibbs–Legendre manifold, where conjugate variables are identified with derivatives of thermodynamic potentials, one has $\left(\frac{\partial s}{\partial p_i}\right)_e = -\left(\frac{\partial e}{\partial p_i}\right)_s \left(\frac{\partial e}{\partial s}\right)_\mathbf{p}^{-1}$ and $\left(\frac{\partial e}{\partial s}\right)_\mathbf{p} = \left(\frac{\partial s}{\partial e}\right)_\mathbf{p}^{-1}$.) The equations are then explicitly

$$\frac{d}{dt} \begin{pmatrix} \mathbf{r} \\ \mathbf{p} \\ s \end{pmatrix} = \begin{pmatrix} 0 & 1 & 0 \\ -1 & 0 & 0 \\ 0 & 0 & 0 \end{pmatrix} \cdot \begin{pmatrix} \mathbf{r}^\dagger \\ \mathbf{p}^\dagger \\ s^\dagger \end{pmatrix} + \begin{pmatrix} 0 \\ -\frac{1}{\tau} \frac{\mathbf{p}^\dagger}{s^\dagger} \\ \frac{1}{\tau} \left(\frac{\mathbf{p}^\dagger}{s^\dagger}\right)^2 \end{pmatrix}, \tag{28}$$

which is the same as Equations (11). The equations thus possess the GENERIC structure.

After the relaxation of the momentum \mathbf{p} , expressed by Equation (15), evolution of positions becomes irreversible, given by Equation (16). Is this equation compatible with GENERIC? In other words, is there a dissipation potential generating that evolution? The answer is affirmative and actually easy to find at least in the case of the damped particle. Indeed, by evaluating dissipation potential $\Xi(\mathbf{p})$ at the constitutive relation (15), we obtain dissipation potential for the lower level

$$\Xi^{(r)}(\mathbf{r}^*) = \Xi^{(p)}|_{\mathbf{p}^* = -\tau \mathbf{r}^\dagger = \tau \frac{\mathbf{r}^*}{e^*}} = \frac{\tau}{2} \left(\frac{\mathbf{r}^*}{e^*} \right)^2, \tag{29}$$

where $e^* = S_e = 1/s^\dagger$, e being total energy of the particle. Derivative of this dissipation potential w.r.t. \mathbf{p}^* reads

$$\dot{\mathbf{r}} = \Xi_{\mathbf{r}^*}^{(r)} = \tau \frac{\mathbf{r}^*}{(e^*)^2} = -\tau s^\dagger \mathbf{r}^\dagger, \tag{30}$$

which is the reduced evolution equation (16). In other words, at least in this particular case the reduced evolution equation for \mathbf{r} is generated by a dissipation potential constructed from the original dissipation potential for \mathbf{p} by a projection, see also [21]. At least in the case of damped particle, the reduced evolution is a particular realization of GENERIC, and the reduced dissipation potential is obtained from the original dissipation potential.

3.4. Summary of the Dynamic MaxEnt Method

A few remarks should be pointed out:

1. MaxEnt with constraints corresponding to a chosen projection linking the two levels of description is equivalent to MinEne with the same constraints. This follows from the same argument as used in ([27], Ch 5.1) only with the addition of constraints which, crucially, describe the same manifold in the phase space of (S, E, \mathbf{x}) .
2. It is important to consider direct and conjugate variables to be independent until reaching the Legendre manifold where they are related via appropriate entropy. This stands out during the MaxEnt procedure as noted above and in the contact-geometric formulation in Section 5.
3. Static MaxEnt should be seen as not providing a relation among conjugate variables but rather only among the direct ones. This can be appreciated in a special case of projection that corresponds to a relaxation of fast variables in the system, hence removing some of the state variables \mathbf{x} when a transition to a less microscopic description is carried out. For this point of view, it is essential to consider direct and conjugate variables as independent.
4. If direct and conjugate variables are not considered independent during MaxEnt and hence MaxEnt would provide MaxEnt values for both reduced and conjugate variables, the dynamics on MaxEnt manifold would be (typically) such that its vector field would be “sticking out”, i.e., driving the dynamics out of the MaxEnt manifold. The correction in finding $\tilde{\mathbf{x}}^*(\mathbf{y}, \mathbf{y}^*)$ is exactly such that the MaxEnt manifold \mathcal{M} in direct variables is never left by the dynamics.
5. The distinction of direct and conjugate variables has several crucial benefits. First, it guarantees the thermodynamic structure of the evolution equations (potentials, reversible and irreversible parts of equations, CR-GENERIC or possibly GENERIC structure). Secondly, this distinction of state variables enables to always sustain the MaxEnt, i.e., the most probable, value of the direct variables on the lower description (as discussed above). This cannot be achieved in an asymptotic framework/approach, where such knowledge is not at hand and the solution is searched in the form of asymptotic corrections to a leading order solution.
6. Parity of the state variables with respect to time reversal typically changes during the DynMaxEnt reduction. For instance, the momentum, which was initially an odd variable, becomes proportional to the gradient of potential, which is even, or the conformation tensor (which is initially even) becomes proportional to the shear rate, which is odd. Similarly, behavior with respect to space-time transformations (e.g., Galilean boost) also changes. For instance, momentum of a particle, the value of which of course depends on the choice of inertial laboratory frame, becomes independent of Galilean boosts after the reduction (being proportional to gradient of the potential). This is compatible with the multiscale point of view of the studied systems. For instance, if one is able to measure the conjugate entropy flux \mathbf{w} (see Section 4.3) directly, one can also see that Galilean boost affects it, and one should stay on the level of description

where \mathbf{w} is among the state variables. On the other hand, if one only measures \mathbf{w} in the relaxed state, where it is proportional to the gradient of temperature, one does not see the effect of Galilean boosts anymore, and one can safely work on the Fourier level, where \mathbf{w} is no longer among the state variables. In summary, the behavior of physical quantities with respect to time reversal and space-time transformations crucially depends on the chosen level of description, and this level-dependent behavior is compatible with the multiscale point of view of physical systems.

The comparison to the asymptotic expansion methods provided further insight into the Dynamic MaxEnt method. For example, the asymptotic analysis provides corrections to the solution at each order, whereas Dynamic MaxEnt provides relations for closures/fluxes. In the particular examples above, it may seem that both methods yield the same set of leading order evolution equations but note that this is only when one can explicitly solve the asymptotic problems in each order. As noted above, typically asymptotic methods do not change the number of equations as opposed to Dynamic MaxEnt, where the number is given by the projection. Asymptotic methods also typically do not change parity with respect to time reversal, whereas DynMaxEnt does [28]. Finally, note that Dynamic MaxEnt does not rely per se on the presence of a small parameter but rather on the existence of a projection which is similar but not the same.

In summary, Dynamic MaxEnt does not have (and perhaps should not have) an aim to find other than the leading order evolution equations on a specified level. From all the observations and discussion above, we propose that the most appropriate choice for this aim is to find and keep the static MaxEnt values of direct variables exactly while identifying the conjugate state variables in such a way that evolution (dynamics) stays exactly on this MaxEnt value of direct variables; entropy is modified in such a way as to correspond to conjugate variables and the first correction of the direct variables. It seems that, if the zero-th order asymptotic solution coincides with the static MaxEnt value of the direct state variable $\bar{\mathbf{x}}(\mathbf{y})$, the asymptotic expansion method yields the same leading order behaviour as the Dynamic MaxEnt (although without the thermodynamic structure and new phenomena linked to the change of entropy accompanying the transition of scales). Interestingly, we found in the studied example that even higher order asymptotic solutions seem to be related to the Dynamic MaxEnt method, although it is yet unclear how exactly and will be subjected to further research.

4. Applications in Continuum Thermodynamics

Let us now demonstrate the Dynamic MaxEnt on a few examples in continuum thermodynamics, namely on relaxation of conformation tensor, relaxation of Reynolds stress, and hyperbolic heat conduction. The former two examples were already discussed in [14].

4.1. Suspension of Hookean Dumbbells

4.1.1. Non-Equilibrium Thermodynamics of Conformation Tensor

First, let the state variables be density of matter ρ , momentum density \mathbf{u} , entropy density s and conformation tensor c^{ij} , which expresses correlations of dumbbell orientation and prolongation. Poisson bracket expressing kinematics of these state variables is

$$\begin{aligned} \{A, B\}^{(c)} &= \{A, B\}^{(FM)} + \int \mathbf{d}\mathbf{r} c_{ij} \left(\partial_k A c_{ij} B_{u_k} - \partial_k B c_{ij} A_{u_k} \right) \\ &+ \int \mathbf{d}\mathbf{r} c_{ij} \left(\left(A_{c_{kj}} + A_{c_{jk}} \right) \partial_i B_{u_k} - \left(B_{c_{kj}} + B_{c_{jk}} \right) \partial_i A_{u_k} \right), \end{aligned} \tag{31}$$

where c^{ij} was identified with c_{ij} for simplicity of notation. Bracket $\{\bullet, \bullet\}^{(FM)}$ is the fluid mechanics Poisson bracket (A3). Note that the conformation tensor is related to the left Cauchy–Green tensor \mathbf{B}

by $\mathbf{c} = \rho \mathbf{B}$. Reversible evolution equations for state variables $\mathbf{x} = (\rho, \mathbf{u}, s, \mathbf{c})$ implied by bracket (31) are

$$\frac{\partial \rho}{\partial t} = -\partial_i (\rho E_{u_i}), \tag{32a}$$

$$\begin{aligned} \frac{\partial u_i}{\partial t} = & -\partial_j (u_i E_{u_j}) - \rho \partial_i E_\rho - u_j \partial_i E_{u_j} - s \partial_i E_s - \\ & -c_{jk} \partial_i E_{c_{jk}} + \partial_k (c_{kj} (E_{c_{ij}} + E_{c_{ji}})), \end{aligned} \tag{32b}$$

$$\frac{\partial s}{\partial t} = -\partial_i (s E_{u_i}), \tag{32c}$$

$$\frac{\partial c_{ij}}{\partial t} = -\partial_k (c_{ij} E_{u_k}) + c_{kj} \partial_k E_{u_i} + c_{ki} \partial_k E_{u_j}, \tag{32d}$$

where E is the total energy of the system.

With energy

$$E = \int d\mathbf{r} \left[\frac{\mathbf{u}^2}{2\rho} + \varepsilon(\rho, s, \mathbf{c}) \right], \tag{33}$$

where internal energy ε still remains unspecified, evolution equation (32d) can be rewritten in terms of the upper-convected time-derivative as

$$\overset{\nabla}{\mathbf{c}} = -\mathbf{c} \nabla \cdot \mathbf{v}, \quad \mathbf{v} = \frac{\mathbf{u}}{\rho}, \tag{34}$$

which is the reversible part of Maxwell rheological model [29].

Considering a suspension of Hookean dumbbells, entropy is

$$S = \int d\mathbf{r} \left[\frac{1}{2} n k_B \ln \det \mathbf{c} + s \left(n, e - \frac{\mathbf{u}^2}{2\rho} - \frac{1}{2} H \text{Tr} \mathbf{c} \right) \right], \tag{35}$$

as derived for instance in [14]. Parameter H is the spring constant of the dumbbells, and n represents concentration of dumbbells. Derivative of this entropy with respect to \mathbf{c} is

$$c_{ij}^* = \frac{\partial S}{\partial c_{ij}} = \frac{1}{2} k_B n c_{ij}^{-1} - \frac{1}{2} \frac{H}{T} \delta_{ij}, \tag{36}$$

which is equal to zero for

$$\bar{\mathbf{c}} = \frac{k_B T n}{H} \mathbf{I}. \tag{37}$$

This is the MaxEnt value of \mathbf{c} . Note that inverse temperature T^{-1} is identified as derivative of entropy with respect to energy density.

Dissipation potential can be prescribed as

$$\Xi^{(\mathbf{c})} = \int d\mathbf{r} \Lambda_c c_{ij} c_{ik}^* c_{jk}^*, \tag{38}$$

the derivative of which is

$$\Xi_{c_{ij}^*}^{(\mathbf{c})} = 2 \Lambda_c c_{ik}^* c_{kj}^*. \tag{39}$$

The evolution equation of \mathbf{c} then gains an irreversible term,

$$\left. \frac{\partial \Xi^{(\mathbf{c})}}{\partial c_{ij}^*} \right|_{\mathbf{c}_s = S_c} = -\frac{\Lambda_c H}{T} \left(c_{ij} - \frac{k_B T n}{H} \delta_{ij} \right). \tag{40}$$

After the transformation to the energetic representation (conjugates with respect to energy rather than entropy), the sum of the reversible and irreversible contributions to evolution equations for $(\rho, \mathbf{u}, \mathbf{c}, s)$ is prepared for the DynMaxEnt reduction.

4.1.2. DynMaxEnt to Hydrodynamics

Let us now apply the Dynamic MaxEnt reduction so that the conformation tensor \mathbf{c} relaxes. The energetic representation reversible Equations (32) and irreversible Equations (40) together are

$$\frac{\partial \rho}{\partial t} = -\partial_i (\rho u_i^\dagger), \tag{41a}$$

$$\begin{aligned} \frac{\partial u_i}{\partial t} = & -\partial_j (u_i u_j^\dagger) - \rho \partial_i \rho^\dagger - u_j \partial_i u_j^\dagger - s \partial_i s^\dagger - \\ & - c_{jk} \partial_i c_{jk}^\dagger + \partial_k (c_{kj} (c_{ij}^\dagger + c_{ji}^\dagger)), \end{aligned} \tag{41b}$$

$$\frac{\partial s}{\partial t} = -\partial_i (s u_i^\dagger) + 2 \frac{\Lambda_c}{(s^\dagger)^2} c_{ij}^\dagger c_{ik} c_{kj}^\dagger \tag{41c}$$

$$\frac{\partial c_{ij}}{\partial t} = -\partial_k (c_{ij} u_k^\dagger) + c_{kj} \partial_k u_i^\dagger + c_{ki} \partial_k u_j^\dagger - \frac{2\Lambda_c}{s^\dagger} c_{ik} c_{kj}^\dagger. \tag{41d}$$

Consider now the isothermal incompressible case (The compressible case and the origin of incompressibility were discussed in [19].), i.e., $S_e = T = \text{const}$, $n = \text{const}$ and $\nabla \cdot \mathbf{u}^\dagger = 0$. Equations (41b) and (41d) at the MaxEnt value of \mathbf{c} (given by Equation (37)) become

$$\begin{aligned} \frac{\partial u_i}{\partial t} = & -\partial_j (u_i u_j^\dagger) - \rho \partial_i \rho^\dagger - u_j \partial_i u_j^\dagger - s \partial_i s^\dagger - \\ & - \frac{k_B T n}{H} \partial_i \text{Tr} \mathbf{c}^\dagger + \frac{k_B T n}{H} \partial_k (c_{ik}^\dagger + c_{ki}^\dagger), \end{aligned} \tag{42a}$$

$$0 = \partial_j u_i^\dagger + \partial_i u_j^\dagger - 2 \frac{\Lambda_c}{T} c_{ij}^\dagger. \tag{42b}$$

The last equation has a solution

$$\mathbf{c}^\dagger = \frac{T}{2\Lambda_c} (\nabla \mathbf{u}^\dagger + (\nabla \mathbf{u}^\dagger)^T), \quad \text{Tr} \mathbf{c}^\dagger = 0. \tag{43}$$

By plugging this solution into the equation for momentum density, we obtain the Navier–Stokes equation for momentum density

$$\begin{aligned} \frac{\partial u_i}{\partial t} = & -\partial_j (u_i u_j^\dagger) - \rho \partial_i \rho^\dagger - u_j \partial_i u_j^\dagger - s \partial_i s^\dagger \\ & + \frac{k_B T^2 n}{H \Lambda_c} \partial_k (\partial_i u_k^\dagger + \partial_k u_i^\dagger), \end{aligned} \tag{44}$$

where the coefficient $k_B T^2 n / H \Lambda_c$ corresponds to the shear viscosity and $\mathbf{u}^\dagger = E_{\mathbf{u}} = \mathbf{v} = \mathbf{u} / \rho$ is the velocity.

The Dynamic MaxEnt reduction of the conformation tensor leads to the Newtonian shear stress tensor.

4.2. Reynolds Stress

We now turn to a complex fluid where momentum–momentum correlations between two neighboring particles matter, the correlation being expressed by the Reynolds stress tensor R_{ij} .

4.2.1. Non-Equilibrium Thermodynamics of Reynolds Stress

Let the state variables be $\mathbf{x} = (\rho, \mathbf{u}, s, \mathbf{R})$. The Poisson bracket expressing kinematics of \mathbf{x} is

$$\{A, B\}^{(\mathbf{R})} = \{A, B\}^{(EM)} + \int d\mathbf{r} R_{ij} \left(\partial_k A_{R_{ij}} B_{u_k} - \partial_k B_{R_{ij}} A_{u_k} \right) - \int d\mathbf{r} R_{ij} \left((A_{R_{kj}} + A_{R_{jk}}) \partial_k B_{u_i} - (B_{R_{kj}} + B_{R_{jk}}) \partial_k A_{u_i} \right), \tag{45}$$

see, e.g., [14,30]. The reversible evolution equations are then

$$\frac{\partial \rho}{\partial t} = -\partial_i (\rho E_{u_i}), \tag{46a}$$

$$\frac{\partial u_i}{\partial t} = -\partial_j (u_i E_{u_j}) - \rho \partial_i E_\rho - u_j \partial_i E_{u_j} - s \partial_i E_s - R_{kj} \partial_i E_{R_{kj}} - \partial_k (R_{ij} (E_{R_{kj}} + E_{R_{jk}})), \tag{46b}$$

$$\frac{\partial s}{\partial t} = -\partial_i (s E_{u_i}), \tag{46c}$$

$$\frac{\partial R_{ij}}{\partial t} = -\partial_k (R_{ij} E_{u_k}) - R_{kj} \partial_i E_{u_k} - R_{ki} \partial_j E_{u_k}. \tag{46d}$$

Let entropy be given by

$$S^{(\mathbf{R})} = \int d\mathbf{r} \left[s \left(\rho, e - \frac{\mathbf{u}^2}{2\rho} - \frac{1}{2m} \text{Tr} \mathbf{R} \right) + \frac{1}{2} k_B \frac{\rho}{m} \ln \det \frac{\mathbf{R}}{Q_R} \right], \tag{47}$$

where Q_R is an appropriately chosen constant. The reason for this entropy is analogical to the entropy (35). A derivative of entropy (47) with respect to \mathbf{R} is

$$R_{ij}^* = \frac{\partial S^{(\mathbf{R})}}{\partial R_{ij}} = -\frac{1}{2m} S_e \delta_{ij} + \frac{k_B \rho}{2m} (R^{-1})_{ij}, \tag{48}$$

which is equal to zero if and only if

$$R_{ij} = k_B T \rho \delta_{ij}. \tag{49}$$

This is the MaxEnt value of \mathbf{R} , at which the Reynolds stress is proportional to the unit matrix. Similarly as in the preceding section, we choose dissipation potential

$$\Xi^{(\mathbf{R})} = \int d\mathbf{r} \Lambda_R R_{ij}^* R_{jk} R_{ki}^*, \tag{50}$$

the derivative of which is

$$\Xi_{R_{ij}^*}^{(\mathbf{R})} = 2 \Lambda_R R_{jk} R_{ki}^*. \tag{51}$$

Note that R^{ij} was identified with R_{ij} and similarly for \mathbf{R}^* for simplicity of notation. Evolution equation of \mathbf{R} then gains an irreversible term

$$\frac{\partial \Xi^{(\mathbf{R})}}{\partial R_{ij}^*} \Big|_{\mathbf{R}^* = S_{\mathbf{R}}} = -\frac{\Lambda_R}{Tm} (\mathbf{R} - k_B T \rho \mathbf{I}). \tag{52}$$

By combining the reversible evolution (46) and irreversible (52), we obtain

$$\frac{\partial \rho}{\partial t} = -\partial_i (\rho E u_i), \tag{53a}$$

$$\begin{aligned} \frac{\partial u_i}{\partial t} = & -\partial_j (u_i E u_j) - \rho \partial_i E \rho - u_j \partial_i E u_j - s \partial_i E s - \\ & -R_{kj} \partial_i E R_{kj} - \partial_k (R_{ij} (E R_{kj} + E R_{jk})), \end{aligned} \tag{53b}$$

$$\frac{\partial s}{\partial t} = -\partial_i (s E u_i) + 2 \frac{\Lambda_R}{(E_s)^2} E R_{ij} R_{jk} E R_{ki}, \tag{53c}$$

$$\begin{aligned} \frac{\partial R_{ij}}{\partial t} = & -\partial_k (R_{ij} E u_k) - R_{kj} \partial_i E u_k - R_{ki} \partial_j E u_k \\ & - 2 \frac{\Lambda_R}{E_s} R_{jk} E R_{ki}, \end{aligned} \tag{53d}$$

which are the GENERIC evolution equations for fluid mechanics with Reynolds stress. For instance, the last equation can be rewritten as

$$\begin{aligned} \frac{\partial R_{ij}}{\partial t} = & -\partial_k (R_{ij} v_k) - R_{kj} \partial_i v_k - R_{ki} \partial_j v_k \\ & - \frac{\Lambda_R}{Tm} (\mathbf{R} - k_B T \rho \mathbf{I}), \end{aligned} \tag{54}$$

from which the tendency to relaxation of the Reynolds stress tensor to the respective MaxEnt value is obvious.

4.2.2. DynMaxEnt to Hydrodynamics

As in the case of the conformation tensor in Section 4.1, let us now show how the Reynolds stress relaxes. The MaxEnt value (49) can be plugged into Equations (53). Assuming again isothermal incompressible flow, $\rho = \text{const}$, $\nabla \cdot \mathbf{u}^\dagger = 0$ and $S_e = T = \text{const}$, the equations become

$$\begin{aligned} \frac{\partial u_i}{\partial t} = & -\partial_j (u_i u_j^\dagger) - \rho \partial_i \rho^\dagger - u_j \partial_i u_j^\dagger - s \partial_i s^\dagger - \\ & -k_B T \rho \partial_i R_{kk}^\dagger - k_B T \rho \partial_k (R_{ki}^\dagger + R_{ik}^\dagger), \end{aligned} \tag{55a}$$

$$0 = -k_B T \rho (\partial_i u_j^\dagger + \partial_j u_i^\dagger) - 2 \Lambda_R k_B \rho R_{ji}^\dagger. \tag{55b}$$

The last equation has a solution

$$\tilde{\mathbf{R}}^\dagger = -\frac{T}{2\Lambda_R} (\nabla \mathbf{u}^\dagger + (\nabla \mathbf{u}^\dagger)^T) \quad \text{and} \quad \text{Tr} \tilde{\mathbf{R}} = 0. \tag{56}$$

Plugging this solution back into the equation for \mathbf{u} leads to

$$\begin{aligned} \frac{\partial u_i}{\partial t} = & -\partial_j (u_i u_j^\dagger) - \rho \partial_i \rho^\dagger - u_j \partial_i u_j^\dagger - s \partial_i s^\dagger \\ & + \frac{k_B T^2 \rho}{\Lambda_R} \partial_k (\partial_k u_i^\dagger + \partial_i u_k^\dagger), \end{aligned} \tag{57}$$

which is again the Navier–Stokes equation with shear viscosity. Relaxation of Reynolds stress thus leads to extra (also called turbulent) viscosity by means of the Dynamic MaxEnt reduction.

4.3. Hyperbolic Heat Conduction

4.3.1. Non-Equilibrium Thermodynamics of Heat

Kinematics of heat transfer can be thought of as kinematics of phonons, and kinematics of phonons has been successfully described by Boltzmann-like dynamics, where the distribution function of phonons plays the role of state variable, see e.g., book [31]. By the reduction from the kinetic theory to fluid mechanics, see e.g., [1,14], kinematics of phonons can be expressed in terms of the entropy density and momentum related to entropy transport, the kinematics of which is expressed by a hydrodynamic-like Poisson bracket (see [32]). Subsequent transformation to density of matter ρ , total momentum of matter and phonons \mathbf{m} , entropy density s and conjugate entropy flux \mathbf{w} , which is equal to the ratio of phonon momentum and entropy density, leads to bracket

$$\begin{aligned} \{F, G\}^{(Cat)} &= \{F, G\}^{(FM)} \Big|_{\mathbf{u}=\mathbf{m}} + \int d\mathbf{r} (G_{w_i} \partial_i F_s - F_{w_i} \partial_i G_s) \\ &+ \int d\mathbf{r} w_j (\partial_i F_{w_i} G_{m_j} - \partial_i G_{w_i} F_{m_j}) \\ &+ \int d\mathbf{r} (\partial_i w_j - \partial_j w_i) (F_{w_i} G_{m_j} - G_{w_i} F_{m_j}) \\ &+ \int d\mathbf{r} \frac{1}{s} (\partial_i w_j - \partial_j w_i) F_{w_i} G_{w_j}, \end{aligned} \tag{58}$$

expressing kinematics of matter and heat—the Cattaneo Poisson bracket. The name Cattaneo is due to the implied hyperbolicity of heat transport [19]. The Poisson bracket (58) generates reversible evolution equations

$$\frac{\partial \rho}{\partial t} = -\partial_k (\rho E_{m_k}), \tag{59a}$$

$$\begin{aligned} \frac{\partial m_i}{\partial t} &= -\partial_j (m_i E_{m_j}) - \partial_j (w_i E_{w_j}) - \rho \partial_i E_\rho - m_j \partial_i E_{m_j} - s \partial_i E_s \\ &- w_k \partial_i E_{w_k} + \partial_i (E_{w_k} w_k), \end{aligned} \tag{59b}$$

$$\frac{\partial s}{\partial t} = -\partial_k (s E_{m_k} + E_{w_k}), \tag{59c}$$

$$\frac{\partial w_k}{\partial t} = -\partial_k E_s - \partial_k (w_j E_{m_j}) + (\partial_k w_j - \partial_j w_k) \left(E_{m_j} + \frac{1}{s} E_{w_j} \right). \tag{59d}$$

These evolution equations express reversible dynamics of fluid mechanics and conjugate entropy flux \mathbf{w} . Note that, for the heat flux, i.e., flux of energy, the usual relation $\mathbf{q} = E_s E_{w_k} = T \mathbf{J}^{(s)}$ holds true, see [14] for more details.

Local dissipation is enforced by adopting an algebraic dissipation potential, the simplest of which is

$$\Xi(\mathbf{w}^*) = \int d\mathbf{r} \frac{1}{2} \frac{1}{\tau} (\mathbf{w}^*)^2 = \int d\mathbf{r} \frac{1}{2} \frac{1}{\tau} \left(\frac{1}{s^\dagger} \mathbf{w}^\dagger \right)^2, \tag{60}$$

where the last equality follows from the transformation between energetic and entropic representation. Then, the irreversible terms generated by this dissipation potential are added to the reversible evolution, Equations (59),

$$\frac{\partial \rho}{\partial t} = -\partial_k(\rho m_k^\dagger), \tag{61a}$$

$$\begin{aligned} \frac{\partial m_i}{\partial t} = & -\partial_j(m_i m_j^\dagger) - \partial_j(w_i w_j^\dagger) - \rho \partial_i \rho^\dagger - m_j \partial_i m_j^\dagger - s \partial_i s^\dagger \\ & - w_k \partial_i w_k^\dagger + \partial_i(w_k^\dagger w_k), \end{aligned} \tag{61b}$$

$$\frac{\partial s}{\partial t} = -\partial_k \left(s m_k^\dagger + w_k^\dagger \right) + \frac{1}{\tau (s^\dagger)^2} (\mathbf{w}^\dagger)^2, \tag{61c}$$

$$\begin{aligned} \frac{\partial w_k}{\partial t} = & -\partial_k s^\dagger - \partial_k(w_j m_j^\dagger) + (\partial_k w_j - \partial_j w_k) \left(m_j^\dagger + \frac{1}{s} w_j^\dagger \right) \\ & - \frac{1}{\tau s^\dagger} w_k^\dagger. \end{aligned} \tag{61d}$$

These are the GENERIC equations for fluid mechanics with hyperbolic heat conduction.

4.3.2. DynMaxEnt to Fourier Heat Conduction

The simplest possible dependence of entropy on the extra field \mathbf{w} is quadratic (keeping in mind that S has to be a concave and even with respect to time reversal functional),

$$S(\rho, \mathbf{m}, e, \mathbf{w}) = \int d\mathbf{r} s \left(\rho, e - \frac{\mathbf{m}^2}{2\rho} - \frac{1}{2} \alpha \mathbf{w}^2 \right). \tag{62}$$

Consequently, entropy is highest (for given fields ρ , \mathbf{u} and e) at $\mathbf{w} = 0$, which is the MaxEnt estimate $\tilde{\mathbf{w}}$. Plugging this value into Equations (61) leads to

$$\frac{\partial \rho}{\partial t} = -\partial_k(\rho m_k^\dagger), \tag{63a}$$

$$\frac{\partial m_i}{\partial t} = -\partial_j(m_i m_j^\dagger) - \rho \partial_i \rho^\dagger - m_j \partial_i m_j^\dagger - s \partial_i s^\dagger, \tag{63b}$$

$$\frac{\partial s}{\partial t} = -\partial_k \left(s m_k^\dagger + w_k^\dagger \right) + \frac{1}{\tau (s^\dagger)^2} (\mathbf{w}^\dagger)^2, \tag{63c}$$

$$0 = -\partial_k s^\dagger - \frac{1}{\tau s^\dagger} w_k^\dagger. \tag{63d}$$

Equation (63d) has the solution

$$\tilde{\mathbf{w}}^\dagger = -\tau s^\dagger \nabla s^\dagger. \tag{64}$$

Plugging this value into the rest of Equations (63), we obtain

$$\frac{\partial \rho}{\partial t} = -\partial_i(\rho E_{m_i}), \tag{65a}$$

$$\frac{\partial m_i}{\partial t} = -\partial_j(m_i E_{m_j}) - \rho \partial_i E_\rho - m_j \partial_i E_{m_j} - s \partial_i E_s, \tag{65b}$$

$$\frac{\partial s}{\partial t} = -\partial_k (s E_{m_k} - \tau E_s \partial_k E_s) + \tau (\nabla E_s)^2, \tag{65c}$$

which are Euler equations with Fourier heat conduction. Indeed, denoting local temperature E_s as T , the entropy flux is

$$\mathbf{J}^{(s)} = -\tau T \nabla T = \frac{-\lambda \nabla T}{T}, \tag{66}$$

where $\lambda = T^2 \tau$ is the heat conductivity and $\mathbf{q} = -\lambda \nabla T$ is the heat flux.

One can also seek higher order corrections by means of the infinite DynMaxEnt chain. The corrected value of \mathbf{w} implied by Equation (63d) is

$$\tilde{\mathbf{w}}^{(2)} = -\frac{\tau}{\alpha} T \nabla T, \tag{67}$$

which leads to energy

$$E = \int d\mathbf{r} \left(\frac{\mathbf{m}^2}{2\rho} + \varepsilon(\rho, s) + \frac{1}{2} \tau \alpha \varepsilon_s^2 (\nabla \varepsilon_s)^2 \right). \tag{68}$$

This is a weakly non-local energy implied by the second-order DynMaxEnt correction.

In summary, Fourier’s law, which tells us that heat flows from a hotter body to a colder body, can be derived by the dynamic MaxEnt reduction from the coupled dynamics of phonons and fluid mechanics. The only irreversibility on the higher level of description is present in the evolution equation for \mathbf{w} . After the reduction, this irreversibility leads to irreversible terms in the equation for entropy (irreversible entropy flux and entropy production). Note that this reduction is again compatible with the asymptotic expansion carried out in [33].

4.4. Magnetohydrodynamics

Let us now turn to DynMaxEnt when the electromagnetic field is present.

4.4.1. Non-Equilibrium Thermodynamics of Charged Mixtures

Dynamics of charged mixtures is governed by the Maxwell equations interacting with fluid mechanics of the species, see ([14] Section 6.4). Let us start with a Poisson bracket for the binary mixture of oppositely charged species endowed with a single entropy, total momentum density, displacement field and magnetic field, that is,

$$\begin{aligned} \{F, G\}^{(\text{EMHD-2})}(\rho_+, \rho_-, \mathbf{m}, s, \mathbf{D}, \mathbf{B}) &= \{F, G\}^{(\text{CIT-2})}(\rho_+, \rho_-, \mathbf{m}, s) \\ \{F, G\}^{(\text{EM})}(\mathbf{D}, \mathbf{B}) &\left\{ \begin{aligned} &+ \int d\mathbf{r} \left(F_{D_i} \varepsilon_{ijk} \partial_j G_{B_k} - G_{D_i} \varepsilon_{ijk} \partial_j F_{B_k} \right) \\ &+ \int d\mathbf{r} D_i \left(\partial_j F_{D_i} G_{m_j} - \partial_j G_{D_i} F_{m_j} \right) \\ &+ \int d\mathbf{r} \partial_j D_j \left(F_{m_i} G_{D_i} - G_{m_i} F_{D_i} \right) \\ &+ \int d\mathbf{r} D_j \left(F_{m_i} \partial_j G_{D_i} - G_{m_i} \partial_j F_{D_i} \right) \end{aligned} \right. \\ \{F, G\}^{(\text{SP})}(\mathbf{D}, \mathbf{m}) &\left\{ \begin{aligned} &+ \int d\mathbf{r} B_i \left(\partial_j F_{B_i} G_{m_j} - \partial_j G_{B_i} F_{m_j} \right) \\ &+ \int d\mathbf{r} \partial_j B_j \left(F_{m_i} G_{B_i} - G_{m_i} F_{B_i} \right) \\ &+ \int d\mathbf{r} B_j \left(F_{m_i} \partial_j G_{B_i} - G_{m_i} \partial_j F_{B_i} \right), \end{aligned} \right. \\ \{F, G\}^{(\text{SP})}(\mathbf{B}, \mathbf{m}) &\left\{ \begin{aligned} &+ \int d\mathbf{r} B_i \left(\partial_j F_{B_i} G_{m_j} - \partial_j G_{B_i} F_{m_j} \right) \\ &+ \int d\mathbf{r} \partial_j B_j \left(F_{m_i} G_{B_i} - G_{m_i} F_{B_i} \right) \\ &+ \int d\mathbf{r} B_j \left(F_{m_i} \partial_j G_{B_i} - G_{m_i} \partial_j F_{B_i} \right), \end{aligned} \right. \end{aligned} \tag{69}$$

where the CIT2 (binary classical irreversible thermodynamics [1,34]) bracket stands for

$$\begin{aligned} \{F, G\}^{(\text{CIT-2})}(\rho_+, \rho_-, \mathbf{m}, s) &= \int d\mathbf{r} \rho_+ \left(\partial_i F_{\rho_+} G_{m_i} - \partial_i G_{\rho_+} F_{m_i} \right) \\ &+ \int d\mathbf{r} \rho_- \left(\partial_i F_{\rho_-} G_{m_i} - \partial_i G_{\rho_-} F_{m_i} \right) \\ &+ \int d\mathbf{r} m_i \left(\partial_j F_{m_i} G_{m_j} - \partial_j G_{m_i} F_{m_j} \right) \\ &+ \int d\mathbf{r} s \left(\partial_i F_s G_{m_i} - \partial_i G_s F_{m_i} \right), \end{aligned} \tag{70}$$

cf. bracket (A3).

This system is additionally required to satisfy the Gauß laws for electric and magnetic charge, respectively. We have

$$\partial_i D_i = qe_0 \left(\frac{\rho_+}{m_+} - \frac{\rho_-}{m_-} \right) \quad \text{and} \quad \partial_i B_i = 0, \tag{71}$$

where the right-hand side of Equation (71)_{left} is the free charge density.

Total density $\rho = \rho_+ + \rho_-$ and the free charge density can be used for the description instead of ρ_+ and ρ_- . Such transformation allows for the projection to the state variables without free charge density (i.e., where free charge density is relaxed) by letting the functionals depend only on $(\rho, \mathbf{m}, s, \mathbf{D}, \mathbf{B})$. Consequently, bracket (69) transforms into

$$\begin{aligned} \{F, G\}^{(\text{EMHD})}(\rho, \mathbf{m}, s, \mathbf{D}, \mathbf{B}) &= \{F, G\}^{(\text{FM})}(\rho, \mathbf{m}, s) + \{F, G\}^{(\text{EM})}(\mathbf{D}, \mathbf{B}) \\ &+ \{F, G\}^{(\text{SP})}(\mathbf{D}, \mathbf{m}) + \{F, G\}^{(\text{SP})}(\mathbf{B}, \mathbf{m}), \end{aligned} \tag{72}$$

and it is equipped with the updated constraint on the displacement field (given by the relaxed value of free charge density, typically zero) and magnetic field. Bracket (72) describes reversible evolution of electroneutral continuum coupled with the Maxwell equations.

Although the continuum described by bracket (72) is electroneutral, it can conduct electric current. This can be seen as a dissipation of the displacement field as suggested in [35]. Let us define dissipation potential

$$\Xi(\mathbf{D}^*) = \int d\mathbf{r} \frac{\sigma}{2} (\mathbf{D}^*)^2 = \int d\mathbf{r} \frac{\sigma}{2} \left(\frac{\mathbf{D}^\dagger}{s^\dagger} \right)^2. \tag{73}$$

The reversible evolution generated by (72) and the irreversible evolution due to (73) give together

$$\frac{\partial \rho}{\partial t} = -\partial_k (\rho m_k^\dagger), \tag{74a}$$

$$\begin{aligned} \frac{\partial m_i}{\partial t} &= -\partial_j (m_i m_j^\dagger) - \rho \partial_i \rho^\dagger - m_j \partial_i m_j^\dagger - s \partial_i s^\dagger - D_j \partial_i D_j^\dagger - B_j \partial_i B_j^\dagger \\ &+ \partial_j (D_j D_i^\dagger + B_j B_i^\dagger), \end{aligned} \tag{74b}$$

$$\frac{\partial s}{\partial t} = -\partial_k (s m_k^\dagger) + \frac{\sigma}{(s^\dagger)^2} (\mathbf{D}^\dagger)^2, \tag{74c}$$

$$\frac{\partial D_i}{\partial t} = \varepsilon_{ijk} \partial_j B_k^\dagger - \partial_j (D_i m_j^\dagger - m_i^\dagger D_j) - m_i^\dagger \partial_j D_j - \frac{\sigma}{s^\dagger} D_i^\dagger, \tag{74d}$$

$$\frac{\partial B_i}{\partial t} = -\varepsilon_{ijk} \partial_j D_k^\dagger - \partial_j (B_i m_j^\dagger - m_i^\dagger B_j) - m_i^\dagger \partial_j B_j. \tag{74e}$$

The conjugate displacement field \mathbf{D}^\dagger is interpreted as electric intensity \mathbf{E} , and the irreversible (last) term in Equation (74d) then tells that the electric current is $\mathbf{J} = \frac{\sigma}{s^\dagger} \mathbf{E}$. Dissipation in the \mathbf{D} field can be thus seen as Ohm’s law (Alternatively, Ohm’s law can be derived from the relaxation of matter in the presence of the electric field, see [14]).

4.4.2. DynMaxEnt to the Displacement Field—Passage to MHD

Let us apply the DynMaxEnt reduction to the displacement field in Equations (73) so that we approach the magnetohydrodynamics (MHD). The reversible part of the MHD equations can be obtained easily by projection to variables $(\rho, \mathbf{m}, s, \mathbf{B})$ as in [14], but we wish to also obtain the irreversible part of the equations.

Assuming energy quadratic in \mathbf{D} , the MaxEnt value is $\tilde{\mathbf{D}} = 0$, which erases all terms containing the displacement field (but not \mathbf{D}^\dagger) from the equations. Except for the evolution of entropy, \mathbf{D}^\dagger only remains in Equation (74d), which can be solved and gives

$$\tilde{D}_i^\dagger = \frac{s^\dagger}{\sigma} \varepsilon_{ijk} \partial_j B_k^\dagger. \tag{75}$$

Introducing the *curl* of Equation (75) into Equation (74d) yields a dissipative evolution equation for the magnetic field. The complete set of equations after this reduction reads

$$\frac{\partial \rho}{\partial t} = -\partial_k (\rho m_k^\dagger), \tag{76a}$$

$$\frac{\partial m_i}{\partial t} = -\partial_j (m_i m_j^\dagger) - \rho \partial_i \rho^\dagger - m_j \partial_i m_j^\dagger - s \partial_i s^\dagger - B_j \partial_i B_j^\dagger + \partial_j (B_j B_i^\dagger), \tag{76b}$$

$$\frac{\partial s}{\partial t} = -\partial_k (s m_k^\dagger) + \frac{1}{\sigma} (\nabla \times \mathbf{B}^\dagger)^2, \tag{76c}$$

$$\frac{\partial B_i}{\partial t} = -\partial_j (B_i m_j^\dagger - m_i^\dagger B_j) - m_i^\dagger \partial_j B_j - \varepsilon_{ijk} \partial_j \left(\frac{s^\dagger}{\sigma} \varepsilon_{klm} \partial_l B_m^\dagger \right), \tag{76d}$$

which is compatible with [36]. The first terms on the right-hand side of Equation (76d) can be further simplified for constant σ/s^\dagger , provided that the contribution of the magnetic field to the energy is $\frac{B^2}{\mu_0}$. We can then write

$$\frac{\partial \mathbf{B}}{\partial t} = \frac{s^\dagger}{\mu_0 \sigma} \Delta \mathbf{B} - \nabla \times (\mathbf{B} \times \mathbf{m}^\dagger), \tag{77}$$

where $\partial_i B_i = 0$ was finally used. Keeping in mind that $\mathbf{m}^\dagger = \mathbf{v}$, Equation (77) is the advection–diffusion equation for the magnetic field, cf. ([37] Equation 2.15) or [38]. The coefficient $\frac{s^\dagger}{\mu_0 \sigma}$ is referred to as the magnetic diffusivity.

In summary, after the relaxation of free charge density, one gets the electroneutral continuum coupled with Maxwell equations. Further dissipation in the displacement field then leads by the DynMaxEnt reduction to the MHD equations including magnetic diffusivity.

5. Contact Geometry

Contact geometry seems to be the so far most general geometric formulation of non-equilibrium thermodynamics. It started with works of Hermann [11] in equilibrium thermodynamics and continued to non-equilibrium thermodynamics, e.g., [12,15,39–41] and many others. Here, we adopt a recent version of contact-geometric formulation of GENERIC from [14].

6. Contact GENERIC

We begin by introducing a space

$$\mathbb{M}^{(cont)} = \mathbf{M} \times \mathbf{M}^* \times \mathbf{N}_{eq}^* \times \mathbf{N}_{eq} \times \mathbb{R} \tag{78}$$

with coordinates (x, x^*, y^*, y, ϕ) . The space \mathbf{M} with elements x is the state space, the space \mathbf{M}^* with elements x^* is its dual. Similarly, \mathbf{N}_{eq} with elements y is the state space on the equilibrium level, \mathbf{N}_{eq}^* with elements y^* is its dual. We recall that $y = (E, N)$ and $y^* = (E^*, N^*)$, where $E^* = \frac{1}{T}$ and $N^* = -\frac{\mu}{T}$. We moreover introduce the fundamental thermodynamic relation $S = S(x), y = y(x)$ represented in $\mathbf{M} \times \mathbf{N}_{eq} \times \mathbb{R}$ by the Gibbs manifold $\mathcal{M}^{(G)}$ that is the image of the mapping

$$x \mapsto (x, y(x), S(x)). \tag{79}$$

Corresponding to the fundamental thermodynamic relation is the thermodynamic potential $\Phi(x, y^*) = -S(x) + \langle y^*, y(x) \rangle$, where $\langle \cdot, \cdot \rangle$ denotes the inner product.

The Gibbs manifold $\mathcal{M}^{(G)}$ can be now extended to the **Gibbs–Legendre manifold** $\mathcal{M}^{(GL)}$ (in the shorthand notation *GL manifold*) that is the image of the mapping

$$(x, y^*) \mapsto (x, \Phi_x(x, y^*), y^*, \Phi_{y^*}(x, y^*), \Phi(x, y^*)) \tag{80}$$

in $\mathbb{M}^{(cont)}$.

The thermodynamics in \mathbf{M} is completely expressed in the GL manifold $\mathcal{M}^{(GL)}$. Note that $[\mathcal{M}^{(GL)}]_{y^*=0}$ (i.e., the image of the mapping

$$(x, 0) \mapsto (x, -S_x(x), 0, y(x), -S(x)) \tag{81}$$

in the space $\mathbf{M} \times \mathbf{M}^* \times \mathbf{N}_{eq} \times \mathbb{R}$) is an extension of the Gibbs manifold $\mathcal{M}^{(G)}$ by including the conjugate variable x^* . Moreover, the manifold $[\mathcal{M}^{(GL)}]_{x^*=S_x=0}$ displays the states $x_{eq}(y^*)$ that represent in \mathbf{M} the equilibrium states and also the fundamental thermodynamic relation $S^*(y^*), y(y^*)$ in \mathbf{N}_{eq} implied by the fundamental thermodynamic relation $S(x), y(x)$ in \mathbf{M} . Indeed, $[\mathcal{M}^{(GL)}]_{x^*=0}$ is the image of the mapping

$$(x, y^*) \mapsto (x_{eq}(y^*), 0, y^*, y(x_{eq}(y^*)), S^*(y^*)). \tag{82}$$

Let us turn to the time evolution in $\mathbb{M}^{(cont)}$. We begin by introducing in $\mathbb{M}^{(cont)}$ a bracket

$$\begin{aligned} \{A, B\}^{(cont)} &= (\langle A_x, B_{x^*} \rangle - \langle B_x, A_{x^*} \rangle) \\ &\quad - (\langle A_y, B_{y^*} \rangle - \langle B_y, A_{y^*} \rangle) \\ &\quad - (\langle x^*, A_{x^*} \rangle B_\phi - \langle x^*, B_{x^*} \rangle A_\phi) \\ &\quad + (AB_\phi - BA_\phi) \\ &\quad + (\langle A_y, y \rangle B_\phi - \langle B_y, y \rangle A_\phi), \end{aligned} \tag{83}$$

where A and B are sufficiently regular functions $\mathbb{M}^{(cont)} \rightarrow \mathbb{R}$. This bracket consists of two contact brackets (95) of paper [41]. With such bracket, we introduce the time evolution in $\mathbb{M}^{(cont)}$ by an equation

$$\dot{A} = \{A, H^{(cont)}\}^{(cont)} - AH_\phi^{(cont)} \tag{84}$$

that is required to hold for all A . The function $H^{(cont)} : \mathbb{M}^{(cont)} \rightarrow \mathbb{R}$, called a contact Hamiltonian, will be specified below. The last term on the right-hand side corresponds to the non-conservation of the phase-space volume [40]. Written explicitly, the time evolution equations (84) take the form

$$\dot{x} = H_{x^*}^{(cont)}, \tag{85a}$$

$$\dot{x}^* = -H_x^{(cont)} - x^* H_\phi^{(cont)}, \tag{85b}$$

$$\dot{y}^* = H_y^{(cont)}, \tag{85c}$$

$$\dot{y} = -H_{y^*}^{(cont)} + y H_\phi^{(cont)}, \tag{85d}$$

$$\dot{\phi} = -H^{(cont)} + \langle x^*, H_{x^*}^{(cont)} \rangle - \langle H_y^{(cont)}, y \rangle. \tag{85e}$$

These are the evolution equations in \mathbb{M} .

Next, we specify the contact Hamiltonian $H^{(cont)}$

$$H^{(cont)}(x, x^*, y^*, y, \phi) = -S^{(cont)}(x, x^*, y^*) + \frac{1}{E^*} E^{(cont)}(x, x^*, y^*), \tag{86}$$

where

$$\begin{aligned} S^{(cont)}(x, x^*, y^*) &= \Xi(x, x^*, y^*) - [\Xi(x, x^*, y^*)]_{x^*=\Phi_x}, \\ E^{(cont)}(x, x^*, y^*) &= \langle x^*, L\Phi_x \rangle. \end{aligned} \tag{87}$$

Ξ is the dissipation potential entering GENERIC and L is the Poisson bivector also entering GENERIC. Both Ξ and L are degenerate in the sense

$$\begin{aligned} \langle x^*, LS_x \rangle &= \langle x^*, LN_x \rangle = 0, \quad \forall x^*, \\ \langle E_x, \Xi_{x^*} \rangle &= \langle N_x, \Xi_{x^*} \rangle = 0, \quad \forall x^*, \\ \langle x^*, [\Xi_{x^*}]_{x^*=E_x} \rangle &= \langle x^*, [\Xi_{x^*}]_{x^*=M_x} \rangle = 0, \quad \forall x^*. \end{aligned} \tag{88}$$

We note in particular that the contact Hamiltonian (86) is independent of y and ϕ . With (86), the time evolution Equations (85a) become

$$\dot{x} = \frac{1}{E^*} L\Phi_x - \Xi_{x^*}, \tag{89a}$$

$$\begin{aligned} \dot{x}^* &= \Phi_{xx} \left(\frac{1}{E^*} Lx^* - [\Xi_{x^*}]_{x^*=\Phi_x} \right) \\ &\quad - \frac{1}{E^*} \langle x^*, L_x \Phi_x \rangle + \Xi_x - [\Xi_x]_{x^*=\Phi_x}, \end{aligned} \tag{89b}$$

$$\dot{\phi} = -\langle x^*, \Xi_{x^*} + \Xi - [\Xi]_{x^*=\Phi_x} \rangle, \tag{89c}$$

$$\dot{y}^* = 0, \tag{89d}$$

$$\dot{y} = \Xi_{y^*} - \Xi_{y^*}|_{x^*=\Phi_x}. \tag{89e}$$

If we now evaluate (89a) on the GL manifold $\mathcal{M}^{(GL)}$ (note that $[H^{(cont)}]_{\mathcal{M}^{(GL)}} = 0$), we arrive at

$$\dot{x} = \frac{1}{E^*} L\Phi_x - \Xi_{x^*}|_{(x^*=\Phi_x, y=\Phi_{y^*})}, \tag{90a}$$

$$\dot{x}^* = \Phi_{xx} \left(\frac{1}{E^*} L\Phi_x - [\Xi_{x^*}]_{(x^*=\Phi_x, y=\Phi_{y^*})} \right), \tag{90b}$$

$$\dot{\phi} = -\langle x^*, \Xi_{x^*} \rangle|_{(x^*=\Phi_x, y=\Phi_{y^*})}, \tag{90c}$$

$$\dot{y}^* = 0, \tag{90d}$$

$$\dot{y} = 0, \tag{90e}$$

which are the GENERIC evolution equations. See [14] for more details.

6.1. Relation to DynMaxEnt

Consider state variables $\mathbf{x} = (\mathbf{r}, \mathbf{p})$ as in the Section 3.3 on the damped particle (disregarding entropy for simplicity). The Poisson bivector is then canonical, $\mathbf{L} = \begin{pmatrix} 0 & 1 \\ -1 & 0 \end{pmatrix}$, and the dissipation potential is quadratic in conjugate momentum, $\Xi = \frac{1}{2\gamma} (\mathbf{p}^*)^2$. This conjugate momentum, according to Equation (89b), approaches the value where GENERIC evolution equations hold, Equation (11), and eventually reaches the value given by the derivative of thermodynamic potential.

Now, assume that state variable \mathbf{p} evolves faster to the corresponding equilibrium (zero) than both \mathbf{r} and conjugate variables. The GENERIC evolution equations then become Equations (11a) and (15). The conjugate variable \mathbf{p}^* approaches the value where the GENERIC equations are valid, which means that it approaches solutions to Equation (15) as in the DynMaxEnt procedure. Conjugate variables approach the Gibbs–Legendre manifold (80). Contact geometry provides motivation and geometric meaning to the Dynamic MaxEnt reduction.

7. Conclusions

In this paper, we have presented a method for reduction of detailed dynamics to less detailed dynamics called Dynamic MaxEnt. The key feature of the method is that conjugate variables are promoted to independent variables and as such they can relax to a quasi-equilibrium in a different way than state variables. While relaxation of the state variables generates the entropy on the lower level of description, relaxation of conjugate variables ensures that the vector field on the higher level becomes tangent to the quasi-equilibrium manifold.

First, in Section 2, the usual MaxEnt is recalled, which gives state variables on the higher (detailed) level as functions of state variables on the lower (less detailed) level. The DynMaxEnt method is then presented in Section 3 including the infinite chain of higher order DynMaxEnt corrections, and it is compared to asymptotic expansions in Section 3.3.3. Then, the method is used on the reduction of dynamics of complex fluids equipped with conformation tensor and Reynolds stress to the Navier–Stokes equations, reduction of hyperbolic heat conduction to the Fourier law, where we again compare the result to the formal asymptotic methods, and reduction of electromagnetohydrodynamics to magnetohydrodynamics. Finally, motivation for the DynMaxEnt method by contact geometry is shown in Section 5.

In summary, this paper contains a relatively straightforward method for reduction from dynamics on a detailed level of description to dynamics on a less detailed level of description.

Author Contributions: M.G. stands behind the main ideas for DynMaxEnt, V.K. and M.P. formulated the energetic DynMaxEnt and wrote most of the text. P.V. formulated the application of DynMaxEnt on electromagnetic field.

Funding: This work was supported by the Czech Science Foundation, project No. 17-15498Y, and by Charles University Research program No. UNCE/SCI/023. This research has been supported partially by the Natural Sciences and Engineering Research Council of Canada, Grants 3100319 and 3100735.

Acknowledgments: We are grateful to Petr Pelech and Ilya Peshkov for discussing the DynMaxEnt method.

Conflicts of Interest: The authors declare no conflict of interest.

Abbreviations

The following abbreviations are used in this manuscript:

MaxEnt	Maximum Entropy Principle
DynMaxEnt	Dynamic Maximum Entropy Principle
GENERIC	General Equation for Non-Equilibrium Reversible-Irreversible Coupling
FM	Fluid Mechanics
MHD	Magnetohydrodynamics
CIT	Classical Irreversible Thermodynamics

Appendix A.

Appendix A.1. Correction of Upper Entropy $\uparrow S$

Appendix A.1.1. General Case

Let us now discuss the possibility to correct the higher level entropy instead of the infinite chain presented above. As a sequence of correction will be produced, we introduce a more detailed notation. Static MaxEnt starts with $\uparrow S(x)$, which we shall now denote as $\uparrow S_0$. Static MaxEnt provides $\downarrow S_0(\mathbf{y})$ and $\tilde{x}_0^{ME}(\mathbf{y})$ and the reduction of the upper evolution equations to the lower MaxEnt manifold yields $\tilde{x}_0^*(\mathbf{y})$ (where we rewrote the lower conjugate variables in terms of direct ones $\mathbf{y}^* = \partial_{\mathbf{y}} \downarrow S(\mathbf{y})$).

As generally $\tilde{x}_0^{ME}(\mathbf{y})$ and $\tilde{x}_0^*(\mathbf{y})$ are independent and hence likely are not conjugate to each other via $\uparrow S$ evaluated at the lower MaxEnt manifold, we correct the upper entropy so that they are conjugate

variables. Let us denote the conjugate counterpart to $\tilde{\mathbf{x}}_0^*(\mathbf{y})$ via $\uparrow S_0^*$ as $\tilde{\mathbf{x}}_0^{evo}(\mathbf{y}) \neq \tilde{\mathbf{x}}_0^{ME}(\mathbf{y})$. Hence, we find $\uparrow S_1^*$ (or equivalently $\uparrow S_1$ via Legendre transformation) such that

$$\partial_{\mathbf{x}^*} \uparrow S_1^* |_{\mathbf{x}^*=\tilde{\mathbf{x}}_0^*(\mathbf{y})} = \tilde{\mathbf{x}}_0^{ME}(\mathbf{y}),$$

which may be rewritten as

$$\partial_{\mathbf{x}^*} \left(\uparrow S_1^* - \uparrow S_0^* \right) \Big|_{\mathbf{x}^*=\tilde{\mathbf{x}}_0^*(\mathbf{y})} = \tilde{\mathbf{x}}_0^{ME}(\mathbf{y}) - \tilde{\mathbf{x}}_0^{evo}(\mathbf{y}). \tag{A1}$$

It might be difficult in practice to find such a correction to the upper entropy in general. However, we provide a worked out example below.

The change in the upper entropy $\uparrow S_1$ entails a change in static MaxEnt value and in everything that follows: $\tilde{\mathbf{x}}_1^{ME}(\mathbf{y})$, $\tilde{\mathbf{x}}_0^*(\mathbf{y})$, $\downarrow S_1(\mathbf{y}) = \uparrow S_1(\tilde{\mathbf{x}}_1^{ME}(\mathbf{y}))$, $\tilde{\mathbf{x}}_1^{evo}(\mathbf{y})$. Hence, a sequence of correction is produced and if they are “small” they may provide a converging sequence.

Appendix A.1.2. The Correction of the Upper Energy for the Damped Particle

Let us illustrate the outlined difficulty of the correction of the upper energy on the simple example of a damped particle. This method corrects upper energy so that the direct and conjugate variables are indeed conjugate. The natural choice

$$\uparrow E_0 = \frac{(\mathbf{p} + \mathbf{p}_0^{evo})^2}{2m} + V(\mathbf{r}) + \varepsilon(s) = \frac{(\mathbf{p} - m\frac{\tau}{\zeta}V_{\mathbf{r}}(\mathbf{r}))^2}{2m} + V(\mathbf{r}) + \varepsilon(s) \tag{A2}$$

entails

$$\mathbf{p}^\dagger = \partial_{\mathbf{p}} \uparrow E_0 = \frac{1}{m}(\mathbf{p} + \mathbf{p}_0^{evo})$$

and hence indeed the conjugate value to $\mathbf{p} = 0$ is $\mathbf{p}^\dagger = \frac{1}{m}\mathbf{p}_0^{evo}$. Similarly,

$$\mathbf{r}^\dagger = \partial_{\mathbf{r}} \uparrow E_1 = \frac{1}{m}(\mathbf{p} - m\frac{\tau}{\zeta}V_{\mathbf{r}})(-m\frac{\tau}{\zeta}V_{\mathbf{r}\mathbf{r}}) + V_{\mathbf{r}}.$$

Static MaxEnt of $\uparrow E_1$ gives (minimum energy for given \mathbf{r}, s)

$$\mathbf{p}_1^{ME} = m\frac{\tau}{\zeta}V_{\mathbf{r}}$$

with a conjugate value $\mathbf{p}^\dagger = 0$ and also $\mathbf{r}^\dagger = V_{\mathbf{r}}$. Note that lower energy is the same as in the previous step $\uparrow E_1|_{\mathbf{p}_1^{ME}} = \uparrow E_0|_{\mathbf{p}_0^{ME}}$. Finally, the evolution equation yields dependent relations

$$\partial_t \mathbf{p}_1^{ME} = m\frac{\tau}{\zeta}V_{\mathbf{r}\mathbf{r}}\partial_t \mathbf{r} = m\frac{\tau}{\zeta}V_{\mathbf{r}\mathbf{r}}\mathbf{p}_1^\dagger = -\mathbf{r}^\dagger - \frac{\zeta}{\tau}\mathbf{p}_1^\dagger,$$

requiring that

$$\mathbf{p}_1^\dagger = -\frac{\tau}{\zeta}\mathbf{r}^\dagger \frac{1}{1 + m\frac{\tau^2}{\zeta^2}V_{\mathbf{r}\mathbf{r}}} \approx \mathbf{p}_0^\dagger - m\frac{\tau^2}{\zeta^2}V_{\mathbf{r}\mathbf{r}}\mathbf{p}_0^\dagger.$$

Note that this correction method seems to be working well, cf. (25). Namely, both correction methods of dynamic MaxEnt yield an asymptotic type series solution for small τ and, although it does not match the formal asymptotic expansion solution, some similarities can be seen.

However, a second inspection of the proposed upper energy (A2) reveals that energy is no longer an even function with respect to time reversal. One can show that, under the assumption of energy being an analytic function of state variables, the requirement that the conjugate value to \mathbf{p}^{ME} is non-zero requires a presence of a linear term of \mathbf{p} in the corrected energy $\uparrow E_1$. In turn, energy cannot

be even with respect to time reversal when \mathbf{p} is odd. Additionally, note that a natural term appearing in the correction is of the form $(\mathbf{p} - \mathbf{p}_0^{ME} + \mathbf{p}_0^{evo})^2$, thus again failing to satisfy the requirement of being even with respect to time reversal once there is a change of parity during the transition (as it is here: the odd parity variable \mathbf{p} evolves in such a way that it is enslaved to \mathbf{r}^\dagger on the lower level, which is a variable with even parity).

Appendix B. Fluid Mechanics

The reversible part of fluid mechanics, where the state variables are density, momentum density and entropy density (per volume), (ρ, \mathbf{m}, s) , is generated by the Poisson bracket of classical hydrodynamics (see, e.g., [42,43]),

$$\begin{aligned} \{A, B\} = & \int d\mathbf{r} \rho (\partial_i A_\rho B_{m_i} - \partial_i B_\rho A_{m_i}) \\ & + \int d\mathbf{r} m_i (\partial_i A_{m_i} B_{m_j} - \partial_j B_{m_i} A_{m_j}) \\ & + \int d\mathbf{r} s (\partial_i A_s B_{m_i} - \partial_i B_s A_{m_i}). \end{aligned} \tag{A3}$$

Supplied with energy, e.g.,

$$E = \int d\mathbf{r} \frac{\mathbf{m}^2}{2\rho} + \varepsilon(\rho, s), \tag{A4}$$

the reversible evolution of an arbitrary functional of the hydrodynamic variables $A(\rho, \mathbf{m}, s)$ is

$$\dot{A} = \{A, E\}. \tag{A5}$$

By rewriting the time-derivative of the functional as

$$\dot{A} = \int d\mathbf{r} A_\rho \partial_t \rho + A_{m_i} \partial_t m_i + A_s \partial_t s, \tag{A6}$$

and comparing with Equation (A5), one can read the reversible part of evolution equations for the hydrodynamic fields,

$$\partial_t \rho = -\partial_i (\rho E_{m_i}) = -\partial_i m_i, \tag{A7a}$$

$$\partial_t m_i = -\partial_j (m_i E_{m_j}) - \rho \partial_i E_\rho - m_j \partial_i E_{m_j} - s \partial_i E_s = -\partial_j \left(\frac{m_i m_j}{\rho} \right) - \partial_i p, \tag{A7b}$$

$$\partial_t s = -\partial_i (s E_{m_i}) = -\partial_i \left(\frac{s m_i}{\rho} \right), \tag{A7c}$$

where $p = -\varepsilon(\rho, s) + \rho \varepsilon_\rho + s \varepsilon_s$ is the pressure. The reversible evolution of hydrodynamic fields with energy (A4) is of course the Euler equations.

References

1. De Groot, S.R.; Mazur, P. *Non-Equilibrium Thermodynamics*; Dover Publications: New York, NY, USA, 1984.
2. Struchtrup, H. *Macroscopic Transport Equations for Rarefied Gas Flows*; Springer: Berlin, Germany, 2005.
3. Zwanzig, R. *Nonequilibrium Statistical Mechanics*; Oxford University Press: New York, NY, USA, 2001.
4. Öttinger, H. *Beyond Equilibrium Thermodynamics*; Wiley: New York, NY, USA, 2005.
5. Gorban, A.N.; Karlin, I.V.; Öttinger, H.C.; Tatarinova, L.L. Ehrenfest’s argument extended to a formalism of nonequilibrium thermodynamics. *Phys. Rev. E* **2001**, *63*, 066124. [[CrossRef](#)] [[PubMed](#)]
6. Karlin, I.V.; Tatarinova, L.L.; Gorban, A.N.; Öttinger, H.C. Irreversibility in the short memory approximation. *Phys. A Stat. Mech. Appl.* **2003**, *327*, 399–424. [[CrossRef](#)]
7. Gorban, A.; Karlin, I. *Invariant Manifolds for Physical and Chemical Kinetics*; Lecture Notes in Physics; Springer: Berlin, Germany, 2005.
8. Pavelka, M.; Klika, V.; Grmela, M. Thermodynamic explanation of Landau damping by reduction to hydrodynamics. *Entropy* **2018**, *20*, 457. [[CrossRef](#)]

9. Jaynes, E.T. *Delaware Seminar in the Foundation of Physics*; Bunge, M., Ed.; Springer: New York, NY, USA, 1967; chapter Foundations of probability theory and statistical mechanics.
10. Cimmelli, V.; Jou, D.; Ruggeri, T.; Ván, P. Entropy principle and recent results in non-equilibrium theories. *Entropy* **2014**, *16*, 1756–1807. [[CrossRef](#)]
11. Hermann, R. *Geometry, Physics and Systems*; Marcel Dekker: New York, NY, USA, 1984.
12. Grmela, M. Contact Geometry of Mesoscopic Thermodynamics and Dynamics. *Entropy* **2014**, *16*, 1652–1686. doi:10.3390/e16031652. [[CrossRef](#)]
13. Grmela, M. Geometry of Multiscale Nonequilibrium Thermodynamics. *Entropy* **2015**, *17*, 5938–5964. [[CrossRef](#)]
14. Pavelka, M.; Klika, V.; Grmela, M. *Multiscale Thermo-Dynamics*; de Gruyter: Berlin, Germany, 2018.
15. Grmela, M. Role of thermodynamics in multiscale physics. *Comput. Math. Appl.* **2013**, *65*, 1457–1470. doi:10.1016/j.camwa.2012.11.019. [[CrossRef](#)]
16. Grmela, M.; Klika, V.; Pavelka, M. Reductions and extensions in mesoscopic dynamics. *Phys. Rev. E* **2015**, *92*. [[CrossRef](#)]
17. Beris, A.; Edwards, B. *Thermodynamics of Flowing Systems*; Oxford University Press: Oxford, UK, 1994.
18. Dzyaloshinskii, I.E.; Volovick, G.E. Poisson brackets in condense matter physics. *Ann. Phys.* **1980**, *125*, 67–97. [[CrossRef](#)]
19. Peshkov, I.; Pavelka, M.; Romenski, E.; Grmela, M. Continuum Mechanics and Thermodynamics in the Hamilton and the Godunov-type Formulations. *Contin. Mech. Thermodyn.* **2018**, *30*, 1343–1378. [[CrossRef](#)]
20. Jizba, P.; Korbek, J. Maximum Entropy Principle in Statistical Inference: Case for Non-Shannonian Entropies. *Phys. Rev. Lett.* **2019**, *122*, 120601. doi:10.1103/PhysRevLett.122.120601. [[CrossRef](#)] [[PubMed](#)]
21. Grmela, M.; Pavelka, M.; Klika, V.; Cao, B.Y.; Bendian, N. Entropy and Entropy Production in Multiscale Dynamics. *J. Non-Equilibrium Thermodyn.* **2019**, *44*. [[CrossRef](#)]
22. Chapman, S.; Cowling, T.; Burnett, D.; Cercignani, C. *The Mathematical Theory of Non-uniform Gases: An Account of the Kinetic Theory of Viscosity, Thermal Conduction and Diffusion in Gases*; Cambridge Mathematical Library; Cambridge University Press: Cambridge, UK, 1990.
23. Grmela, M.; Öttinger, H.C. Dynamics and thermodynamics of complex fluids. I. Development of a general formalism. *Phys. Rev. E* **1997**, *56*, 6620–6632. doi:10.1103/PhysRevE.56.6620. [[CrossRef](#)]
24. Öttinger, H.C.; Grmela, M. Dynamics and thermodynamics of complex fluids. II. Illustrations of a general formalism. *Phys. Rev. E* **1997**, *56*, 6633–6655. doi:10.1103/PhysRevE.56.6633. [[CrossRef](#)]
25. Beretta, G.P. Steepest entropy ascent model for far-nonequilibrium thermodynamics: Unified implementation of the maximum entropy production principle. *Phys. Rev. E* **2014**, *90*, 042113. doi:10.1103/PhysRevE.90.042113. [[CrossRef](#)] [[PubMed](#)]
26. Montefusco, A.; Consonni, F.; Beretta, G.P. Essential equivalence of the general equation for the nonequilibrium reversible-irreversible coupling (GENERIC) and steepest-entropy-ascent models of dissipation for nonequilibrium thermodynamics. *Phys. Rev. E* **2015**, *91*, 042138. doi:10.1103/PhysRevE.91.042138. [[CrossRef](#)] [[PubMed](#)]
27. Callen, H. *Thermodynamics: An Introduction to the Physical Theories of Equilibrium Thermostatistics and Irreversible Thermodynamics*; Wiley: New York, NY, USA, 1960.
28. Pavelka, M.; Klika, V.; Grmela, M. Time reversal in nonequilibrium thermodynamics. *Phys. Rev. E* **2014**, *90*, 062131. [[CrossRef](#)] [[PubMed](#)]
29. Bird, R.B.; Hassager, O.; Armstrong, R.C.; Curtiss, C.F. *Dynamics of Polymeric Fluids*; Wiley: New York, NY, USA, 1987; Volume 2..
30. Pavelka, M.; Klika, V.; Esen, O.; Grmela, M. A hierarchy of Poisson brackets in non-equilibrium thermodynamics. *Phys. D Nonlinear Phenom.* **2016**, *335*, 54–69. [[CrossRef](#)]
31. Müller, I.; Ruggeri, T. *Rational Extended Thermodynamics*; Springer Tracts in Natural Philosophy; Springer: Berlin, Germany, 1998.
32. Grmela, M.; Lebon, G.; Dubois, C. Multiscale thermodynamics and mechanics of heat. *Phys. Rev. E* **2011**, *83*. [[CrossRef](#)]
33. Dumbser, M.; Peshkov, I.; Romenski, E.; Zanotti, O. High order ADER schemes for a unified first order hyperbolic formulation of continuum mechanics: Viscous heat-conducting fluids and elastic solids. *J. Comput. Phys.* **2016**, *314*, 824–862. [[CrossRef](#)]

34. Jou, D.; Casas-Vázquez, J.; Lebon, G. *Extended Irreversible Thermodynamics*, 4th ed.; Springer: New York, NY, USA, 2010.
35. Dumbser, M.; Peshkov, I.; Romenski, E.; Zanotti, O. High order ADER schemes for a unified first order hyperbolic formulation of Newtonian continuum mechanics coupled with electro-dynamics. *J. Comput. Phys.* **2017**, *348*, 298–342. doi:10.1016/j.jcp.2017.07.020. [[CrossRef](#)]
36. Godunov, S. Symmetric form of the magnetohydrodynamic equation. *Chislennyye Metody Mekh. Sploshnoi Sredy* **1972**, *3*, 26–34.
37. Biskamp, D. *Magnetohydrodynamic Turbulence*; Cambridge University Press: Cambridge, UK, 2003.
38. Landau, L.; Bell, J.; Kearsley, J.; Pitaevskii, L.; Lifshitz, E.; Sykes, J. *Electrodynamics of Continuous Media*; Course of Theoretical Physics; Elsevier Science: Oxford, United Kingdom, 1984.
39. Favache, A.; Dochain, D.; Maschke, B. An entropy-based formulation of irreversible processes based on contact structures. *Chem. Eng. Sci.* **2010**, *65*, 5204–5216. [[CrossRef](#)]
40. Bravetti, A.; Cruz, H.; Tapias, D. Contact Hamiltonian Mechanics. *Ann. Phys.* **2017**, *376*, 17–39. [[CrossRef](#)]
41. Esen, O.; Gümral, H. Geometry of Plasma Dynamics II: Lie Algebra of Hamiltonian Vector Fields. *J. Geom. Mech.* **2012**, *4*, 239–269. [[CrossRef](#)]
42. Arnold, V. Sur la géométrie différentielle des groupes de Lie de dimension infini et ses applications dans l'hydrodynamique des fluides parfaits. *Annales de l'institut Fourier* **1966**, *16*, 319–361. [[CrossRef](#)]
43. Grmela, M. Particle and Bracket Formulations of Kinetic Equations. *Contemp. Math.* **1984**, *28*, 125–132.



© 2019 by the authors. Licensee MDPI, Basel, Switzerland. This article is an open access article distributed under the terms and conditions of the Creative Commons Attribution (CC BY) license (<http://creativecommons.org/licenses/by/4.0/>).

Article

A Fourth Order Entropy Stable Scheme for Hyperbolic Conservation Laws

Xiaohan Cheng 

School of Science, Chang'an University, Xi'an 710064, China; xhcheng@chd.edu.cn

Received: 7 April 2019; Accepted: 17 May 2019; Published: 19 May 2019

Abstract: This paper develops a fourth order entropy stable scheme to approximate the entropy solution of one-dimensional hyperbolic conservation laws. The scheme is constructed by employing a high order entropy conservative flux of order four in conjunction with a suitable numerical diffusion operator that based on a fourth order non-oscillatory reconstruction which satisfies the sign property. The constructed scheme possesses two features: (1) it achieves fourth order accuracy in the smooth area while keeping high resolution with sharp discontinuity transitions in the nonsmooth area; (2) it is entropy stable. Some typical numerical experiments are performed to illustrate the capability of the new entropy stable scheme.

Keywords: conservation laws; entropy stable; entropy conservative; non-oscillatory reconstruction; sign property

1. Introduction

During the past few decades, abundant numerical methods for solving hyperbolic conservation laws have been designed; one can consult the review papers [1,2] and the references therein. Among the various methods, high order schemes, such as total variation diminishing (TVD) schemes, weighted essentially non-oscillatory (WENO) schemes and discontinuous Galerkin (DG) schemes, have achieved great success. However, it seems that there are few entropy stability results for high order numerical schemes for hyperbolic conservation laws, especially for the nonlinear hyperbolic conservation laws. In view of the above discussion, we limit our research on high order entropy stable methods for solving hyperbolic conservation laws.

In accordance with the idea of Tadmor, entropy schemes are often constructed by utilizing entropy conservative flux in conjunction with suitable numerical diffusion [3]. For example, physical viscosity was discretized and used as numerical diffusion in [4]. Roe-type numerical diffusion was selected for various systems like Euler equations, shallow water equations and ideal magnetohydrodynamic equations [5–7]. Based on the limiter mechanism, Liu et al. constructed a family of entropy consistent schemes with high resolution [8]. Recently, Dubey discussed the amount of suitable diffusion for the sake of devising non-oscillatory entropy stable schemes in the TVD sense [9]. To obtain high order entropy stable schemes, Fjordholm et al. firstly proved that ENO reconstruction satisfies a sign property and presented entropy stable schemes based on ENO reconstruction of arbitrary order accuracy [10,11]. To overcome the drawbacks of ENO reconstruction, we presented a third order reconstruction which is non-oscillatory and satisfies the sign property to construct a third order entropy stable scheme [12]. WENO reconstruction was modified to satisfy the sign property and also used to construct an entropy stable scheme in [13,14], although they are limited to third order accuracy.

In this paper, we are aiming at presenting a new entropy stable scheme of fourth order accuracy to solve hyperbolic conservation laws in one dimension. First, we employ a fourth order entropy conservative flux which is a linear combination of two-point entropy conservative fluxes. Then, we present a non-oscillatory reconstruction of fourth order accuracy which possesses the sign property

to obtain a fourth order accurate numerical diffusion operator. By adding this numerical diffusion operator to the entropy conservative flux, the resulting flux is entropy stable.

The remainder of this paper is given as follows. Section 2 describes the procedure for building our fourth order entropy scheme. After that, we present some typical numerical experiments to show the effectiveness of the newly developed scheme. Finally, concluding remarks are given in Section 4.

2. Numerical Method

Consider the scalar conservation law

$$\frac{\partial}{\partial t} u + \frac{\partial}{\partial x} f(u) = 0. \tag{1}$$

The weak solutions for Equation (1) are not unique and we are interested in the so-called entropy solution, which satisfies the entropy condition

$$\frac{\partial}{\partial t} \eta(u) + \frac{\partial}{\partial x} q(u) \leq 0. \tag{2}$$

Here, the entropy function $\eta(u)$ is convex and the entropy flux function $q(u)$ satisfies $\frac{\partial q}{\partial u} = v \frac{\partial f}{\partial u}$ with the entropy variable $v = \frac{\partial \eta}{\partial u}$. To solve Equation (1) with the conservative difference method, we have the semi-discrete scheme

$$\frac{du_i}{dt} = -\frac{f_{i+1/2} - f_{i-1/2}}{\Delta x}, \tag{3}$$

where u_i represents the point value at the node x_i on a uniform Cartesian mesh with the mesh size $x_{i+1} - x_i = \Delta x$. The scheme (3) is said to be entropy stable if it satisfies a discrete version of the entropy condition (2), namely,

$$\frac{\partial}{\partial t} \eta(u_i) + \frac{q_{i+1/2} - q_{i-1/2}}{\Delta x} \leq 0; \tag{4}$$

the scheme is said to be entropy conservative if it satisfies the discrete entropy equality

$$\frac{\partial}{\partial t} \eta(u_i) + \frac{q_{i+1/2} - q_{i-1/2}}{\Delta x} = 0. \tag{5}$$

In this work, we utilize the familiar Runge–Kutta scheme of order four to solve the ordinary Equation (3). Now, we focus on how to build the entropy stable numerical flux $f_{i+1/2}$.

First, the numerical flux is split into an entropy conservative part and a numerical diffusion part

$$f_{i+1/2} = f_{i+1/2}^{EC} - \frac{1}{2} \delta_{i+1/2} (v_{i+1/2}^+ - v_{i+1/2}^-). \tag{6}$$

Here, $f_{i+1/2}^{EC}$ is a fourth order entropy conservative flux [15] expressed as

$$f_{i+1/2}^{EC} = \frac{4}{3} \tilde{f}(u_i, u_{i+1}) - \frac{1}{6} (\tilde{f}(u_{i-1}, u_{i+1}) - \tilde{f}(u_i, u_{i+2})) \tag{7}$$

with $\tilde{f}(\alpha, \beta)$ being the second order entropy conservative flux defined by Tadmor [3]. Generally, $\delta_{i+1/2}$ in the numerical diffusion part is chosen to be $|f'(u_{i+1/2})|$. If the reconstructed values $v_{i+1/2}^\pm$ at the interfaces from the entropy variable v_i satisfy

$$\text{sign}(v_{i+1/2}^+ - v_{i+1/2}^-) = \text{sign}(v_{i+1} - v_i), \tag{8}$$

the numerical flux (6) achieves entropy stability. Property (8) in which the jump of the reconstructed point values at each cell interface has the same sign as the jump of the underlying point values across that interface is called the sign property. We present the fourth order reconstruction satisfying the sign property as follows to obtain $v_{i+1/2}^\pm$.

Consider a polynomial reconstruction of the form

$$p_i(x) = v_i + d_i \left(\frac{x - x_i}{\Delta x} \right) + \left(\frac{v_{i-1} - 2v_i + v_{i+1}}{2} \right) \left(\frac{x - x_i}{\Delta x} \right)^2 + \left(\frac{-v_{i-1} + v_{i+1} - 2d_i}{2} \right) \left(\frac{x - x_i}{\Delta x} \right)^3 \quad (9)$$

with d_i being a slope function. For convenience, we introduce the following notation

$$\begin{aligned} ds_i &= \frac{2}{3}v_{i+1} - \frac{2}{3}v_{i-1} - \frac{1}{12}v_{i+2} + \frac{1}{12}v_{i-2}, \\ WC_i &= v_{i+1} - v_{i-1}, \quad WR_i = v_{i+1} - v_i, \quad WC2_i = v_{i+2} - v_{i-2}, \\ ds1_i &= 0, \quad ds2_i = \frac{1}{2}(WC_i - 8WR_i), \quad ds3_i = \frac{1}{2}(8WR_i - 7WC_i), \\ S_i &= \text{sign}(WC_i), \\ C_1 &= \frac{\sqrt{3}}{6}, \quad C_2 = \frac{6}{12 + \sqrt{3}}, \end{aligned} \quad (10)$$

and define the slope d_i in the following way:

1. If $S_i = 0$, then $d_i = 0$.
2. If $S_i \neq 0$ and $(2S_i \cdot WC_i \geq S_i \cdot WC2_i)$, then $d_i = ds_i$.
3. If $S_i \neq 0$ and $(2S_i \cdot WC_i < S_i \cdot WC2_i)$, then the following hold:

(a) If $v_i = \frac{v_{i+1} + v_{i-1}}{2}$, we define

$$d_i = \begin{cases} \max(ds1_i, ds_i), & \text{if } S_i > 0, \\ \min(ds1_i, ds_i), & \text{if } S_i < 0. \end{cases}$$

(b) If $v_i \neq \frac{v_{i+1} + v_{i-1}}{2}$, then the following hold:

i. If $\left| WR_i - \frac{1}{2}WC_i \right| \geq \frac{1}{8} |WC2_i - 2WC_i|$, then

$$d_i = \begin{cases} \max(ds2_i, ds3, ds_i), & \text{if } S_i > 0, \\ \min(ds2_i, ds3, ds_i), & \text{if } S_i < 0. \end{cases}$$

ii. If $\left| WR_i - \frac{1}{2}WC_i \right| < \frac{1}{8} |WC2_i - 2WC_i|$, then

$$d_i = \begin{cases} \frac{WC_i}{2} - S_i \cdot C_1 \cdot |2WR_i - WC_i|, & \text{if } \left| \frac{WR_i}{WC_i} - \frac{1}{2} \right| \leq C_2, \\ \frac{WC_i}{2}, & \text{if } \left| \frac{WR_i}{WC_i} - \frac{1}{2} \right| > C_2. \end{cases}$$

Theorem 1. With this definition of the slope, the polynomial reconstruction (9) fulfills the shape preserving property, namely,

- $p_i(x)$ is monotone in $[x_{i-1/2}, x_{i+1/2}]$ iff the point values $\{v_{i-1}, v_i, v_{i+1}\}$ are;
- $p_i(x)$ generates an extremum in the interior of $[x_{i-1/2}, x_{i+1/2}]$ iff v_i is an extremum value.

The proof of this theorem can be found in [16]. According to this property, the polynomial $p_i(x)$ does not create new extrema in the interior of $[x_{i-1/2}, x_{i+1/2}]$. In other words, the polynomial $p_i(x)$ may create new extrema at the interfaces $\{x_{i\pm 1/2}\}$. To keep away from such spurious extrema,

we can employ a similar strategy as in [17]. Let us modify the polynomial reconstruction to be the following form:

$$\varphi_i(x) = (1 - \theta_i)v_i + \theta_i p_i(x), \quad 0 < \theta_i < 1. \tag{11}$$

The limiter θ_i is determined by

$$\theta_i = \begin{cases} \min \left\{ \frac{M_{i+1/2} - v_i}{M_i - v_i}, \frac{m_{i-1/2} - v_i}{m_i - v_i}, 1 \right\}, & \text{if } v_{i-1} < v_i < v_{i+1}, \\ \min \left\{ \frac{M_{i-1/2} - v_i}{M_i - v_i}, \frac{m_{i+1/2} - v_i}{m_i - v_i}, 1 \right\}, & \text{if } v_{i-1} > v_i > v_{i+1}, \\ 1, & \text{otherwise,} \end{cases} \tag{12}$$

with

$$M_i = \max_{x \in [x_{i-1/2}, x_{i+1/2}]} p_i(x), \quad m_i = \min_{x \in [x_{i-1/2}, x_{i+1/2}]} p_i(x),$$

and

$$\begin{cases} M_{i\pm 1/2} = \max \left\{ \frac{1}{2}(v_i + v_{i\pm 1}), p_{i\pm 1}(x_{i\pm 1/2}) \right\}, \\ m_{i\pm 1/2} = \min \left\{ \frac{1}{2}(v_i + v_{i\pm 1}), p_{i\pm 1}(x_{i\pm 1/2}) \right\}. \end{cases}$$

Theorem 2. *The polynomial reconstruction (11) is fourth order accurate and fulfills the sign property (8).*

Theorem 3. *With the definitions of the reconstructed values $v_{i+1/2}^+ = \varphi_{i+1}(x_{i+1/2})$ and $v_{i+1/2}^- = \varphi_i(x_{i+1/2})$, the numerical flux (6) is entropy stable and fourth order accurate.*

Remark 1. *The proofs for Theorems 2 and 3 can be carried out very similarly as in [12,17]. We omit the simple but trivial procedure here.*

Remark 2. *For hyperbolic systems, the reconstruction procedure should be implemented in the local characteristic directions for the purpose of achieving entropy stability. The detailed steps can be found in our previous paper [12].*

3. Numerical Examples

In this section, we illustrate the effectiveness of the presented scheme which is abbreviated by ES4 by means of three typical examples. Numerical results include the convergence order and the capacity of dealing with discontinuous problems.

Example 1. *Consider the linear advection equation $u_t + u_x = 0$ on the domain $[-1, 1]$ with two initial data $u(x, 0) = \sin(\pi x)$ and $u(x, 0) = \sin^4(\pi x)$. For a comparison, a third order entropy stable scheme (ES3) [12] is also implemented for this example. The numerical errors (L^1 error and L^∞ error) and convergence orders are displayed in Tables 1 and 2. We can observe that the fourth order convergence of the proposed scheme is confirmed and ES4 performs better than ES3.*

Table 1. The numerical errors and convergence orders for $u_t + u_x = 0$ with $u(x, 0) = \sin(\pi x)$ at $t = 8$.

Method	N	L^1 Error	L^1 Order	L^∞ Error	L^∞ Order
ES3	40	7.8941×10^{-3}	2.9838	6.1563×10^{-3}	2.9528
	80	9.8686×10^{-4}	2.9999	7.7371×10^{-4}	2.9922
	160	1.2332×10^{-4}	3.0004	9.6812×10^{-5}	2.9985
	320	1.5413×10^{-5}	3.0002	1.2104×10^{-5}	2.9997
	640	1.9266×10^{-6}	3.0000	1.5131×10^{-6}	2.9999
ES4	40	7.2962×10^{-4}		5.5350×10^{-4}	
	80	4.4746×10^{-5}	4.0273	3.4513×10^{-5}	4.0034
	160	2.7650×10^{-6}	4.0164	2.1523×10^{-6}	4.0032
	320	1.7178×10^{-7}	4.0086	1.3430×10^{-7}	4.0023
	640	1.0702×10^{-8}	4.0046	8.3862×10^{-9}	4.0013

Table 2. The numerical errors and convergence orders for $u_t + u_x = 0$ with $u(x, 0) = \sin^4(\pi x)$ at $t = 1$.

Method	N	L^1 Error	L^1 Order	L^∞ Error	L^∞ Order
ES3	80	3.8419×10^{-3}		3.7835×10^{-3}	
	160	4.9986×10^{-4}	2.9422	5.8676×10^{-4}	2.6889
	320	6.7841×10^{-5}	2.8813	8.6901×10^{-5}	2.7553
	640	1.0357×10^{-5}	2.7115	1.5669×10^{-5}	2.4715
	1280	1.4533×10^{-6}	2.5625	4.9399×10^{-6}	1.6654
ES4	80	8.1572×10^{-4}		1.2001×10^{-3}	
	160	5.9041×10^{-5}	3.7883	1.4743×10^{-4}	3.0249
	320	4.9006×10^{-6}	3.5907	2.7023×10^{-5}	1.3202
	640	1.6184×10^{-7}	4.9203	1.4716×10^{-7}	7.5207
	1280	1.0013×10^{-8}	4.0146	8.6289×10^{-9}	4.0921

Example 2. Consider the Burgers equation

$$u_t + (u^2/2)_x = 0 \tag{13}$$

subjected to the initial data

$$u(x, 0) = \begin{cases} 1, & \text{for } |x| \leq 1/3, \\ -1, & \text{for } 1/3 < |x| \leq 1. \end{cases}$$

For this problem, we can deduce the analytical solution that evolves a rarefaction fan and a stationary shock on the left-hand and right-hand side, respectively. Figure 1 presents the numerical result at time $t = 0.3$ on a mesh of 100 grids. Our scheme resolves the shock wave and the rarefaction wave very well.

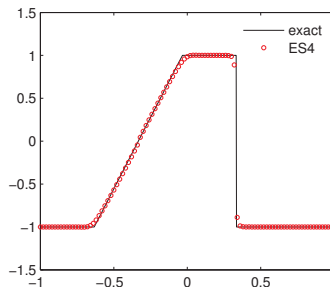


Figure 1. The numerical result for Burgers equation.

Example 3. Consider the Euler equations from aerodynamics

$$\frac{\partial}{\partial t} \begin{pmatrix} \rho \\ \rho\mu \\ E \end{pmatrix} + \frac{\partial}{\partial x} \begin{pmatrix} \rho\mu \\ \rho\mu^2 + p \\ \mu(E + p) \end{pmatrix} = 0 \tag{14}$$

with ρ, μ, p and E being the density, velocity, pressure and total energy, respectively. For an idea gas, the total energy E is given by the relation

$$E = \frac{p}{\gamma - 1} + \frac{1}{2}\rho\mu^2 \tag{15}$$

with the specific heats ratio $\gamma = 1.4$. Three Riemann problems are tested by the presented scheme.

Case 1: Sod’s shock tube problem. The initial data is given as

$$(\rho, \mu, p) = \begin{cases} (1, 0, 1), & \text{for } x < 0, \\ (0.125, 0, 0.1), & \text{for } x > 0. \end{cases}$$

The numerical simulation is carried out on a mesh of 200 grids on $[-0.5, 0.5]$ up to time $t = 0.16$. The computed density is plotted in Figure 2. We can see that the ES4 scheme performs well by capturing the shock, the contact discontinuity and the rarefaction wave accurately.

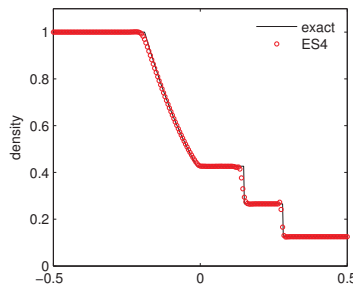


Figure 2. The density for Sod’s shock tube problem.

Case 2: Toro’s 123 problem. The initial data is given as

$$(\rho, \mu, p) = \begin{cases} (1, -2, 0.4), & \text{for } x < 0, \\ (1, 2, 0.4), & \text{for } x > 0. \end{cases}$$

The difficulty for simulating this problem lies in the fact that the pressure between the evolved rarefactions is very small (near vacuum) and may bring about the blow-ups of the code if the numerical method is not robust. The numerical simulation is carried out on a mesh of 200 grids on $[-0.5, 0.5]$ up to time $t = 0.1$. Figure 3 displays the computed density. It can be observed that the computed result by ES4 compares well with the reference solution.

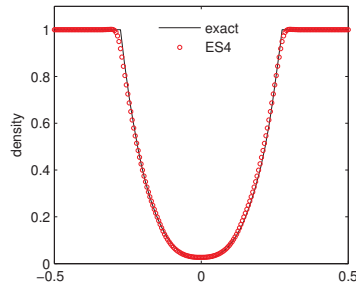


Figure 3. The density for Toro’s 123 problem.

Case 3: Shu–Osher problem. The initial data is given as

$$(\rho, u, p) = \begin{cases} (3.857, 2.629, 10.333), & \text{for } x < -4, \\ (1 + 0.2 \sin(5x), 0, 1), & \text{for } x > -4. \end{cases}$$

This problem, also called the shock density-wave interaction problem, describes a moving Mach 3 shock interacting with sine waves in density. The numerical simulation is carried out on a mesh of 500 grids on $[-5, 5]$ up to time $t = 1.8$. We present the results of density in Figure 4. It can be seen clearly that the ES4 scheme produces accurate results and captures the sine wave well.

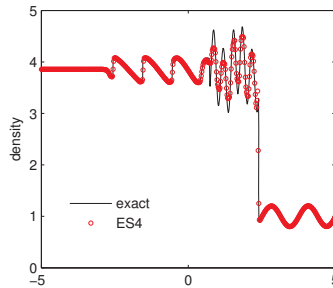


Figure 4. The density for the Shu–Osher problem.

4. Conclusions

This paper presents a fourth order entropy stable scheme for solving one-dimensional hyperbolic conservation laws. Along the lines of [10,12], our scheme is also obtained by utilizing entropy conservative flux in conjunction with suitable numerical diffusion. We first select the existing fourth order entropy conservative scheme based on the combination of the two-point entropy conservative flux. The main novelty lies in the construction of numerical diffusion by presenting a fourth order non-oscillatory reconstruction possessing the sign property. Compared to other high order schemes, the main advantage of our scheme is the entropy stability. Some numerical results are displayed to show the accuracy and shock capturing capacity of our scheme. Ongoing work involves generalizing the idea of this paper to multidimensional cases and other hyperbolic systems such as shallow water equations and magnetohydrodynamic equations.

Funding: This research is supported by the National Natural Science Foundation of China (Grant No. 11601037) and the Natural Science Foundation of Shaanxi Province (Grant No. 2018JQ1027).

Conflicts of Interest: The author declares no conflict of interest.

References

1. Tadmor, E. A review of numerical methods for nonlinear partial differential equations. *Bull. Am. Math. Soc.* **2012**, *49*, 507–554. [[CrossRef](#)]
2. Shu, C. High order WENO and DG methods for time-dependent convection-dominated PDEs. *J. Comput. Phys.* **2016**, *316*, 598–613. [[CrossRef](#)]
3. Tadmor, E. Entropy stability theory for difference approximations of nonlinear conservation laws and related time-dependent problems. *Acta Numer.* **2003**, *12*, 451–512. [[CrossRef](#)]
4. Tadmor, E.; Zhong, W.G. Entropy stable approximations of Navier-Stokes equations with no artificial numerical viscosity. *J. Hyperbolic Differ. Equ.* **2006**, *3*, 529–559. [[CrossRef](#)]
5. Ismail, F.; Roe, P.L. Affordable, entropy-consistent Euler flux functions II: Entropy production at shocks. *J. Comput. Phys.* **2009**, *228*, 5410–5436. [[CrossRef](#)]
6. Fjordholm, U.S.; Mishra, S.; Tadmor, E. Well-balanced and energy stable schemes for the shallow water equations with discontinuous topography. *J. Comput. Phys.* **2011**, *230*, 5587–5609. [[CrossRef](#)]
7. Chandrashekar, P.; Klingenberg, C. Entropy stable finite volume scheme for ideal compressible MHD on 2-D Cartesian meshes. *SIAM J. Numer. Anal.* **2016**, *54*, 1313–1340. [[CrossRef](#)]
8. Liu, Y.; Feng, J.; Ren, J. High Resolution, Entropy-Consistent Scheme Using Flux Limiter for Hyperbolic Systems of Conservation Laws. *J. Sci. Comput.* **2015**, *64*, 914–937. [[CrossRef](#)]
9. Dubey, R.K.; Biswas, B. Suitable diffusion for constructing non-oscillatory entropy stable schemes. *J. Comput. Phys.* **2018**, *372*, 912–930. [[CrossRef](#)]
10. Fjordholm, U.S.; Mishra, S.; Tadmor, E. Arbitrarily high-order accurate entropy stable essentially nonoscillatory schemes for systems of conservation laws. *SIAM J. Numer. Anal.* **2012**, *50*, 544–573. [[CrossRef](#)]
11. Fjordholm, U.S.; Mishra, S.; Tadmor, E. ENO reconstruction and ENO interpolation are stable. *Found. Comput. Math.* **2013**, *13*, 139–159. [[CrossRef](#)]
12. Cheng, X.; Nie, Y. A third order entropy stable scheme for hyperbolic conservation laws. *J. Hyperbolic Differ. Equ.* **2016**, *13*, 129–145. [[CrossRef](#)]
13. Fjordholm, U.S.; Ray, D. A Sign Preserving WENO Reconstruction Method. *J. Sci. Comput.* **2016**, *68*, 42–63. [[CrossRef](#)]
14. Biswas, B.; Dubey, R.K. Low dissipative entropy stable schemes using third order WENO and TVD reconstructions. *Adv. Comput. Math.* **2018**, *44*, 1153–1181. [[CrossRef](#)]
15. Lefloch, P.G.; Mercier, J.M.; Rohde, C. Fully discrete, entropy conservative schemes of arbitrary order. *SIAM J. Numer. Anal.* **2002**, *40*, 1968–1992. [[CrossRef](#)]
16. Balaguer, A.; Conde, C. Fourth-order nonoscillatory upwind and central schemes for hyperbolic conservation laws. *SIAM J. Numer. Anal.* **2005**, *43*, 455–473. [[CrossRef](#)]
17. Liu, X.D.; Osher, S. Nonoscillatory high order accurate self-similar maximum principle satisfying shock capturing schemes I. *SIAM J. Numer. Anal.* **1996**, *33*, 760–779. [[CrossRef](#)]



© 2019 by the author. Licensee MDPI, Basel, Switzerland. This article is an open access article distributed under the terms and conditions of the Creative Commons Attribution (CC BY) license (<http://creativecommons.org/licenses/by/4.0/>).

Spin Isoenergetic Process and the Lindblad Equation

Congjie Ou ¹, Yuho Yokoi ² and Sumiyoshi Abe ^{1,2,3,4,*}

¹ Physics Division, College of Information Science and Engineering, Huaqiao University, Xiamen 361021, China; jcou@hqu.edu.cn

² Department of Physical Engineering, Mie University, Mie 514-8507, Japan; yuho_451@yahoo.co.jp

³ Institute of Physics, Kazan Federal University, 420008 Kazan, Russia

⁴ ESIEA, 9 Rue Vesale, 75005 Paris, France

* Correspondence: suabe@sf6.so-net.ne.jp

Received: 21 March 2019; Accepted: 6 May 2019; Published: 17 May 2019

Abstract: A general comment is made on the existence of various baths in quantum thermodynamics, and a brief explanation is presented about the concept of weak invariants. Then, the isoenergetic process is studied for a spin in a magnetic field that slowly varies in time. In the Markovian approximation, the corresponding Lindbladian operators are constructed without recourse to detailed information about the coupling of the subsystem with the environment called the energy bath. The entropy production rate under the resulting Lindblad equation is shown to be positive. The leading-order expressions of the power output and work done along the isoenergetic process are obtained.

Keywords: quantum thermodynamics of spin; weak invariants; isoenergetic process; Lindblad equation

1. Introduction

Besides its importance for nanoscience, nanotechnology and quantum engineering in general, quantum thermodynamics has a particular status in contemporary physics. It sheds fresh light on both classical and quantum theories. For instance, the quantum-mechanical violation of the law of equipartition of energy seems to require careful reexaminations of even the isothermal process of the ideal gas. It is also the case for the connection between the adiabatic and isentropic processes. Classical mechanics is described by a set of dynamical variables, whereas quantum mechanics contains not only dynamical variables but also the Hilbert space. Accordingly, quantum mechanics may lead to novel concepts that have no counterparts in classical thermodynamics. The dephasing bath [1] and energy bath [2,3] can be thought of as typical such examples. Therefore, it is of significance to elucidate the implications of such baths to thermodynamics.

In the present paper, we develop a discussion about the isoenergetic process associated with the energy bath within the framework of finite-time quantum thermodynamics. We employ a single Pauli spin in a time-dependent magnetic field and describe its nonequilibrium subdynamics based on the Lindblad equation [4,5], which is known to be unique in the Markovian approximation. It is shown how the Lindbladian operators can be determined without detailed information about the interaction between the subsystem and the energy bath. The resulting subdynamics is seen to be unital [6] and accordingly has a non-negative entropy production rate. The power output and work done are evaluated in the leading order.

The paper is organized as follows. In Section 2, a succinct explanation is presented about the concept of weak invariants, which is directly connected to the isoenergetic process. In Section 3, the Lindbladian operators are determined for the Pauli spin in a time-dependent magnetic field, and the entropy production rate under the Lindblad equation thus obtained is discussed. Then, based on the result in Section 3, finite-time thermodynamics of the power output and work in the leading order is studied in Section 4. Section 5 is devoted to concluding remarks.

2. Weak Invariant and Isoenergetic Process

The concept of weak invariants has wide universality. Let us consider a master equation

$$i \hbar \frac{\partial \rho}{\partial t} = \mathcal{E}(\rho) \tag{1}$$

for the density matrix ρ describing the state of a quantum subsystem, where \mathcal{E} is a certain linear superoperator. Henceforth, \hbar is set equal to unity for the sake of simplicity. Then, a weak invariant $I = I(t)$ associated with this master equation is defined as a solution of the following equation [7]:

$$i \frac{\partial I}{\partial t} + \mathcal{E}^*(I) = 0. \tag{2}$$

In this equation, \mathcal{E}^* stands for the adjoint of \mathcal{E} defined by $\text{tr}(Q \mathcal{E}(R)) = \text{tr}(\mathcal{E}^*(Q) R)$, provided that $Q \mathcal{E}(R)$ and therefore also $\mathcal{E}^*(Q) R$ should be trace-class. Then, it follows from Equations (1) and (2) that the expectation value of I is conserved:

$$\frac{d\langle I \rangle}{dt} = 0 \tag{3}$$

with the notation $\langle Q \rangle \equiv \text{tr}(Q\rho)$, although the spectrum of I is time-dependent, in general.

Our purpose is to clarify the implication of the energy bath to quantum thermodynamics. For it, what to be contemplated is the isoenergetic processes, along which the internal energy of the subsystem is kept constant through energy transfer between the subsystem and the energy bath. A point is that the energy transfer that may be realized not in the form of heat but rather in the dynamical manner [8,9].

The isoenergetic processes have been discussed for a “three-stroke” engine [3,10], in which however no explicit time evolution of the subsystem has been considered. In view of finite-time quantum thermodynamics, a density matrix evolves in time according to a master equation. Here, let us assume Markovianity of the subdynamics. In this case, the superoperator in Equation (1) has the Lindblad form [4,5]:

$$\mathcal{E}(\rho) = [H(t), \rho] - \frac{i}{2} \sum_i a_i (L_i^\dagger L_i \rho + \rho L_i^\dagger L_i - 2L_i \rho L_i^\dagger), \tag{4}$$

where $H(t)$ is the time-dependent Hamiltonian and a_i 's are nonnegative c -number coefficients. Both the coefficients and the Lindbladian operators L_i 's may also depend on time, explicitly.

The weak invariant relevant to the isoenergetic process is the time-dependent Hamiltonian itself. Thus, the internal energy

$$U = \text{tr}(H(t) \rho) \tag{5}$$

is required to be conserved under time evolution generated by the Lindblad equation. Such a condition is fulfilled if the Hamiltonian obeys the following equation:

$$\frac{\partial H(t)}{\partial t} - \frac{1}{2} \sum_i a_i (L_i^\dagger L_i H(t) + H(t) L_i^\dagger L_i - 2L_i^\dagger H(t) L_i) = 0, \tag{6}$$

which comes from Equation (2) with Equation (4).

In general, it is a nontrivial task to determine the Lindbladian operators in Equations (4) and (6), since it needs detailed knowledge of how the subsystem interacts with the environment. However, Equation (6) tends to make it possible to determine them without such knowledge [11].

Closing this section, we make some comments on the concept of weak invariants. Firstly, it has recently been discovered [12] that there exists a connection between weak invariants and the action principle for corresponding master equations. Secondly, such quantities clearly have their

classical analogs. For instance, a weak invariant associated with the classical Fokker-Planck equation is discussed in Reference [13]. Thirdly, it is worth mentioning that the Lindblad equation with a time-dependent Hamiltonian can describe the dynamics toward an “instantaneous attractor” in the nonadiabatic regime [14], inside which isoenergeticity is realized.

3. Weak Invariant of Spin in Time-Dependent Magnetic Field and Lindbladian Operators

In recent years, quantum thermodynamics of a two-level system has been discussed in the literature [15,16]. Here, we consider a single spin in a time-dependent magnetic field $\mathbf{B}(t)$. The Hamiltonian reads

$$H(t) = \mathbf{B}(t) \cdot \sigma \tag{7}$$

with σ being the Pauli-matrix vector. The constant involving the gyromagnetic ratio is set equal to unity. In the thermodynamic context, variation of the magnetic field should be slow. That is, the time scale of the variation is much longer than those of relaxation and quantum dynamics.

From the linearity of Equation (6) with respect to the Hamiltonian and the $su(2)$ Lie algebra of the spin, it is natural to examine the following Lindbladian operators:

$$L_i = \sigma_i \quad (i = 1, 2, 3). \tag{8}$$

These are Hermitian, and accordingly the subdynamics is unital [6]. Substituting Equation (8) into Equation (6) and using linear independence of the Pauli matrices, we have

$$\dot{\mathbf{B}}(t) = -2A \mathbf{B}(t) + 2c \mathbf{B}(t), \tag{9}$$

where the overdote denotes differentiation with respect to time, and A and c are given by

$$A = \begin{pmatrix} a_1 & 0 & 0 \\ 0 & a_2 & 0 \\ 0 & 0 & a_3 \end{pmatrix}, \tag{10}$$

$$c = \text{tr } A = a_1 + a_2 + a_3, \tag{11}$$

respectively. From Equation (9), we see that

$$\mathbf{B}(t) \cdot \dot{\mathbf{B}}(t) = 2(a_2 + a_3) B_1^2(t) + 2(a_3 + a_1) B_2^2(t) + 2(a_1 + a_2) B_3^2(t), \tag{12}$$

which is positive since a_i 's are nonnegative and not all of them can be zero. Therefore, the magnitude $B(t) = |\mathbf{B}(t)|$ has to monotonically increase in time. In addition, from Equation (9), we find the coefficients to be given by

$$a_1 = \frac{1}{4} \left(\frac{\dot{B}_1}{B_1} + \frac{\dot{B}_2}{B_2} + \frac{\dot{B}_3}{B_3} \right), \quad a_2 = \frac{1}{4} \left(\frac{\dot{B}_1}{B_1} - \frac{\dot{B}_2}{B_2} + \frac{\dot{B}_3}{B_3} \right), \quad a_3 = \frac{1}{4} \left(\frac{\dot{B}_1}{B_1} + \frac{\dot{B}_2}{B_2} - \frac{\dot{B}_3}{B_3} \right). \tag{13}$$

Thus, without detailed information about the interaction between the subsystem and the environment, the explicit form of the Lindblad equation is now fully determined as follows:

$$i \frac{\partial \rho}{\partial t} = [H(t), \rho] - \frac{i}{2} \sum_{i=1}^3 a_i [\sigma_i, [\sigma_i, \rho]]. \tag{14}$$

We note that the second term on the right-hand side, termed the dissipator, is small and is of the order $\dot{B}_i(t)$'s. Equation (14) belongs to a class of finite-level systems in contact with a singular reservoir consisting of particles with the vanishing correlation time [17]. On the other hand, what is

peculiar here is highlighted in Equation (13) that purely comes from isoenergeticity, without recourse to the detailed property of the energy bath.

Hermiticity of the Lindbladian operators in Equation (8), or equivalently the fact that the subdynamics is unital, can have a significant implication for the isoenergetic process. As shown in Reference [18] (see, also Reference [11] and a discussion generalized to the Rényi entropy in Reference [19]), time evolution of the von Neumann entropy

$$S[\rho] = -\text{tr}(\rho \ln \rho) \tag{15}$$

under the Lindblad equation in its general form in Equation (1) with Equation (4) satisfies

$$\frac{dS}{dt} = \sum_i a_i \Gamma_i, \tag{16}$$

$$\Gamma_i \geq \langle [L_i^\dagger, L_i] \rangle, \tag{17}$$

where the Boltzmann constant is set equal to unity. Since the Lindbladian operators in the present case are Hermitian, the subdynamics tends to produce the entropy in time,

$$\frac{dS}{dt} \geq 0, \tag{18}$$

as desired.

4. Temporally-Local Equilibrium State, Power Output and Work along Isoenergetic Process

A nonequilibrium thermodynamic system with a slowly-varying Hamiltonian is dominantly described by a locally-equilibrium state, in which the thermodynamic variables also vary slowly. In the present case, what is relevant is the temporally-local equilibrium state given by

$$\rho^{(0)} = \frac{1}{Z(t)} \exp(-\beta(t)H(t)), \tag{19}$$

where $Z(t)$ is the partition function

$$Z(t) = \text{tr} \exp(-\beta(t) H(t)). \tag{20}$$

$\beta(t)$ is the time-dependent inverse temperature that slowly varies in time [see Equation (26) below].

For the Hamiltonian in Equation (7), the explicit expression of Equation (19) is the familiar one

$$\rho^{(0)} = \frac{1}{2} \{I - (\mathbf{n}(t) \cdot \sigma) \tanh(\beta(t) B(t))\}, \tag{21}$$

where I is the 2×2 unit matrix and $\mathbf{n}(t)$ is a unit vector defined by $\mathbf{n}(t) = \mathbf{B}(t)/B(t)$.

The full density matrix may be expanded around the state in Equation (21) as follows:

$$\rho = \rho^{(0)} + \rho^{(1)} + \dots, \tag{22}$$

where the expansion should be performed in terms of the elements of $\dot{\mathbf{B}}(t)$ and its higher-order derivatives. It is natural to assume that all of the correction terms are traceless. Substituting Equation (22) into Equation (14), the first-order correction is found to satisfy

$$[H(t), \rho^{(1)}] = i \frac{\partial \rho^{(0)}}{\partial t} + \frac{i}{2} \sum_{i=1}^3 a_i [\sigma_i, [\sigma_i, \rho^{(0)}]], \tag{23}$$

for instance.

In accordance with Equation (22), the internal energy is also expanded as follows:

$$U = U^{(0)} + U^{(1)} + \dots \tag{24}$$

The isoenergeticity condition should be satisfied in each order. For the leading-order term

$$U^{(0)} = \text{tr}(H(t) \rho^{(0)}) = -B(t) \tanh(\beta(t) B(t)), \tag{25}$$

we find that the isoenergeticity condition, $dU^{(0)}/dt = 0$, in the leading order gives rise to

$$\dot{B}(t) [\sinh(2\beta(t) B(t)) + 2\beta(t) B(t)] = -2B^2(t) \dot{\beta}(t). \tag{26}$$

Since $\dot{B}(t)$ is positive due to Equation (12) resulting from the Lindblad equation, $\dot{\beta}(t)$ is necessarily negative, implying that the temperature monotonically increases in time.

Now, let us discuss the power output defined by

$$P(t) = -\text{tr}(\dot{H}(t) \rho). \tag{27}$$

The leading-order contribution comes from the temporally-local equilibrium state and is calculated to be

$$P(t) = -\dot{\mathbf{B}}(t) \cdot \text{tr}(\sigma \rho^{(0)}) = \dot{\mathbf{B}}(t) \cdot \mathbf{n}(t) \tanh(\beta(t) B(t)). \tag{28}$$

An interesting point is that, similarly to the case of the time-dependent harmonic oscillator [20], this quantity can be expressed in terms of the internal energy as follows:

$$P(t) = -\frac{\dot{B}(t)}{B(t)} U^{(0)}. \tag{29}$$

From this expression, the work done during the time interval $t_i \leq t \leq t_f$ along the isoenergetic process is given, in the leading order, by

$$W = \int_{t_i}^{t_f} dt P(t) = -U^{(0)}(t_i) \int_{t_i}^{t_f} dt \frac{\dot{B}(t)}{B(t)} = B(t_i) \tanh(\beta(t_i) B(t_i)) \ln \left[\frac{B(t_f)}{B(t_i)} \right], \tag{30}$$

where the initial value is used for the conserved internal energy.

5. Concluding Remarks

Toward clarifications of the physical properties of exotic baths present in quantum thermodynamics but absent in classical thermodynamics, we have focused our attention on the isoenergetic process that is connected with the energy bath. For this purpose, we have studied a single spin in a magnetic field slowly varying in time based on the Lindblad equation. We have shown how the isoenergeticity condition can determine the Lindbladian operators without recourse to detailed knowledge of the interaction between the subsystem and the energy bath. We have developed a discussion about finite-time thermodynamics of such a system and evaluated the power output and the work in the leading order.

The result given in Equation (30) implies that the work is determined only by the initial and final values of the variables without depending on paths of the magnetic field in the parameter \mathbf{B} -space. This would be a common feature of the isoenergetic processes in the leading order.

In the present work, we have treated a single Pauli spin. As known, by virtue of the structure of spin algebra, any density matrix of a multispin system can be expanded in terms of the spin matrices,

their tensor products as well as the unit matrix. Therefore, the temporally-local equilibrium state in Equation (21) can be generalized to the multispin case [21].

Here, we have considered only the energy bath, which is nothing but one of the exotic baths in quantum thermodynamics. Existence of various baths indicates that there may be ensemble-dependent dynamics. In this point, it is worth mentioning that such dynamics are also suggested in nanothermodynamics of classical small systems, in which fluctuations can be very large [22,23]. Much is yet to be clarified about the quantum-classical correspondence in thermodynamics.

Author Contributions: S.A. has provided the idea of the study, performed the calculations and written the manuscript. C.O. and Y.Y. have checked the calculations, made the critical comments and contributed to the improvement of the manuscript. All authors have read and approved the final manuscript.

Funding: The authors would like to thank the support by a grant from the National Natural Science Foundation of China (No. 11775084). The work of S.A. has also been supported in part by the programs of Fujian Province, China, and of Competitive Growth of Kazan Federal University from the Ministry of Education and Science, Russian Federation.

Acknowledgments: This work has been completed while S.A. has stayed at the Wigner Research Centre for Physics with the support of the Distinguished Guest Fellowship of the Hungarian Academy of Sciences. He would like to express his sincere thanks to the Wigner Research Centre for Physics for the warm hospitality extended to him.

Conflicts of Interest: The authors declare no conflict of interest.

References

- Giusteri, G.G.; Recrosi, F.; Schaller, G.; Celardo, G.L. Interplay of different environments in open quantum systems: Breakdown of the additive approximation. *Phys. Rev. E* **2017**, *96*, 012113. [[CrossRef](#)]
- Wang, J.; He, J.; He, X. Performance analysis of a two-state quantum heat engine working with a single-mode radiation field in a cavity. *Phys. Rev. E* **2011**, *84*, 041127. [[CrossRef](#)]
- Liu, S.; Ou, C. Maximum power output of quantum heat engine with energy bath. *Entropy* **2016**, *18*, 205. [[CrossRef](#)]
- Lindblad, G. On the generators of quantum dynamical semigroups. *Commun. Math. Phys.* **1976**, *48*, 119–130. [[CrossRef](#)]
- Gorini, V.; Kossakowski, A.; Sudarshan, E.C.G. Completely positive dynamical semigroups of N -level systems. *J. Math. Phys.* **1976**, *17*, 821–825. [[CrossRef](#)]
- Bhatia, R. *Matrix Analysis*; Springer: New York, NY, USA, 1997.
- Abe, S. Weak invariants of time-dependent quantum dissipative systems. *Phys. Rev. A* **2016**, *94*, 032116. [[CrossRef](#)]
- Gorman, D.J.; Hemmerling, B.; Megidish, E.; Moeller, S.A.; Schindler, P.; Sarovar, M.; Haeffner, H. Engineering vibrationally assisted energy transfer in a trapped-ion quantum simulator. *Phys. Rev. X* **2018**, *8*, 011038. [[CrossRef](#)]
- Henao, I.; Serra, R.M. Role of quantum coherence in the thermodynamics of energy transfer. *Phys. Rev. E* **2018**, *97*, 062105. [[CrossRef](#)]
- Ou, C.; Abe, S. Exotic properties and optimal control of quantum heat engine. *EPL* **2016**, *113*, 40009. [[CrossRef](#)]
- Ou, C.; Chamberlin, R.V.; Abe, S. Lindbladian operators, von Neumann entropy and energy conservation in time-dependent quantum open systems. *Physica A* **2017**, *466*, 450–454. [[CrossRef](#)]
- Abe, S.; Ou, C. Action principle and weak invariants. *Results Phys.* **2019**. [[CrossRef](#)]
- Abe, S. Invariants of Fokker-Planck equations. *Eur. Phys. J. Special Topics* **2017**, *226*, 529–532. [[CrossRef](#)]
- Dann, R.; Levy, A.; Kosloff, R. Time-dependent Markovian quantum master equation. *Phys. Rev. A* **2018**, *98*, 052129. [[CrossRef](#)]
- Kieu, T.D. The second law, Maxwell's demon, and work derivable from quantum heat engines. *Phys. Rev. Lett.* **2004**, *93*, 140403. [[CrossRef](#)]
- Peterson, J.P.S.; Batalhão, T.B.; Herrera, M.; Souza, A.M.; Sarthour, R.S.; Oliveira, I.S.; Serra, R.M. Experimental characterization of a spin quantum heat engine. *arXiv* **2018**, arXiv:1803.06021.

17. Gorini, V.; Kossakowski, A. *N*-level system in contact with a singular reservoir. *J. Math. Phys.* **1976**, *17*, 1298–1305. [[CrossRef](#)]
18. Benatti, F.; Narnhofer, H. Entropy behavior under completely positive maps. *Lett. Math. Phys.* **1988**, *15*, 325–334. [[CrossRef](#)]
19. Abe, S. Time evolution of Rényi entropy under the Lindblad equation. *Phys. Rev. E* **2016**, *94*, 022106. [[CrossRef](#)] [[PubMed](#)]
20. Ou, C.; Abe, S. Weak invariants, temporally local equilibria, and isoenergetic processes described by the Lindblad equation. *EPL* **2019**, *125*, 60004. [[CrossRef](#)]
21. Kosloff, R.; Feldmann, T. Optimal performance of reciprocating demagnetization quantum refrigerators. *Phys. Rev. E* **2010**, *82*, 011134. [[CrossRef](#)]
22. Hill, T.L.; Chamberlin, R.V. Fluctuations in energy in completely open small systems. *Nano Lett.* **2002**, *2*, 609–613. [[CrossRef](#)]
23. Chamberlin, R.V. The big world of nanothermodynamics. *Entropy* **2015**, *17*, 52–73. [[CrossRef](#)]



© 2019 by the authors. Licensee MDPI, Basel, Switzerland. This article is an open access article distributed under the terms and conditions of the Creative Commons Attribution (CC BY) license (<http://creativecommons.org/licenses/by/4.0/>).

MDPI
St. Alban-Anlage 66
4052 Basel
Switzerland
Tel. +41 61 683 77 34
Fax +41 61 302 89 18
www.mdpi.com

Entropy Editorial Office
E-mail: entropy@mdpi.com
www.mdpi.com/journal/entropy



MDPI
St. Alban-Anlage 66
4052 Basel
Switzerland

Tel: +41 61 683 77 34
Fax: +41 61 302 89 18

www.mdpi.com



ISBN 978-3-03936-233-2